Forschungszentrum Karlsruhe
Technik und Umwelt
Wissenschaftliche Berichte
FZKA 6287

TRITEX

A Ferritic Steel Loop with Pb-15.8Li Behavior of Metals and Corrosion Products

H. Feuerstein, L. Hörner, S. Horn, S. Bucké
Hauptabteilung Ingenieurtechnik

Juni 1999

Forschungszentrum Karlsruhe
Technik und Umwelt
Wissenschaftliche Berichte
FZKA 6287

TRITEX

A Ferritic Steel Loop with Pb-15.8Li

Behavior of Metals and Corrosion Products

H.Feuerstein, L.Hörner, S.Horn and S.Bucké*

Hauptabteilung Ingenieurtechnik

*Institut für Biopharmazie und Pharmazeutische Technologie, Universität Marburg

FORSCHUNGSZENTRUM KARLSRUHE GmbH, KARLSRUHE
1999

Als Manuskript gedruckt
Für diesen Bericht behalten wir uns alle Rechte vor

Forschungszentrum Karlsruhe GmbH
Postfach 3640, 76021 Karlsruhe

Mitglied der Hermann von Helmholtz-Gemeinschaft
Deutscher Forschungszentren (HGF)

ISSN 0947-8620

TRITEX

A Ferritic Steel Loop with Pb-15.8Li*

BEHAVIOR OF METALS AND CORROSION PRODUCTS

Abstract

TRITEX was a pumped loop with Pb-15.8Li, operated for 13000 hours at temperatures between 260 and 480 °C. Many features were comparable to ITER blankets. The behavior of metals and corrosion products were investigated, and different purification devices tested.

In spite of good **wetting**, drain of Pb-15.8Li left a residue film of 87 mg/cm^2 on surfaces. In TRITEX 1 kg or 1 % of the inventory was not drained. Generally structural materials showed the expected behavior. For **α-iron** a volume swelling by 5 % was observed, an effect not described before. A **H_2 background** in all covergas spaces was caused by the reaction of steel 1.4922 with humidity. This has to be considered in experiments with low concentrations of deuterium or tritium.

The behavior of **lithium** is of special concern. Because of an initially hyper-eutectic mixture, LiPb with a melting point of 482°C was formed and deposited, flow blocking in some parts observed. On the other hand, the Li concentration can easily be controlled by a simple diffusion cold trap with a solid phase, e.g. with freeze valves. But also a **lead** phase was found and has to be considered when designing systems.

118 grams **Corrosion Products** in form of particles with different compositions were formed. The chemistry of corrosion products was complex, even compounds like NiMn and $Ni_{1.22\text{-}1.9}V$ were identified. Because of the density difference to the eutectic mixture, a fraction floated to liquid metal/covergas interfaces. 78 % of particles were magnetic, but only 30 % were trapped in magnetic fields. Cold traps were effective because of hydraulic conditions and not because of low temperature. Purification devices trapped also LiPb. Always more than 90 % of deposited material was a mixture of LiPb and Pb-15.8Li.

In TRITEX **bismuth** concentrations in the circulating mixture were below 10 wppm. Any excess was deposited at liquid/solid phase boundaries. The concentrations of **Cu**, **Ag** and **Zn** in circulating Pb-15.8Li were unchanged. **Oxygen** transport to a cold trap was seen, and elemental **carbon** observed. Metallic **aerosol** deposits were found in all covergas areas. A small fraction contained up to 93 at.% Li and reacted with oxygen and humidity. When opening components deflagration of hydrogen, colored by lithium, was observed several times. **Cadmium** was evaporating from the molten eutectic and found mainly in aerosol deposits.

* In the literature mostly Pb-17Li is written. However the eutectic mixture contains only 15.8 at.% lithium.

TRITEX

Ein Kreislauf aus ferritischem Stahl mit Pb-15.8Li*

Verhalten von Metallen und Korrosionsprodukten

Zusammenfassung

TRITEX war ein gepumpter Pb-15.8Li Kreislauf. Er wurde 13000 Stunden bei Temperaturen zwischen 260 und 480 °C betrieben. Viele Eigenschaften waren vergleichbar zu ITER. Das Verhalten von Metallen und Korrosionsprodukten wurde untersucht, und verschiedene Reinigungssysteme getestet.

Trotz guter Benetzung verbleibt beim Ablassen der eutektischen Mischung ein Restfilm von 87 mg/cm^2 auf den Oberflächen. In TRITEX verblieben so 1 kg oder 1 % des Inventars im Kreislauf. Die Strukturmaterialien zeigten das erwartete Verhalten. Bei **α-Eisen** wurde jedoch eine Volumenvergrößerung von 5 % gefunden, ein bisher nicht beschriebener Effekt. Ein **H_2 Untergrund** im Schutzgas wurde durch die Korrosion von Stahl 1.4922 in Luft verursacht. Das muß bei Versuchen mit niedrigen Partialdrucken an Deuterium oder Tritium berücksichtigt werden.

Besonders das Verhalten von **Lithium** muß beachtet werden. LiPb mit einem Schmelzpunkt von 482 °C wurde gebildet und abgeschieden, was eine Strömungsblockade in einigen Komponenten verursachte. Andererseits ist die Li-Konzentration mit einer Diffusions-Kaltfalle einfach zu kontrollieren. Jedoch auch eine **Blei**phase wurde gefunden, das muß bei der Auslegung von Systemen beachtet werden.

118 Gramm **Korrosionsprodukte** in Form von Partikeln mit unterschiedlicher Zusammensetzung wurden gebildet. Ihre Chemie ist komplex. Verbindungen wie NiMn und $Ni_{1.22\text{-}1.9}V$ wurden identifiziert. Wegen Dichtunterschieden zur eutektischen Mischung sammelte sich ein Teil der Partikel an der Phasengrenze flüssiges Metall-Schutzgas an. Obwohl 78 % der Partikel magnetisch waren, wurden nur 30 % in Magnetfeldern abgeschieden. Hauptsächlich wegen der Strömungsbedingungen waren Kaltfallen effektiv, nicht jedoch wegen der niedrigen Temperaturen. Alle Reinigungssysteme fingen jedoch hauptsächlich LiPb ein. Immer waren über 90 % des abgeschiedenen Materials eine Mischung aus LiPb und Pb-15.8Li.

Die **Bismuth** Konzentration im zirkulierenden Pb-15.8Li war stets unter 10 wppm. Ein anfänglich vorhandener Überschuß wurde in Gefrierventilen abgeschieden. Die Konzentrationen von **Cu**, **Ag** und **Zn** in Pb-15.8Li waren unverändert. **Sauerstoff** Transport zur Kaltfalle, und elementarer **Kohlenstoff** wurden beobachtet. Metallische **Aerosol**-Niederschläge wurden in allen Schutzgasräumen gefunden. Ein kleiner Teil davon enthielt bis zu 93 at.% Lithium. Aerosole reagierten mit Sauerstoff und Luftfeuchte. Wenn Komponenten an Luft geöffnet wurden, erfolgte manchmal eine Wasserstoff-Deflagration. Cadmium verdampfte aus der eutektischen Mischung und wurde überwiegend in Aerosolen gefunden.

* In der Literatur wird Pb-17Li is geschrieben. Das eutektische Gemisch enthält jedoch nur 15.8 at.% Lithium.

Used abbreviations

at.% Li	Li concentrations, calculated from |Li+Pb|
Pb-15.8Li	eutectic mixture
LM	liquid metal
EMP	electro magnetic pump
FM	electro magnetic flow meter
MFM	mass flow meter
CT	cold trap
MT	magnetic trap
MH	main heater
ET	expansion tank
SS	sampling station
TS	test section
V	valve
FV	freeze valve
DT	drain tank
LI	LM level indicator
CS	corrosion sample
crusts	deposited material at LM/covergas interfaces
deposits	deposited material in magnetic fields and cold traps

Table of Contents

Abstract
Zusammenfassung
Used abbreviations

Part I Measurements and results 1

Table of Contents 2
List of tables and figures 4

1. Introduction 5
2. Loop TRITEX 6
3. Investigations and Chemistry 8
4. Results 10
5. Purification of Pb-15.8 Li 26
6. Other effects 32
7. Summary and conclusion 33

Part II Investigation of components 35

Table of Contents 36
List of tables and figures 37

1. Phase IV 40
2. Phase V 41
3. Phase VI 44
4. Phase VII 46

Tables 49
Figures 71
References 105
Acknowledgment 106

Part I

Measurements and results

Table of Contents

List of tables and figures 4

1. Introduction 5

2. Loop TRITEX 6

3. Investigations and Chemistry 8

3.1 Treatment of lithium-lead samples 8
3.2 Treatment of crusts and deposits 8
3.3 Measurements 9
3.4 Other observations 10

4. Results 10

4.1 Behavior of materials in air 10
4.1.1 Steel 1.4922, hydrogen background
4.1.2 Vanadium in air

4.2 Behavior of lithium 12
4.2.1 Introduction
4.2.2 Samples of Pb-15.8Li
4.2.3 Crusts and deposits
4.2.4 Discussion

4.3 Corrosion in TRITEX 14
4.3.1 Introduction
4.3.2 Behavior of materials
4.3.3 Dissolved corrosion products
4.3.4 Composition of particles
4.3.5 Total corrosion products
4.3.6 Distribution of corrosion products
4.3.7 Discussion

4.4 Other impurities 21
4.4.1 Oxygen
4.4.2 Carbon
4.4.3 Bismuth
4.4.4 Cu, Ag, Zn and Cd

4.5	Formation and transport of aerosols	23
	4.5.1 Introduction	
	4.5.2 Evaporated material	
	4.5.3 Li, Pb and Cd in deposits	
5.	**Purification of Pb-15.8 Li**	**26**
5. 1	Introduction	26
5.2	Mechanical filter	27
5.3	Cold traps	27
5.4	Deposition in magnetic fields	30
5.5	Bath tube effect and other observations	31
5.6	Discussion	31
6.	**Other effects**	**32**
6.1	Residue film	32
6.2	Lithium in steels	32
6.3	Others	33
7.	**Summary and conclusion**	**33**

List of Tables and Figures

Table 1 : Facility TRITEX, main parameters.
Table 2 : Materials in contact with Pb-15.8Li.
Table 3 : Dissolved corrosion products.
Table 4 Fractions and average composition of particles.
Table 5 Distribution of corrosion products in TRITEX.

Fig.1 : Flow sheet of TRITEX in phase VII, 1996.
Fig.2 : Operation of TRITEX, phase I to VII.
Fig.3 : Magnetic particles, trapped from solution with a VITON coated magnet.
Fig.4 : TRITEX, corrosion of steel 1.4922 in air.
Fig.5 : Micro hardness of vanadium after phase V.
Fig.6 : Phase diagram of lithium-lead.
Fig.7 : Experimental phase VI and VII, operation history
Fig.8 : Li and Bi in CT3, phase VI.
Fig.9 : Deposit concentration per cm^2 evaporating surface.
Fig.10 : Li concentration in Test Section deposits, phase IV.
Fig.11 : Beads of a lead phase in CT2, phase III.
Fig.12 : Lead deposits in CT2 after phase V.
Fig.13 : Cadmium in deposits, Phase V.
Fig.14 : Profiles of Li and particles in CT1 after phase V.
Fig.15 : Profiles of Li and particles in CT1 after phase VI.
Fig.16 : Li and particles distribution in CT2 after phase V.
Fig.17 : Phase VI, CT2. Concentration of Li and corrosion products.

1. Introduction

A mixture Pb-15.8Li is proposed for fusion reactor blankets [1]. Tritium will be produced from lithium, lead is a neutron multiplier, and the molten mixture is used for heat extraction. The loop TRITEX was constructed in 1988 [2]. It was operated for 13.003 hours, before the experimental program ended in 1998.

> At start of the experimental program, always $Li_{17}Pb_{83}$ was written. At an international liquid metal workshop in Karlsruhe in 1986, experts agreed to write Pb-17Li. Actually however the eutectic mixture contains 15.8 at.% Li [4][5]. In non-isothermal systems like blankets, always this mixture is circulating [6]. Therefore **in this paper Pb-15.8Li is used**. The as-received material contained as ordered 17 at.%Li [5], only for this material Pb-17Li is written.

TRITEX was originally designed to study methods for tritium extraction. Later goals changed to behavior of impurities and purification methods. Depending on experimental requirements, components were replaced or modified. In parallel to operating TRITEX, other experiments with Pb-15.8Li were performed. Many batch type experiments were done, 25 capsules with thermal gradients heated, and twelve thermal convection loops operated for different purposes. All results were published before, mainly at conferences, and reported at European Liquid Metal Workshops. Furthermore the compatibility of 31 metals and alloys in static Pb-15.8Li was investigated [7].

This report describes the behavior of metals and corrosion products in TRITEX. It is divided into two parts. In **Part I**, measurements are described and results discussed. **Part II** gives details of investigations of components. Many samples were taken and analyzed. Most reliable results are compiled in Tables.

2. Loop TRITEX

Facility and operation history were described in [3].

TRITEX was a forced convection loop with Pb-15.8Li from ferritic steel 1.4922. Tubes of EMP, FM and MT were from TZM or from vanadium 99.5, permeation membranes from armco iron. The main loop was operated in seven operation phases for 13.003 hours between 350 and 500°C, the cold trap bypass between 250 and 280°C [3]. Depending on experimental requirements, components were replaced or modified. **Table 1** shows main parameters, **Fig.1** a flow sheet, **Fig.2** the total operation history.

Table 1 : Facility TRITEX, main parameters.

Materials	
main loop	steel 1.4922
some parts	TZM, V, armco iron
circulating Pb-15.8Li	80 to 100 kg
total inventory	ca. 120 kg
covergas	argon-6.0
heating concept	thermo boxes
temperature range	250 to 550 °C
flow rates	0.02 to 3.0 l/min (main pipes 0.2 to 30 cm/s)
inner diameter of main pipes	15 mm
length of main pipes	10 to 11 m
Pb-15.8Li wetted surface	1.2 to 1.5 m^2

The loop was filled before phase I with Pb-17Li from Metallgesellschaft company. After phase V it was cleaned and filled with Pb-17Li from Meteaux Speciaux company. During and after operation many samples were taken and components investigated. **Part II** gives details of this; most reliable results are compiled in Tables. Results and some observations will be discussed in the next chapters.

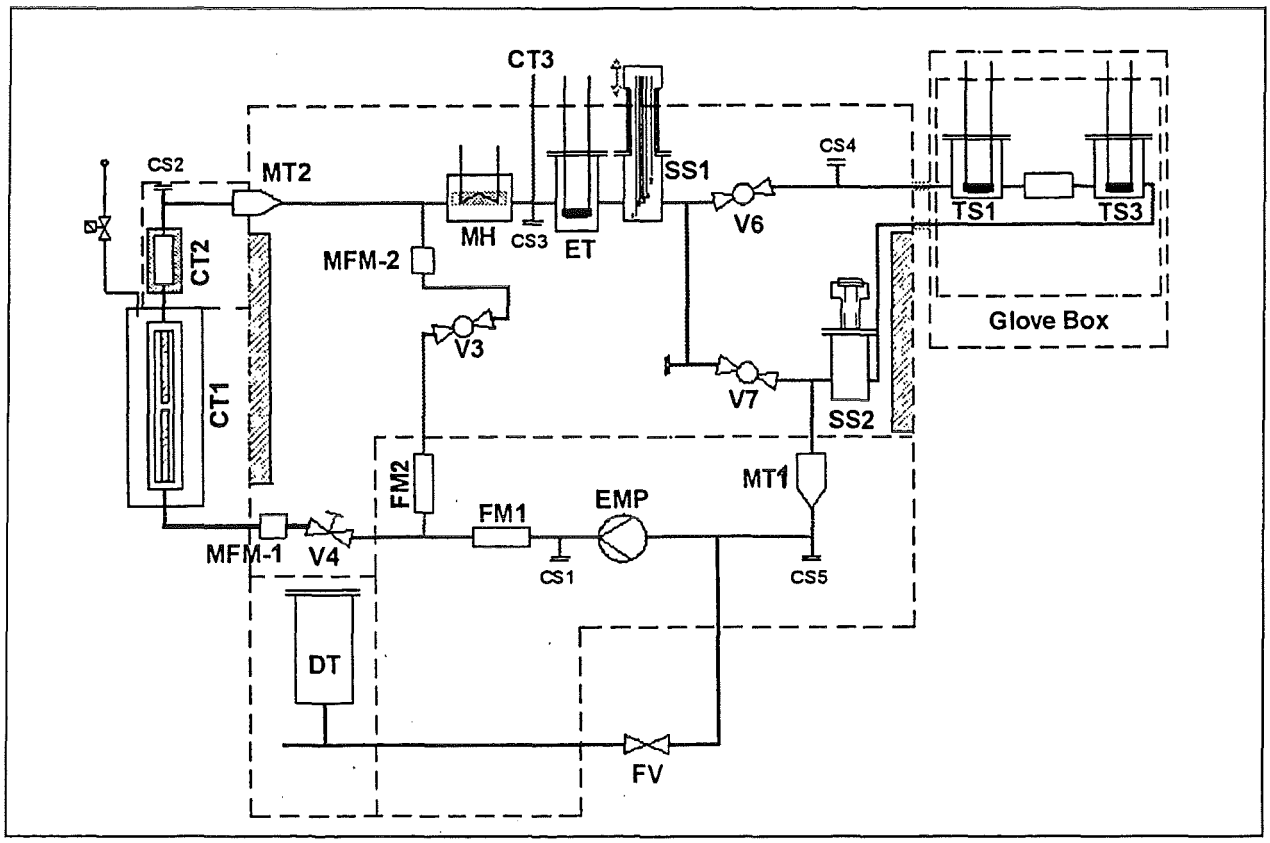

Fig.1 : Flow sheet of TRITEX in phase VII, 1996.

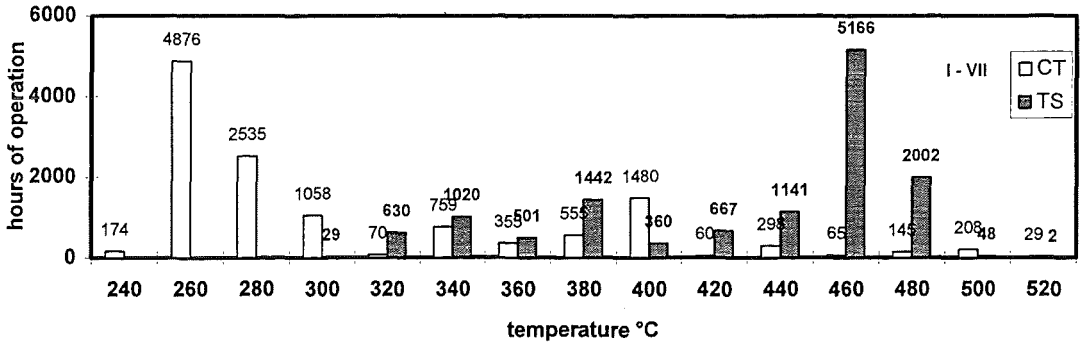

Fig.2 : Operation of TRITEX, phase I to VII.

3. Investigations and Chemistry

Three kinds of samples were investigated. Aerosol deposits were washed from surfaces with diluted acids. Samples of Pb-15.8 from the loop and samples of crusts or deposits were treated different.

3.1 Treatment of lithium-lead samples

Molten Pb-15.8Li samples of up to 100 grams were taken during operation from DT, SS2, TS and some other positions. Because of the risk of segregation effects during solidification especially for Li and Bi [5], the total sample was dissolved in a stoichiometric amount of nitric acid. The technique was described before [7]. Solutions with up to 20 grams/liter Pb+Li could be measured directly by ICP-OES. To improve the sensitivity, lead was in some samples precipitated as $PbSO_4$ or -more often- as $Pb(NO_3)_2$. No co-precipitation of elements to be determined was observed.

3.2 Treatment of crusts and deposits

Crusts were deposited material at LM/covergas interfaces, deposits found in magnetic fields and cold traps. Mainly Li and corrosion products were determined in samples of this kind. Except for a small fraction dissolved, corrosion products were found in form of particles with different composition. With up to 10 gram samples the following procedure was used :

Step 1. The sample was treated at 60°C with a mixture of 2% acetic acid+0.5% H_2O_2. The solution contained Pb, Li, Bi, dissolved corrosion products and some other elements. Especially with high Li concentrations, and depending on shape and size of particles, a small fraction of these was dissolved. But usually found concentrations of Mn, Ni and Fe reflected solubilities in the molten mixture, respectively equilibrium concentrations with structural materials.

Step 2. Using a VITON coated magnet, **'magnetic particles'** were extracted from the residue, **Fig.3**. When putting the magnet in a Pyrex test tube, the particles fell down after removing the magnet. They could easily be dissolved in concentrated HCl.

Step 3. Treating the remaining particles with aqua regia dissolved a fraction of its, called **'non-magnetic particles-I'**.

Step 4. There remains a residue of **'non-magnetic particles-II'.** Most of it could be dissolved with boiling HNO_3/H_2SO_4.

Step 5. Sometimes there was still a small residue, consisting of chromium oxides and/or carbides, called **'non-magnetic particles-III'**. It could be dissolved only by melting with $NaKCO_3/Na_2O_2$ or similar mixtures.

Of course, particle separation is not complete, concentrations, therefore, scattered over a wide range. Nevertheless the four kinds of particles have clearly different compositions.

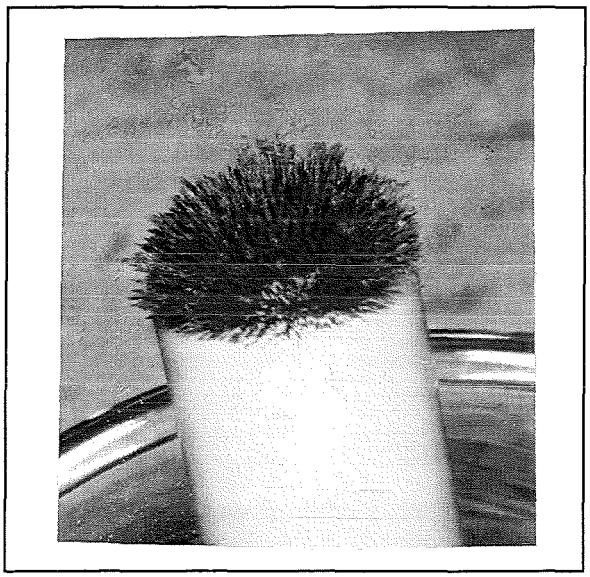

Fig. 3 : Magnetic particles, trapped from solution with a VITON coated magnet.

3.3 Measurements

Simple thermal analysis was occasionally done to see if or not they were metallic. A few times particles were analyzed by Microprobe. But mostly samples were dissolved and solutions analyzed by ICP-OES, using a PLASMA II of Perkin Elmer company. Only Bismuth was determined by polarography [8] [9].

The accuracy of ICP-OES measurements was generally ± 3-5%, in special cases as good as ±0.1% [6], those for polarography not better than ±15%. Analytical results are influenced by many parameters. Smaller samples caused larger errors. Also samples were seldom homogeneous. Usually a sample was divided at least in two parts, dissolved and analyzed separately. Different numbers of digits in tables of results reflect the possible errors. Not in all samples all elements could be determined

3.4 Other observations

Samples with high Li-concentrations dissolve in oxidizing acids often under sparks and fire effects. Because of small mass of deposits this caused however never a hazard.

When dissolving lithium-lead from steel surfaces with mild acids, often the reaction stops. Stronger acids are needed for dissolution. But with this also steel dissolves. We assume formation of an electrochemical element, as seen before [7]. Also with mild acids often a film of pure lead remained at the surface. These effects have to be considered when cleaning Pb-15.8Li wetted surfaces, as done with the whole loop after phase V.

4. Results

4.1 Behavior of materials in air

The compatibility of structural materials with air was not expected to cause problems. Mainly three materials were used. TZM caused at the beginning of the program problems with broken welds. During phases II to VII, no contact was any more to air. Only for steel 1.4922 and vanadium some effects had to be considered.

4.1.1 Steel 1.4922, hydrogen background

There was always a H_2 background in TRITEX covergases. At high temperature steel reacts with humidity and forms H_2. Up to 50% of formed hydrogen diffused into the liquid metal and was found in covergases. The effect is not new and was even used for corrosion studies [11]. For loop operation this H_2 caused no problems, but it had to be considered in experiments with hydrogen isotopes at low concentrations.

In TRITEX $2*10^{-8}$ mol H_2/s were formed at 470°C in operation phase 1. This value dropped during 9520 hours of operation, phase V, to $2.7*10^{-10}$ mol H_2/s. At 330°C the corresponding values were $6.4*10^{-9}$ and $2.7*10^{-11}$ mol H_2/s. The values are comparable with those from thermal convection loops [10]. At the beginning of operation, the calculated corrosion rate in air at 470°C would be as low as 0.08 g/m^2*d. Even if such low corrosion rates were not published, the value seems possible, **Fig.4.**

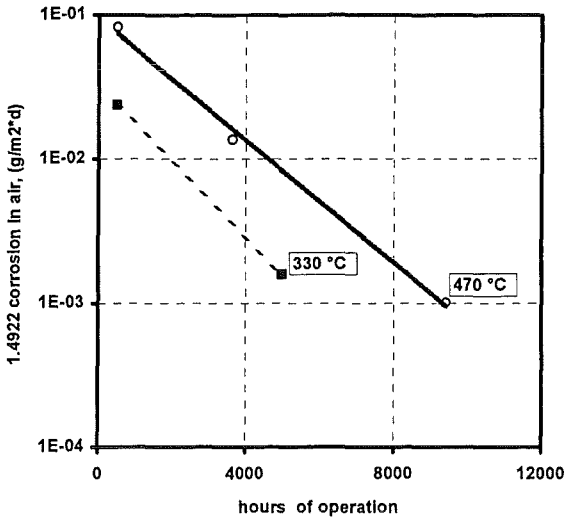

Fig.4 : TRITEX, corrosion of steel 1.4922 in air.

4.1.2 Vanadium in air

Vanadium was used for flow meters, magnetic traps and for hydrogen extraction [12]. It is very stable in Pb-15.8Li [7]. In case of FM's and MT's the out- side was in contact with air. Oxygen dissolves in V at higher temperatures, causing embrittlement. For safety reasons this had to be checked.

FM2 was operated until phase V for 5450 hours at 460 to 480 °C. It was removed from the loop and a hardness profile across the wall was determined. The results show that oxygen had been dissolved in the metal, but only a thin outer layer was involved, **Fig.5**. The harder surface layer at the Pb-15.8Li side is from fabrication of the tube. It was concluded that Vanadium can be used under TRITEX conditions.

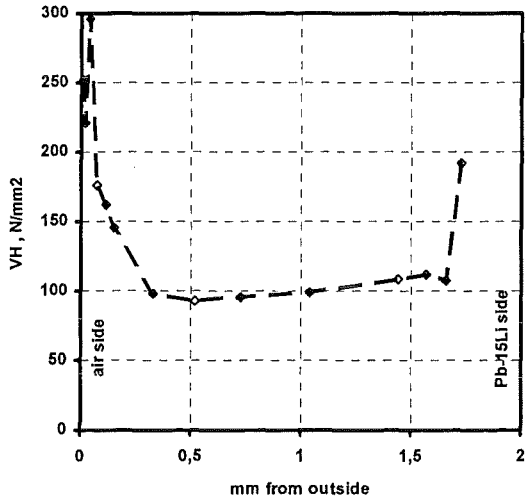

Fig.5 : Micro hardness of vanadium after phase V.

4.2 Behavior of lithium

4.2.1 Introduction

The Pb-Li phase diagram [4] shows several intermetallic compounds and eutectic compositions, **Fig.6**. At the melting point of the interesting mixture, 234°C, a liquid phase with 15.8 at.% lithium in lead is in equilibrium with a solid phase, consisting of LiPb and Pb.

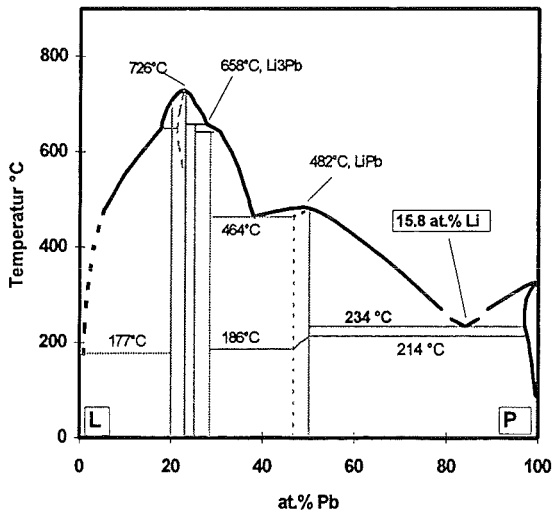

Fig.6 : Phase diagram of lithium-lead, [4].

During operation of a fusion reactor blanket, lithium will be consumed by transmutation to tritium, evaporation and reaction with air. The breeding ratio of ^{3}H decreases, the melting point of the mixture increases. With a loss of 1 at.% Li, the melting point of the mixture increases by 6°C. Pb-17Li too has a melting point 240°C. The lithium concentration in a blanket, therefore, has to be controlled.

The eutectic mixture was always ordered with 17 at.% Li. As an average bars contained this concentration. However Li was not homogeneous distributed. In bars values between 15.5 and 20.7 at.% were found at different positions [5]. Segregation during solidification was responsible for this. The effect is also important in Pb-17Li samples. Reliable results for Li (and Bi) were only obtained if the total sample could be dissolved.

4.2.2 Samples of Pb-15.8Li

During operation dip samples of the molten mixture were taken from time to time at different positions. Even if Pb-17Li was filled in DT and loop before phase I, the average concentration in the flowing eutectic mixture was 15.7±0.4 at.%. This was expected [6]. Fresh Pb-17Li was filled into the loop before phase VI, but the equilibrium was not yet attained after 2000 hours of operation in Nov. 1994.

4.2.3 Crusts and deposits

Crusts from liquid metal-covergas interfaces contained up to 50 at.% Li[1]. Two explanations for the ratio Li/Pb up to 1 are possible :

1. Oxides are deposited, mixed with different fractions of Pb-15.8Li. Li concentrations in oxides are always higher compared to the eutectic [13].

2. Crusts are not permanently washed by liquid metal, LiPb floating around could deposit at interfaces like corrosion product particles. (Bath tube effect.)

The identification of oxides is difficult. Complete oxidation of LiPb would increase the weight only by 11%. This was not found. But partly oxidation is possible. Even if mostly within error range of analytical methods, the sum |Li+Pb+corrosion products| was often smaller than the sample weight. Attempt to identify oxides failed.

Not only crusts, also deposits in cold traps, MT, FM and EMP contained up to 50 at.% Li. There was clearly LiPb deposited. Thermo-analysis showed the metallic phases of LiPb and eutectic mixture. Also when dissolving deposits in acids, H_2 was formed. Often LiPb was without any oxides. For example on deposition rings of CT2 after phase IV, 26 g metallic LiPb was found.

4.2.4 Discussion

TRITEX was a non-isothermal Pb-Li system including a solid phase. In agreement with other experiments a mixture with 15.8 at.% Li was circulating. [5] [6] [14]. Always a hyper-eutectic mixture with 17 at.% Li was filled in. The Li excess should deposit as LiPb at phase boundaries.[2] This was found, all crusts and deposits contained up to 50 at.%Li.

While deposits contained metallic LiPb, for crusts the situation was not so clear. Oxides could deposit at LM-covergas interfaces. Air leaks in the covergas system would deliver the needed oxygen. Such leaks could not be excluded, however complete oxidation was impossible. For example :

> The expansion tank after phase VII contained 18.6 g crusts with 50 at.% Li. To form this mixture as oxides, 1.5 liter O_2 are required. The tank was in operation for 3120 hours with an argon flow rate of 10 (to 20) cm^3/min. The covergas would have to contain all the time for the reaction 800 (400) vpm O_2 to form 18.6 g oxides. The gas at inlet and outlet to the loop contained <0.1 vpm O_2 resp. <10 vpm. Also, the required oxygen would mean an air-in leak of $3*10^{-3}$ ($1.5*10^{-3}$) mbar*l/s, a leak rate never seen.

This shows, that also crusts contained a large fraction of LiPb. However not all LiPb was found. In phase VI + VII changing the concentration from 17 to 15.8 at.% means a loss of 56 grams Li. All deposits and crusts together contained an excess of only 20 grams. The loop was completely dismantled and analyzed after phase VII. The only explanation would be LiPb deposited at a not analyzed cold spot in the drain tank.

---

[1] Li concentrations were calculated from Li in |Li+Pb| .

[2] An initially hypo-eutectic concentration would result in the formation of a lead phase [5].

It remains an important question: Why is **LiPb** deposited at higher temperature, where it should dissolve quickly [14]. Even at the melting point of lead, 327°C, the solubility is 27.5 at.% Li. In addition, as discussed below, also lead was found at positions with higher temperature after phase V. Before drain, TS was at 460, DT at 330, and CT2 for more than one week at 360-385°C. In all these components, LiPb and small amounts of lead were found.

More investigations with special experiments would be needed to understand LiPb formation and behavior in non-isothermal loop systems.

4.3 Corrosion in TRITEX

4.3.1 Introduction

The loop was not designed to study corrosion products, but cold and magnetic traps were installed. Corrosion products were formed from corroding structural materials. This is more comparable to a real blanket than many corrosion experiments, where small samples in a system with a large surface of a different material are tested. Furthermore, the ratio of Pb-15.8Li mass to steel surface was comparable to blankets for ITER, and the LM velocity was similar to those for a water cooled blanket.

During corrosion, elements from the surface get dissolved in the molten metal. If the solubility of an element is exceeded, it will precipitate and form a solid phase. While dissolution takes place mainly in areas with higher temperature, precipitation should occur in cold traps. Several elements are dissolved and mostly compounds or alloys precipitate.

Many samples were taken and components investigated. Details are given in **Part II**. After phase V and after phase VII, the whole loop was dismantled and analyzed.

The following materials were in contact to flowing Pb-15.8 Li, **Table 2.** In this table the cold trap bypass is not considered because it was operated mainly at lower temperature, **Fig.2**. Corrosion products should reflect corrosion of the listed materials.

Table 2 : Materials in contact with Pb-15.8Li.

	m^2
Steel 1.4922	0.9 to 1.2
Steel 1.6770	0.13
αFe	0.19
TZM	0.13
V	0.016

4.3.2 Behavior of materials

No corrosion experiments were performed, but during investigation of components also materials were studied. In agreement with the literature, [7] no reaction zones were seen on ferritic steel, Mo or V. Even if mainly described in Part II, because of its importance for blankets two effects should be given again in this chapter.

1. EMP, and for some time also a MT1, had in the range of the magnet a TZM liner in an austenitic steel tube (1.4571), welded to 1.4922. Still filled with Pb-15.8Li, MT1 it was cut axial, one side for chemical analysis, the other for metallographic examinations. Steel 1.4922 was overlapping TZM by 1 cm, but there was a gap of 20 μm between TZM and the austenitic steel. This gap was filled with eutectic mixture (part II, Fig.8). A ferritic layer was formed on the austenitic steel, showing the effect of Ni-leaching. This was reported many times, an example is given in [15]. Pb-15.8Li clearly exchanged with the circulating mixture, otherwise the thickness of the ferritic layer could not be explained.

Wetting probably needs even at higher temperature more time. After phase V, Pb-15.8Li was a solder between TZM and steel with good wetting (9880 hours of operation), but not after phase VII (3120 hours of operation). Nevertheless the ferritic zone was formed also without wetting.

2. About 0.19 m^2 armco iron was used in TRITEX, mainly for permeation membranes. After about 5000 hours of operation, the iron volume increased by 5 vol.%. This was not seen for ferritic steels 1.4922 and 1.6770. Swelling of materials in liquid metals, as known e.g. for sodium systems [16] was not reported so far for Pb-15.8Li.

4.3.3 Dissolved corrosion products

For determination of dissolved corrosion products, larger samples were treated with diluted acetic acid/H_2O_2. In addition to dissolved metals, 22 wppm (phase I-V) respectively 15 wppm (phase VI and VII) corrosion product particles were floating with Pb-15.8Li. Especially with high Li concentrations in a sample, fractions of these particles got dissolved, giving wrong values. Most reliable average concentrations are listed in **Table 3.**

Table 3 : Dissolved corrosion products.

	wppm	
Fe	6.14	± 3.42
Cr	2.79	± 2.74
Ni	12.24	± 2.49
Mn	0.88	± 0.68
Mo	0.17	
V	0.37	

The wide scattering points to not-homogeneous distribution in loop and/or samples. The found concentrations are comparable with those found before in compatibility tests for 550 °C [7]. The Fe value is higher than given in [7], but lower than a value of Barker [17]. No solubility data for Cr were published, the very wide scattering points to particles, as discussed in [17]. Only Ni is as expected for 1.4922 from a solubility function [17], in spite of additional Ni from austenitic steel in MT and EMP. Mn is a factor of two too low, the values for V and Mo are orders of magnitude too high [7].

TRITEX was operated non-isothermally. Because of observations at cold traps we consider equilibrium at the main-loop temperature of 450 to 480 °C. But it is questionable if the found values are really equilibrium concentrations between steel and molten eutectic. The Mo and V concentrations point more to an equilibrium with TZM (EMP) and vanadium (flow meters), [7]. The chemistry in the molten eutectic, for example formation of NiMn [18] [19], will change equilibrium values, and finally the particle problem has to be considered. Particles with different compositions may have even larger surfaces than structural material. Probably an equilibrium between solution, structural materials and particles has to be considered.

4.3.4 Composition of particles

More than 95% of corrosion products were found in form of particles in crusts or deposits. As described in **chapter 3.2,** four kinds of particles were identified, **magnetic and non-magnetic I, II and III.** Crusts and deposits, usually gray to black, contained up to 50 at.% Li and up to 14 wt.% corrosion product particles.

All particles were composed of several elements. Unfortunately the separation of different kinds of particles by chemical treatment is not perfect. Which fraction of the 'wrong' particles got dissolved in a step could not be controlled. It depended on many different parameters. But in spite of widely scattered concentrations, the four kind of particles have clearly different compositions. Average concentrations of elements in particles are given in **Table 4.**

Table 4 : Fractions and average composition of particles.

	fraction	Fe	Cr	Ni	Mn	Mo	V
		wt.%	wt.%	wt.%	wt.%	wt.%	wt.%
all particles	(1.00)	**89,612**	**9,413**	**0,304**	**0,247**	**0,347**	**0,034**
magn. particles	0,779	92,25	**7,03**	0,30	**0,14**	0,32	0,02
NM-I	0,173	78,32	**19,48**	0,34	**0,95**	**0,74**	**0,17**
NM-II	0,049	31,01	**66,76**	0,26	**1,78**	0,14	0,07
NM-III	< 0.003	11,50	**88,50**				
Steel 1.4922			12,1	0,31	0,53	0,54	0,30

As expected for a ferritic system, the largest fraction were magnetic particles. Only 22% were non-magnetic.

The chromium concentration in all corrosion product particles together is lower than in the loop steel. Probably the corrosion rate of other structural materials (armco iron) is higher than that of 1.4922. Most stable in wet chemistry are non-magnetic particles III. These particles are very hard. They consists probably of chromium oxides or carbides. No detailed analysis could be done because the total amount was very small. Remarkable is the high concentration of manganese in non-magnetic particles, higher than those of Ni. That means not only NiMn was deposited [18] [19]. The concentration of vanadium is far too low. The missing V was not found. Mass transfer between dissimilar metals, e.g. to Mo as found in [7], may be responsible.

Looking however in details of tables in **Part II** shows, that the composition of particles of the same kind was not constant. For example magnetic particles from cold traps contained more chromium and manganese than from other positions, while non-magnetic I particles from cold traps showed a lower concentration of Mo than from other positions. Very high concentrations of Mn and Ni were found in particles from the drain tank after phase VII. NiMn and/or other Mn compounds have deposited there [1] [2]. This was not seen after phase V.

A special kind of particles was found in MF1 near the vanadium surface after phase V : $\mathbf{Ni_{1.2\text{-}1.9}V}$. The compound must be very stable. The chemical activity C/C_s of Ni in the eutectic was only 0.005, that of V near the surface 1. Compounds like this are possible in the system Ni-V [20]. The Ni to V ratio in some particles however points also to other probably more complex compounds.

4.3.5 Total corrosion products

After phase V and after phase VII, the whole loop was dismantled and all components investigated. The total found corrosion products were (**table 5**) :

Phase I to V	79.1	grams
Phase VI+VII	39.3	grams

Published corrosion rates for ferritic steels in eutectic Pb-15.8Li are scattered over a wide range. Tas [15] describes, that all data from pumped loops fit between two lines, about a factor of 25 from each other. TRITEX was a pumped loop with flow velocities in main pipes between 1 and 25 cm/s, well in the range of other loops. Therefore an average function of the two Tas lines was used to calculate the expected corrosion products :

$$\ln CR = 22.96 - 17300/T$$

with corrosion rate CR given in g/m^2*d, T in Kelvin.

Using surfaces of components and operation history, **Fig.2** and **Fig.7**, 164 grams corrosion products should be formed during Phase I to V, and 136 grams during phases VI and VII. Keeping in mind that corrosion rates may be a factor of 5 lower or higher than calculated with the average function from [15], our values are in the expected range.

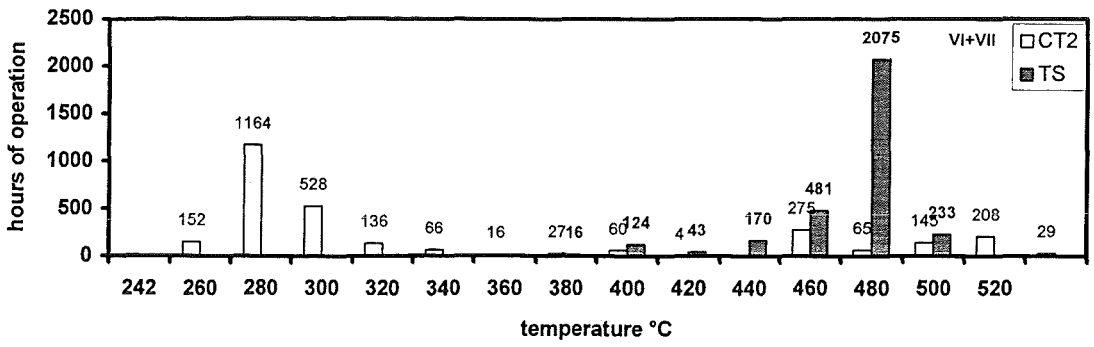

Fig.7 : Experimental phase VI and VII, operation history.

Altogether 118.4 grams corrosion products were formed. They were found dissolved, in crusts and deposits. Fe, Cr, Mn and Mo were found as expected from 1.4922. Too much Ni was found : 3.3 grams instead of 0.36 g. This can be explained by leaching of Ni from austenitic steel below the TZM liner in EMP[3]. Twice 0.13 m^2 steel 1.4571 were in contact to flowing eutectic. On the other hand, only 0.13 grams vanadium was found, 0.36 grams were expected from 1.4922. Mass transfer to TZM, as found in [7], may have been responsible.

4.3.6 Distribution of corrosion products

The distribution of corrosion products will be discussed again together with purification devices. Only a summary is given here :

Table 5 : Distribution of corrosion products in TRITEX.

	Phase I to V		Phase V I + VII	
	grams	%	grams	%
dissolved in Pb-15,8Li	1,59	2,01	2,43	6,19
floating in Pb-15,8Li	2,03	2,57	1,35	3,44
magnetic traps	0,08	0,10	3,62	9,22
flow meters	0,23	0,29	1,06	2,70
EMP	26,63	33,65	7,07	18,01
cold traps	42,02	53,10	22,60	57,56
all crusts	1,21	1,53	1,06	2,70
DT	5,34	6,75	0,07	0,18
total	79,13	100	39,26	100,00

Besides dissolved corrosion products, 2.6 to 3.4 % were floating in form of very fine particles within the flowing eutectic. These stick at walls during drain, only a small fraction is found in drain tank. Because of frequent drain during phases I to V, more particles are found in DT than after phase VII.

Even if 80% of particles were magnetic, only 34 respectively 30% were found deposited in magnetic fields. All crusts and deposits contained magnetic particles. Cold traps were effective for all kind of particles.

[3] 120 kg fresh Pb-17Li were filled in two times, also two new EMP were used.

4.3.7 Discussion

It was reported before [21], that a simple mass transfer model is not valid in ferritic systems. Particles are formed in solution, poorly sticking at walls.

Generally, dissolved metals are in equilibrium between solution, structural materials and also particles. Only the Ni concentration in the eutectic was corresponding to an equilibrium with 1.4922. The concentrations of Mo and V point more to an equilibrium with TZM from EMP and vanadium from flow meters. The formation of compounds like $\mathbf{Ni_{1.2\text{-}1.9}V}$, **NiMn** and others will also influence concentrations in solution. Such compounds may be also in particles with high V or Mn concentrations.

Particles grow while floating in the molten eutectic. Larger particles were trapped in magnetic fields and crusts. Only a small fraction remained in the eutectic and was drained to the drain tank. DT was kept at 350°C during loop operation and particles accumulated in crusts.

More than 95% of the corrosion products were found in form of particles. Four different kinds were identified, with chromium concentrations between 7 and 89 wt.%, and with a high concentration of manganese in non-magnetic particles. Most of the particles were magnetic. However always the main fraction in crusts and deposits were Pb-15.8Li and LiPb. The highest found particle concentration was 14 wt.%.

In case of a ferritic steel loop with no leaching of elements, the composition of all corrosion products together should correspond to the composition of the steel. This was not found. The lower Cr concentration point to stronger corrosion of α-iron[4]. Too much Ni and not enough V were found. The source of Ni is the austenitic steel in EMP, where Ni was leached out in spite of a TZM liner. Mass transfer to TZM [7] may have been responsible for the too small amount of V in corrosion products.

[4] About 0.19 m^2 armco iron were in TRITEX, mainly for permeation membranes.

4.4 Other impurities

4.4.1 Oxygen

If compared to sodium, the solubility of oxygen in Pb-15.8Li is low. Coen supposed that the eutectic will be always saturated [21].

During oxidation Li_2O and PbO will be formed, with relatively more lithium than in the eutectic [13]. Because of low density not dissolved oxides will float to the top of molten eutectic. But even in such crusts the identification of oxides is difficult. This was discussed in chapter 4.2.

The phase diagram, **Fig.6** shows that a metallic phase cannot contain more than 50 at.% Li (LiPb). Higher Li concentrations in crusts point to oxides. This was found in valves 6 and 4 after phase V and VII. Even if there was also LiPb deposited, not identified air leaks caused the formation of oxides.

Until end of phase V, TRITEX was operated for 9700 hours. Most of the time the cold trap temperature was 260 °C. In sections of CT2, up to 55.7 at.% Li were found. This means there was also an oxygen transport by molten Pb-15.8Li to cold traps. With the assumption : only LiPb and Li_2O were deposited, 0.12 gram oxygen was transported to CT2.

4.4.2 Carbon

When dissolving samples from crusts with acetic acid/H_2O_2 or HNO_3, often a black foam was creeping up the walls of beakers, consisting mainly of carbon. No detailed analysis was performed, only estimations are possible.

A few mg carbon may come from degraded oil, low (vpm) concentrations of CH_4 and C_2H_6 were found in covergases. The main fraction comes from loop steel, specified with 0.2 wt.% carbon. Altogether about 118 grams corrosion products were formed, 0.2 g carbon should be found. The total seen carbon was in this range.

Carbon in Pb-15.8Li was described before from loop PICCOLO [22]. It is not possible to conclude if or not there is an additional carbon transport from steel to interfaces, as seen e.g. in sodium systems [23]. No carbon solubility data for Pb-15.8Li are available.

4.4.3 Bismuth

Depending on the blanket concept, up to 10 wppm Bi are formed per year from lead. From Bi the radiological important nuclide Po-210 is formed. To keep this at a low level a Bi concentrations below 10 wppm was requested [25]. With other experiments it could be shown that such low concentration can be attained with a diffusion type cold trap with a solid phase [9][24]. **Cold trap 3** was such a cold trap, but also other positions were comparable to this.

As received Pb-17Li contained 53 and 29 wppm Bi. In agreement with [9] and [24], samples from the loop contained much lower concentrations. Bi was deposited as LiBi or Li_3Bi, **Fig.8**. Enrichment of Bi was not seen in deposits or crusts. The only exception were deposition rings of CT2 after phase V, where 78 wppm Bi were found together with 55 at.% Li.

(The different distribution of Li and Pb in the solid phase of CT3 was found also in thermal convection loops. This will not be discussed in this paper).

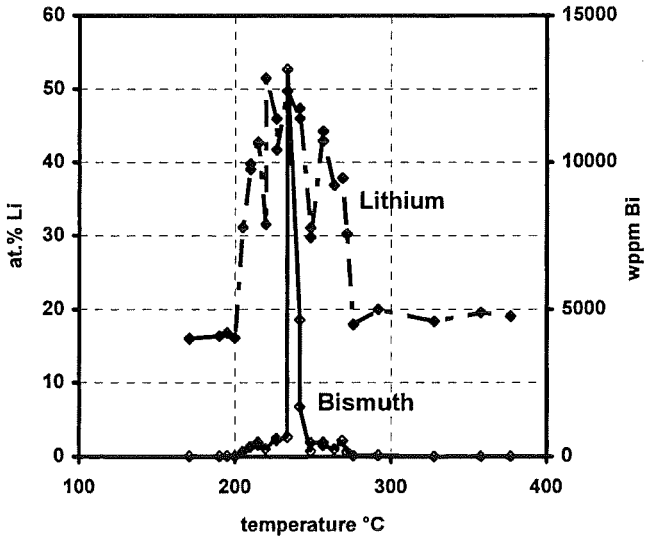

Fig.8 : Li and Bi in CT3, phase VI.

4.4.4 Cu, Ag, Zn and Cd

Only a few elements were determined in samples of the loop. Cu and Ag were within error range of analysis unchanged. The Zn concentration was slightly higher than in as received material, this may be an error in sample preparation.[5] Only the concentration of Cd was reduced. This metal evaporates, chapter 4.5. Never any enrichment of these four elements was seen in crusts or deposits.

[5] Modified chemistry between analysis of samples for Table 3 and Table 4 in part II.

4.5. Formation and transport of aerosols

4.5. 1 Introduction

Evaporation rates in argon are small, aerosol concentrations very low [26]. Nevertheless deposits were found in all covergas areas. They were metallic and reacted with humidity of air. Deflagration of hydrogen, colored by lithium, was observed several times. Because of small mass of deposits this caused never a hazard.

Liquid metal/covergas interfaces were at valves, SS, ET, TS, CT and DT [3]. The total evaporating surface of the main loop was 234 cm^2. Two 0.4 to 0.8 meter long stainless steel gas pipes with 4 mm inner diameter were going from near a LM surface out of thermo boxes. Then up to 3 meters away were 20 microns sintered metal filters. Gas flow rates were generally low, in the range of <1 to 5 cm/s, gas flow laminar. Furthermore often there was no gas flow at all [3], only convection caused transport in components and pipes.

4.5.2 Evaporated material

| **Pb+Li**| . Tubes and filters were analyzed several times for deposits. **Fig.9** shows, that formed aerosols deposit quickly. The surface concentration of | Pb+Li| decreases by a factor of 100 within 200 to 300 mm from an evaporating surface. No | Pb+Li| was found in pipes or behind filters. Only 0.7±0.5 % of evaporated material was in filters. This is more than expected from the distance. It shows that a small fraction of condensed aerosols can be transported over a long distance, but also that it is easily trapped.

Evaporation was proportional to evaporating surfaces. The total mass of evaporated | Pb+Li| was 1.7 grams. Using functions from [26], surfaces and operation history, only 0.05 grams evaporated material was expected. TRITEX was not operated as in evaporation experiments. Before filling the loop it was heated for up to two days under vacuum [3]. Vacuum evaporation rates are 1000 times higher than those in argon. In addition vacuum evaporation took place from the wetted loop surface of ~1 m^2. The high value from TRITEX is therefore not surprising.

4.5.3 Li, Pb and Cd in deposits

As shown before, relatively more **lithium** will evaporate than Pb, and Li concentrations in deposits increases with distance from an evaporating surface [26]. An example from TRITEX, is shown in **Fig.10.** In filters the Li concentration was as high as **85±8 at.% or 16 wt.% !**

Lead. While fractions of deposits contained high Li concentrations, a lead phase was also seen. Mainly near LM-covergas interfaces shiny beads of up to 1 mm diameter remained metallic clean even after several weeks in air, **Fig.11**. The Li concentration was found to be between 0.1 and 4.8 at.%. We assume a kind of rectification effect, leaving lead at positions with higher temperature. After phase V, 1.0g lead was found in covergas area of CT2, and 0.12g in TS. This amount was proportional to evaporating surfaces as found for | Pb+Li| .

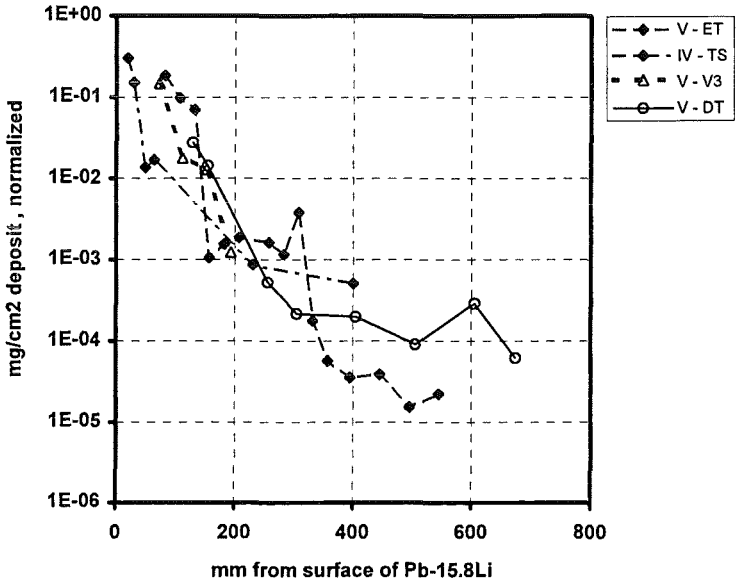

Fig.9 : Deposit concentration per cm^2 evaporating surface.

The density of lead is higher than that of the eutectic. Beads falling down accumulate at the bottom of components, get transported by liquid metal to other components, and are drained with Pb-15.8Li. Below the LM level about 0.3 grams were found in CT2, deposited in basket holes, **Fig.12**. Also at other positions, for example in EMP, lead was found. In the drain tank after phase V, 1 gram was accumulated in the gas phase and 5 gram at the bottom.

An estimation for the whole loop gives about 10 gram lead, only 0.01% of the inventory. This is more than expected from the Li excess in | Pb+Li| deposits, showing that a fraction of evaporated Li re-condenses in the liquid phase. But even if the total amount will be small, it should be considered at positions with narrow gaps and temperatures below 327°C.

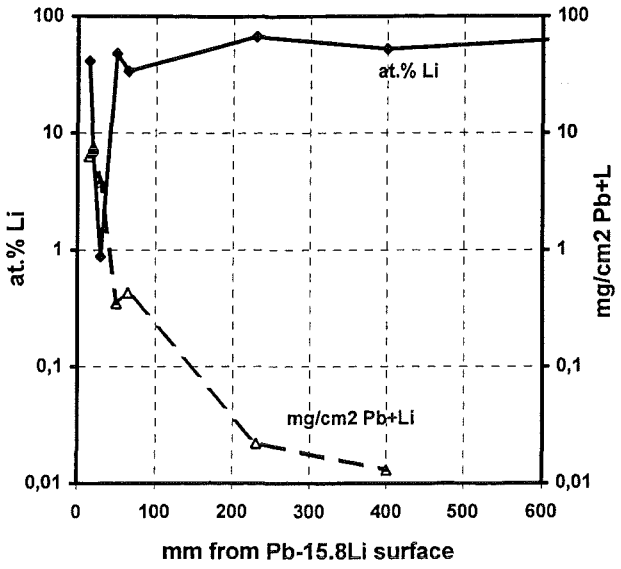

Fig.10 : Li concentration in Test Section deposits, phase IV.

Cadmium. Besides Li and Pb, only Cd was found in aerosol deposits. Its concentration increased with distance from the evaporating surface, **Fig.13.** Altogether only 1 mg Cd were found in covergas spaces. The as received Pb-17Li contained 1 to 2 wppm. Analysis of LM samples from the loop in phase V showed only 0.1 wppm. The difference would be more than 100 mg Cd. Also from calculations, comparing with evaporated lead and using vapor pressure functions from [27], much more Cd than 1 mg should have evaporated. Because the Cd chemistry in Pb-15.8Li was never investigated, no explanation is possible.

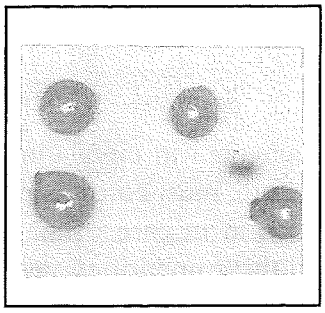

Fig.11 : Beads of a lead phase in CT2, phase III.

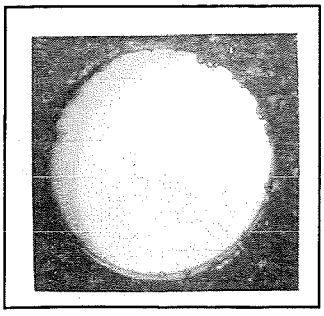

Fig.12 : Lead deposits in CT2 after phase V.

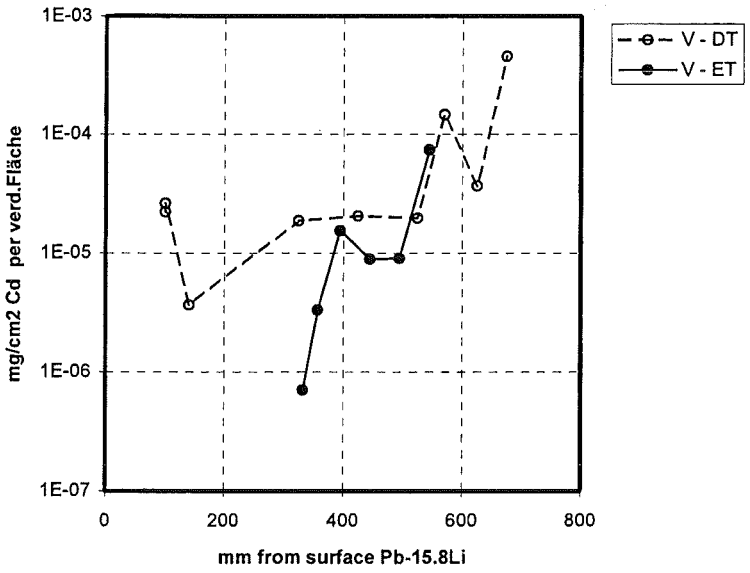

Fig.13 : Cadmium in deposits, Phase V.

5. Purification of Pb-15.8 Li

5. 1 Introduction

Different kinds of impurities will accumulate in circulating Pb-15.8Li. Corrosion products will have the highest mass of all. Therefore, most considerations are done for corrosion products. Oxides of lithium and lead will form in case of air leaks to the system. Bismuth is formed by transmutation from lead. All these impurities have to be removed for different reasons.

In previous chapters it was shown that Li plays an important role in Pb-15.8Li systems. Always Pb-17Li was filled in. The Li excess was deposited in form of LiPb together with corrosion products. Crusts and deposits consisted always mainly of | Li+Pb| . Therefore lithium has to be considered together with impurities.

Different purification devices were described in reference [3], results of investigations in detail in part II. Table 5 shows the distribution of corrosion products in TRITEX. Some components were effective for trapping, others not. In this chapter the efficiency of different devices will be discussed.

5.2 Mechanical filter

Mechanical filter can be used to remove debris and larger particles from the eutectic. In TRITEX a mechanical filter from TZM wire mesh was in the pre-phase between loop and drain tank. It was blocked during the first drain probably by LiPb, and removed from the loop.

5.3 Cold traps

Cold traps are classical devices for liquid metal purification [16]. The solubility of elements is smaller at lower temperature. If it is exceeded, the element (or a compound) will precipitate and form a solid phase. This occurs usually at surfaces, deposition layers or dendrites will grow.

Many attempts failed to find this form of deposited material in TRITEX[6]. 96 to 98 % of the corrosion products were in form of particles. This was not new [21]. Particles with poor sticking properties are formed in ferritic Pb-15.8Li systems and transported by the molten mixture. To deposit such particles hydraulic conditions are more important than temperature differences. That means that the large fraction of corrosion products found in cold traps were deposited because of flow conditions and not because of exceeded solubilities.

Except for CT3, cold traps consisted always of a cooler, CT1 and a deposition device, CT2. A temperature profile was in CT1, while CT2 was operated isothermally at low temperature.

Cold trap 1

Until phase V, CT1 was an 0.72 meter long 8 mm wide annular gap. The LM cross section was 23 cm^2, compared to main pipes the flow velocity was 13 times lower. **Fig.14** shows, that there was no Li profile in CT1, the particle deposition was highest near the exit. 28 g particles were deposited, 36% of total corrosion products.

In Phase VI and VII there were deposition chambers in CT1 in addition to the annular gap. The trap was investigated after phase VI. **Fig.15** shows the profiles, 18 g particles were deposited.

Cold trap 2

Until phase V, CT2 was a tank with a basket, filled with deposition rings. **Fig.16** shows the distribution of Li and corrosion products. At outlet of the dome, 55 at.% Li was found, showing a transport of oxides to the cold trap (chapter 4.4). At this position was also the maximum particle concentration of 6.4%. Together with particles from the tube between CT1 and CT2, 14 grams corrosion products were deposited in CT2. At deposition rings 10 grams of metallic LiPb were found. And finally; as discussed in chapter 4.5.2, a lead phase was seen in CT2.

[6] Only LiPb dendrites were seen in CT1.

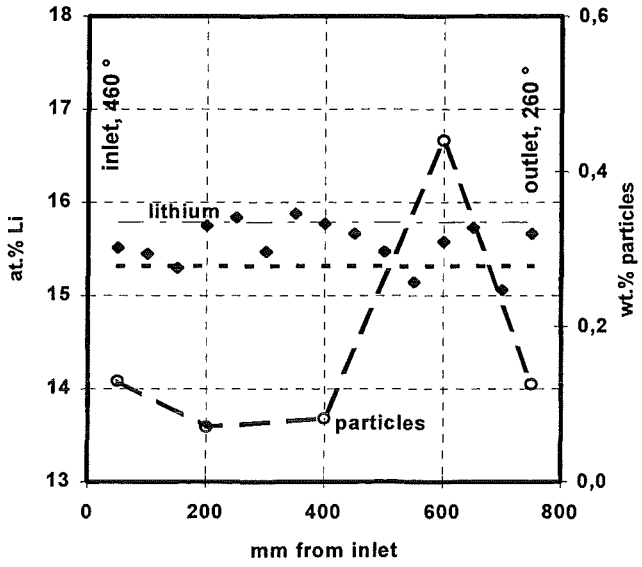

Fig.14 : Profiles of Li and particles in CT1 after phase V.

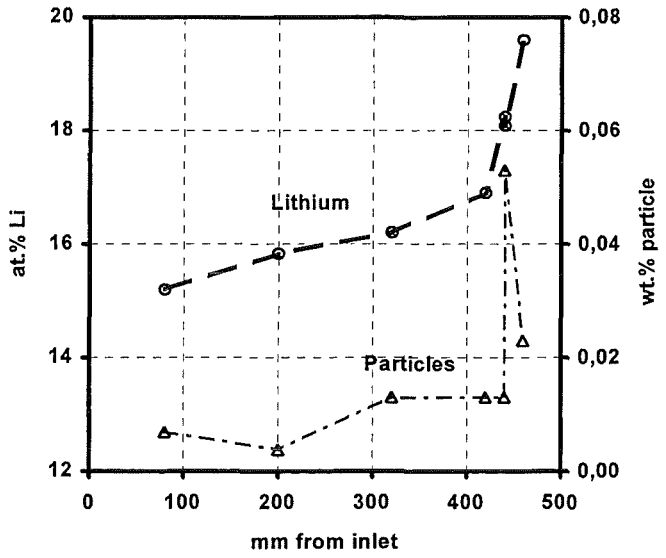

Fig.15 : Profiles of Li and particles in CT1 after phase VI.

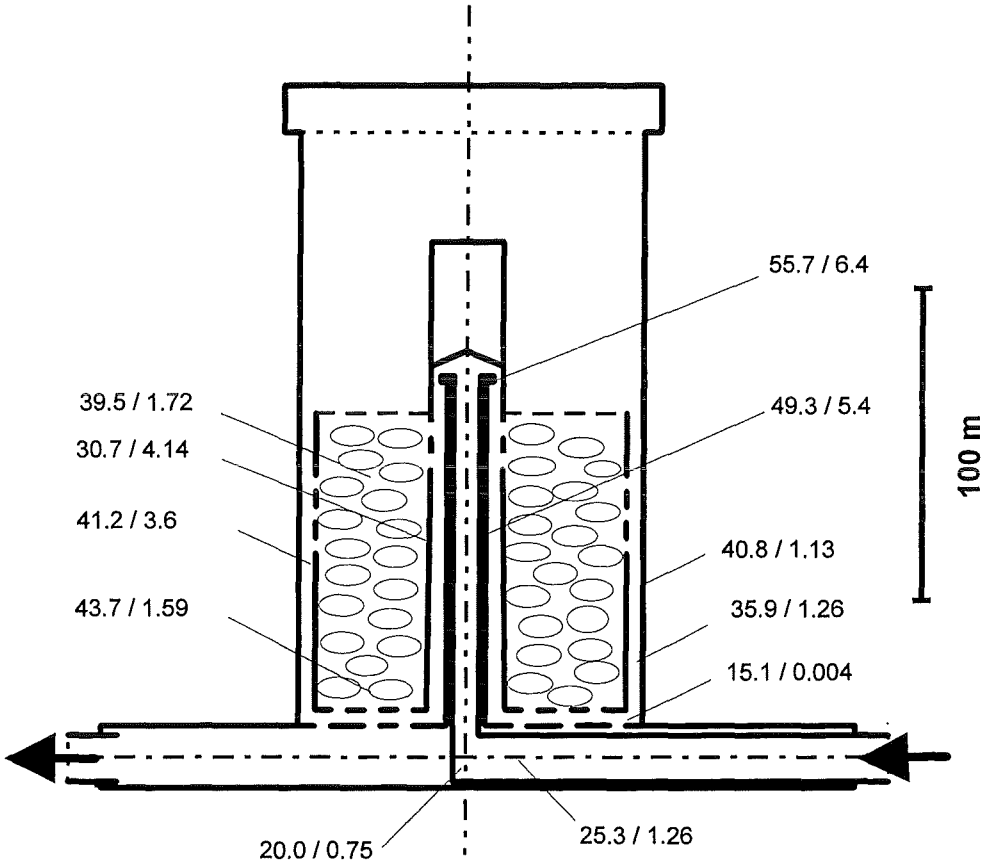

Fig.16 : Li and particles distribution in CT2 after phase V.
First number at.% Li, second number wt.% corrosion product particles.

To check a mass transfer model for corrosion products, CT2 in phase VI contained 1.7 m^2 ferritic steel wire mesh for deposition. The temperature difference between inlet and outlet was <1°C, the flow velocity 15 times lower than in main pipe. Along this cold trap the concentrations of Li and particles increased, **Fig.17.** Phase VI ended after 2398 hours because of a LiPb plug at the outlet of CT2. Fresh Pb-17Li was used in phase VI, excess LiPb deposited. Again, no deposited layers were found on wire mesh, only 2 grams particles deposited. This is a small fraction of total corrosion products.

To investigate deposition of corrosion products in crusts, CT2 with a very large LM-covergas interface was used in phase VII. It was operated at loop temperature (≥450°C). The phase was short, no deposits found.

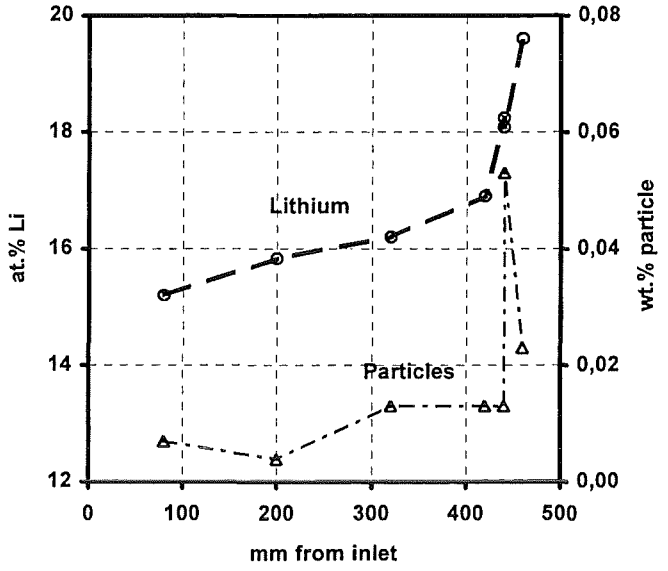

Fig.17 : Phase VI, CT2. Concentration of Li and corrosion products.

Cold trap 3

The lowest possible temperature in a system with molten Pb-15.8Li is the eutectic melting point 234 °C. Any excess of Li will deposit at the liquid/solid phase boundary in form of LiPb, a lead phase will be formed in case of an under-stoichiometric mixture [5] [6]. CT3 was an diffusion type cold trap with a solid phase of Pb-Li. A ferritic steel tube without LM flow was going out of the thermo box. It was used in phase VI and VII. Transport of impurities or lithium to the phase boundary was by diffusion.

Fig.8 showed the distribution of Li and Bi in CT3. The maximum Li concentration was 50 at.%, those of Bi 1.3 wt.% (!). No enrichment of steel elements has been seen. Particles are not expected to diffuse to cold spots. The high enrichment of Bi was expected from [9]. The migration of Bi is a rather fast process, as seen after less than 300 hours in gas pipes of CT2 after phase VII.

5.4 Deposition in magnetic fields

In chapter 4.3 is was shown that 78% of all particles were magnetic. Magnetic traps should therefore be effective. Magnetic fields of comparable intensity were at magnetic traps, electro magnetic flow meters, and in EMP.

A magnetic trap 1 was installed just before EMP. During phases I to V, MT 1 was a empty tube of TZM. Only 0.08 grams particles were found in MT1, together with 5.6 grams Li-Pb with (av.) 24 at.% Li. Similar, flow meters, tubes of vanadium, contained 0.2 grams particles. The most effective magnetic trap was EMP with the large ferritic core. 26 grams particles were deposited after phase V.

For phase VI and VII new MT1 were designed similar to EMP : a ferritic core in a vanadium capsule. They were effective, 3.6 grams particles were deposited, compared to 7.1 grams in EMP. Flow meters after Phase VII contained 1.1 grams particles.

Deposits in magnetic fields contained between 0.5 and 14 wt.% particles, nearly all magnetic. The main fraction however was as before a mixture of |LiPb+Pb-15.8Li|. MT1 was blocked at the end of phase VII mainly because of LiPb. But deposits in magnetic fields contained only 40% of all magnetic particles.

A second magnetic trap was installed behind cold traps in phase VI and VII. It was an empty vanadium capsule with a magnet at the top. CT's and MT2 were operated at loop temperature in phase VII. In 6.8 grams Pb-15.8Li, 0.2 grams particles were hanging there like stalactites.

5.5 Bath tube effect and other observations

Because of density differences, particles in molten Pb-15.8Li may ascend to the top, in case of TRITEX to LM-covergas interfaces. Crusts are formed at such positions. The fraction of non magnetic particles was higher than at other positions. But also crusts contained less than 3% corrosion product particles, the main fraction was always |LiPb+Pb-15.8Li|. In phase VII, a new CT2 was designed with a very large LM-steel-covergas interface. It could not be tested because the experimental program ended.

The small particle fraction floating around with Pb-15.8Li was drained to DT. Because of frequent drain during phase I to V, 6.8% corrosion products were found there.

Compounds like NiMn and $Ni_{1.22\text{-}1.90}V$ were found. They may be used only in some special cases to remove an element [19].

5.6 Discussion

Purification of the eutectic mixture Pb-15.8Li is possible with cold traps and in magnetic fields.

Lithium may cause problems. In all experimental systems Pb-17Li was filled in. The excess lithium was deposited in form of LiPb in traps and at other positions. Phase VI and VII ended because of blocking by LiPb. All deposits and crusts contained mainly a mixture of |LiPb+Pb-15.8Li| in different concentrations. Pure LiPb was found after phase V in CT2, after phase VII behind CT2, and in CT3. Pure Pb-15.8Li was the circulating mixture. In cold traps sometimes a concentration profile for Li was found. This may be a temporary effect, no profile was seen in CT1 after phase V. Probably LiPb particles were floating around, and deposition was dependent on fluid dynamics.

Oxygen transport to cold traps was seen after phase V. More oxides may have deposited in crusts at LM-covergas interfaces. Because of the low solubility oxygen should play no role in Pb-15.8Li systems.

Corrosion products. Except for a small fraction dissolved, corrosion products were found always in form of particles. Particles are probably formed in solution and grow when floating around. If particles are large enough they will deposit. Deposition occurs at positions with longer residence time and particles accumulate for example in cold traps and crusts. On the other hand particle deposition depends on fluid dynamics and is high at positions with high LM velocity (high Reynold's number), as observed in CT2 after phase V and in MT1 after phase VII. Even if 78% of all particles were magnetic, only 30% could be trapped in magnetic fields. There they stick firmly near the magnet, act as mechanical filters and catch non-magnetic particles and especially LiPb. Always particles were soldered together by |LiPb+Pb-15.8Li|.

In agreement with other experiments, Bismuth can easily be removed from Pb-15.8Li with a simple device like CT3. No enrichment of any other element in purification devices has been seen.

6. Other effects

Many effects were observed during TRITEX operation. Only a few will be described in this chapter.

6.1 Residue film

Whenever possible, drain was done at higher temperatures. But there remained still a film of Pb-15.8Li on surfaces. At 477°C drain temperature (phase V) 87 ± 61 mg/cm^2 were found. The wide scattering shows that there is not a homogeneous film. This effect has to be considered when draining a system. In TRITEX nearly 1 kg Pb-15.8Li were not drained, 1% of the inventory[7]. That also
44 ± 5 mg/cm^2 LiPb were found at deposition rings in CT1 after phase V should be considered as a curiosity.

The residue film corresponds to 90±61 μm thickness. It is amazing that for sodium a similar thickness for an remaining film was reported [28]. The mg/cm^2 values for sodium are of course 10 times lower.

6.2 Lithium in steels

Swelling of steels in Pb-15.8Li was only observed for of armco iron. However at least lithium is dissolving also in steel 1.4922. If cleaned and etched samples were kept for a longer time in air, a haze of white lithium oxides appears at the surface. Bulk concentrations of Li or Pb in

[7] In batch type experiments, 45 ± 12 mg/cm^2 were found at walls.

such samples were below 0.01 wt.%. This effect is well known for sodium systems, but it was never reported for Pb-15.8Li.

6.3 Others

For safety considerations two effects will be mentioned again.

1. Samples with high Li-concentrations dissolve in oxidizing acids often under sparks and fire effects. Such samples reacted also with humidity, forming hydrogen.
2. Aerosol deposits were metallic and reacted with humidity of air. Deflagration of hydrogen, colored by lithium, was observed several times.

Because of small mass of deposits this caused never a hazard. In larger systems one should consider such effects.

7. Summary and conclusions

The ferritic steel loop TRITEX was operated for 13000 hours with eutectic Pb-15.8Li. Many features were comparable to ITER blankets. For example : The ratio mass of Pb-15.8Li to steel surface, corrosion products were produced from the corroding loop surface, and the loop was operated non-isothermal.

Wetting
Because of long operation times at higher temperatures, good wetting of Pb-15.8Li to materials was observed in TRITEX. Even narrow gaps in MT and EMP were filled with the eutectic. Inspite of an TZM liner, Ni was leached out from austenitic steel. However, leaching of Ni did not need good wetting, as seen in EMP after phase VII. Drain of Pb-15.8Li left a residue film of 87 mg/cm^2 on surfaces. In TRITEX 1 kg or 1% of the inventory were not drained.

Structural materials in Pb-15.8Li
Generally structural materials showed the expected behavior in the eutectic mixture. Only with α-iron a volume swelling by 5% was observed, an effect not described before. The outside of materials was in air. During the reaction of steel 1.4922 with humidity hydrogen was formed, causing a H_2 background in all covergas spaces. This has to be considered in experiments with low concentrations of deuterium or tritium.

Lithium
Li is a component of the eutectic mixture and not considered as an impurity. But this element may cause serious problems when operating a system like TRITEX. At the beginning of the experimental program the eutectic concentration was given to be 17 at.%. Mixtures with this concentration were filled into the loop. The Li excess precipitated as LiPb with a melting point of 482 °C. This compound was found in all crusts and deposits and caused several times flow-blocking. Not all observations of the behavior of Li and LiPb could be explained. The Li concentration should be controlled carefully, and components should be large enough to avoid blocking because of LiPb. Also freeze valves must have a possibility to be heated higher than 482 °C.

Lead

Pb is the other component of the eutectic mixture. In TRITEX about 10 gram lead were found. It was formed by rectification during evaporation, metallic beads of Pb dropped to the eutectic and got transported around. Even if the found total amount was small, lead has to be considered at positions with narrow gaps and temperatures below 327°C.

Corrosion products

In TRITEX 118 grams of corrosion products were formed. The corrosion rate was in agreement with the literature. The chemistry of corrosion products was complex. 95% were found in form of four different kinds of particles with chromium concentrations between 7 and 89 wt.%. On the other hand compounds like NiMn and $Ni_{1.22\text{-}1.9}V$ were seen in TRITEX. The widely scattered ratios of Ni/Mn or V/Mo in particles point also to other compounds. The amount of vanadium in the loop was lower than expected from corrosion. Mass transfer, e.g. to TZM has to be assumed. The amount of Ni was higher than expected because of Ni-leaching from austenitic steel, in spite of a TZM liner.

Other impurities

Oxides were merely formed at liquid Metal-covergas interfaces. Only a small amount of **oxygen** was transported to cold trap. **Carbon** was seen in samples from crusts, but this element was not investigated in detail. **Bismuth** moved to cold spots, while the concentrations of Cu, Ag and Zn in circulating Pb-15.8Li were unchanged. Only the concentration of Cd was reduced because of evaporation.

Purification methods

Because of the density difference to the eutectic mixture, a fraction of particles floated to liquid metal/covergas interfaces. Different kinds of **cold traps** trapped more that 50% of corrosion product particles. This was an effect of hydraulic conditions and not of temperature. Even if 78% of particles were magnetic, only 30% could be trapped in magnetic fields. Different **magnetic traps** were tested, most effective was an arrangement as in EMP : a ferritic core in a vanadium (or TZM) capsule.

All purification devices were also effective for the deposition of LiPb. Always more than 90% of all deposited material was | LiPb+Pb-15.8Li| . This has to be kept in mind when designing traps. They have to be large enough to avoid blocking because of Li-Pb deposits. A simple diffusion type cold trap was very effective removing excess Li and also Bi from the eutectic. Because freeze valves are such cold traps, they must have a possibility to get heated higher than 480 °C, the melting point of LiPb.

Aerosols

Even if evaporation rates of Li and Pb are small, deposits were found in all covergas spaces. Aerosols can easily be trapped. The deposited amount drops by a factor of 100 within 200-300 mm from evaporating surfaces. On the other hand the lithium concentration increases along the transport path. In filters up to 93 at.% Li (31 wt.% !) were found. Aerosol deposits were metallic and reacted with oxygen and humidity. Deflagration of hydrogen, colored by lithium, was observed several times when opening components. Because of the small mass of deposits this caused never a hazard. The formation of a lead phase was discussed before. Besides Li and Pb only cadmium was seen in aerosol deposits. Nearly all Cd was evaporated from Pb-15.8Li.

Part II

Investigation of components

Table of Contents

List of tables and figures 37

1. Phase IV **40**
1.1 Magnetic Trap and Flow Meters
1.2 Cold Trap 2
1.3 Test Section

2. Phase V **41**
2.1 Magnetic Trap
2.2 Flow Meters
2.3 Electro Magnetic Pump
2.4 Cold Trap 1
2.5 Cold Trap 2
2.5.1 Tank
2.5.2 Basket
2.6 Valves
2.7 Sampling Station and Expansion Tank
2.8 Test Sections
2.9 Drain Tank

3. Phase VI **44**
3.1 Magnetic Trap 1
3.2 Magnetic Trap 2
3.3 Cold Trap 1
3.4 Cold Trap 2
3.5 Cold Trap 3
3.6 Valve 7

4. Phase VII **46**
4.1 Magnetic Trap 1
4.2 Magnetic Trap 2
4.3 Flow Meters
4.4 Electro Magentic Pump
4.5 Cold Trap 1
4.6 Cold Trap 2
4.7 Cold Trap 3
4.8 Valves
4.9 Sampling Station, Expansion Tank and Test Section
4.10 Drain Tank

Tables **49**
Figures **71**
References **105**
Acknowledgment **106**

List of tables

Table 1 : Operation phases of TRITEX.

Table 2 : Materials in contact with Pb-15.8Li.

Table 3 : Analysis of as received bars. Average concentrations.

Table 4 : Analysis of Pb-15.8Li, taken during operation.

Table 5 : Composition of particles from crusts and deposits.

Table 6 : Composition of magnetic particles.

Table 7 : Composition of non-magnetic particles I.

Table 8 : Composition of non-magnetic particles II.

Table 9 : Composition of non-magnetic particles III.

List of Figures

Fig.1 : Operation Phase I to IV.

Fig.2 : Operation Phase III and IV.

Fig.3 : Phase IV. Basket of cold trap 2, filled with rings of steel 1.4922.

Fig.4 : Phase IV. Aerosol deposits in test section.

Fig.5 : Phase IV. Permeation membrane of test section with crusts.

Fig.6 : Operation Phase II to V.

Fig.7 : Phase V , magnetic trap 1, about 3x.

Fig.8 : Phase V , magnetic trap 1. Metallographic examination.

Fig.9 : Operation Phase III to V.

Fig.10 : Phase V. Looking into the tube of flow meter 1 after melt-out.

Fig.11 : Phase V, vanadium tube of flow meter 2. Metallographic examination.

Fig.12 : Phase V, flow meter 1. Particles of $Ni_{1.2\text{-}1.9}V$.

Fig.13 : Operation Phase I to V.

Fig.14 : Phase V, TZM tube of electro magnetic pump inlet.

Fig.15 : Phase V, ferritic core of electro magnetic pump inlet.

Fig.16 : Phase V, core of electro magnetic pump. Corrosion product particles.

Fig.17 : Phase V. Cold trap 1 and cold trap 2 after phase V.

Fig.18 : Temperature profile in cold trap 1, 1990.

Fig.19 : Phase V. Sections of cold trap 1.

Fig.20 : Phase V. Cold trap 1, distribution of Li and corrosion products.

Fig.21 : Phase V. Outlet cold trap 1. Dendrites and corrosion product particles.

Fig.22 : Phase V. Cold trap 1 inlet. Metallographic and SEM picture.

Fig.23 : Phase V. Cold trap 1 outlet. Microprobe analysis.

Fig.24 : Operation phase V.

Fig.25 : Phase V. Cold trap 2. Results.

Fig.26 : Phase V. Cold trap 2. Tank without basket.

Fig.27 : Phase V. Cold trap 2, dome.

Fig.28 : Phase V. Cold trap 2. Dome, metallographic examination.

Fig.29 : Phase V. Cold trap 2. Basket with deposition rings.

Fig.30 : Phase V. Stem of valve 5 with crusts.

Fig.31 : Phase V. Photo of expansion tank and sampling station 1.

Fig.32 : Phase V. Permeation membrane of expansion tank.

Fig.33 : Operation phase IV and V.

Fig.34 : Phase V. Drain Tank.

Fig.35 : Operation phase VI.

Fig.36 : Phase VI. Cold traps and magnetic trap 2 .

Fig.37 : Phase VI. Part of cold trap 1, outlet.

Fig.38 : Phase VI. Cold trap 1 and wire mesh filled chamber.

Fig.39 : Phase VI. Cooler, CT1. Distribution of Li and corrosion products.

Fig.40 : Phase VI. Cold trap 2.

Fig.41 : Phase VI. Wire mesh packing of cold trap 2.

Fig.42 : Phase VI. Cold trap 2. Distribution of Li and corrosion products.

Fig.43 : Phase VI. Cold trap 3. Distribution of Li and Bi.

Fig.44 : Phase VI. Cold trap 3. Axial cut , after 5 hours at room temperature.

Fig.45 : Operation Phase VII.

Fig.46 : Phase VII. Magnetic trap 1 in TRITEX.

Fig.47 : Phase VII. Cross section of magnetic trap 1 near inlet.

Fig.48 : Phase VII. Magnetic trap 1.

Fig.49 : Phase VII. Concentration of Li in magnetic trap 1.

Fig.50 : Phase VII. Arrangement of magnetic trap 2.

Fig.51 : Phase VII. Deposits in magnetic trap 2.

Fig.52 : Operation Phase VI+VII.

Fig.53 : Phase VII. Axially cut of flow meter 1.

Fig.54 : Phase VII. Particle deposition in flow meter 1.

Fig.55 : Phase VII. Cold trap 2 after phase VII. Closed and cut open.

TRITEX was operated in 7 operation phases for 13003 hours, **Table 1**. More details are given in [3]. At the end of an operation phase and drain of the eutectic mixture, components were investigated. Three kinds of deposits were found : Crusts at liquid metal-covergas interfaces, deposits in magnetic traps, flow meters, EMP and cold traps, and aerosol deposits in covergas spaces. As described in **Part I**, four kinds of corrosion product particles were identified: magnetic and non-magnetic 1 to 3. Non-magnetic particles 3 were found only in a few samples, the amount was very small.

No detailed analysis was done after phases I to III. Looking especially for corrosion products and other impurities started with phase IV. **Table 2** shows a list of materials in contact with the eutectic mixture, **Table 3** the analysis of as received Pb-17Li. All reliable results from TRITEX are compiled in **Tables 4** to **9**.

1. Phase IV

Only a few components were replaced after phase IV.

1.1 Magnetic Trap and Flow Meters

MT1 and FM's were operated in phase I to IV, **Fig.1**.
MT1 had in the range of the magnet a TZM liner in an austenitic steel tube (1.4301) with an inner diameter of 15 mm, welded to 1.4922. FM's were tubes from vanadium, inner diameter 12 mm. Vissible deposits were removed mechanically and analyzed. The Li concentration was in the range of the eutectic mixture, the main fraction of particles in FM's was magnetic.

1.2 Cold Trap 2

CT2 was operated in phase III and IV, **Fig.2.**

CT2, **Fig.3,** was filled since phase III with rings from steel 1.4922 for deposition. Some construction details are given in chapter 2.5. The basket was removed, rings, crusts and aerosol deposits analyzed. Crusts, as usually gray to black, contained 50 at.% Li and 10 wt.% corrosion product particles, half of these magnetic. Rings were covered with a clean metallic layer of LiPb with 55 at.% Li. This layer contained also 11 wt.% corrosion product particles. They were analyzed as one fraction, not dividing in magnetic and non-magnetic particles. In the covergas space small beads of lead were seen, but lead was also found below the LM level. The lead formation was discussed in Part I.

1.3 Test Section

TS was operated in phase I to IV, **Fig.1.**

Fig.4 shows a drawing with results from analysis, **Fig.5** a photo of the permeation membrane with crusts. Besides crusts, aerosol deposits were investigated, as discussed in Part I.

2. Phase V

After phase V all loop components were investigated.

2.1 Magnetic Trap

MT1 was operated in phase II to V, **Fig.6**

Only one MT was used in TRITEX during phase I-V. MT1 had in the range of the magnet a TZM liner in an austenitic steel tube (1.4301) with an inner diameter of 15 mm, welded to 1.4922. Still filled with Pb-15.8Li, MT1 it was cut open axial, one side for chemical analysis, the other for metallographic examinations.

Fig.7 shows, that the steel 1.4922 was overlapping TZM by 1 cm, but also that there was a gap of 20 µm between TZM and steel. This gap was filled with eutectic mixture, **Fig.8**. A ferritic layer was formed on the austenitic steel, showing the effect of Ni-leaching [15]. Pb-15.8Li was a solder between TZM and steel with good wetting. It clearly exchanged with the circulating mixture, otherwise the thickness of the ferritic layer could not be explained. Not much deposits were found in MT1, not even near the magnet.

2.2 Flow Meters

Both flow meters were operated in phase III to V, **Fig.9.**

Both electromagnetic flow meters were tubes from vanadium, inner diameter 12 mm. They remained filled after phase V.

FM1 was molten out under argon. The melt-out material contained 15.5 at.% Li and only 0.002 wt.% steel components. FM's trap magnetic particles like MT. After melt-out a solid body remained at the positions of the magnet, **Fig.10,** with 5 wt.% metallic particles, mostly magnetic. Amazing was the low Li concentration in these deposits, pointing to deposited lead. But Pb should not dissolve in 2% acetic acid+0.5% H_2O_2, as used for this samples. The effect can not be explained.

FM2 was used for metallographic examination, only a few small samples were analyzed. Also a micro-hardnes profil of vanadium was measured (Part I). **Fig.11** shows no reaction zone on vanadium. Microprobe analysis showed near the vanadium surface small particles embedded in Pb-15.8, **Fig.12,** consisting of a compound $\mathbf{Ni_{1.2\text{-}1.9}V}$. Compounds like this are possible in the system Ni-V [20]. The chemical activity C/C_s of Ni in the eutectic was only 0.005 [15], that of V near the surface probably 1. The Ni-V compound therefore must be very stable.

2.3 Electro Magnetic Pump

EMP was operated in phase I to V, **Fig.13.**

It was of the same construction as MT1 : a TZM liner in an austenitic steel tube, welded to steel 1.4922. The core of steel 1.6770 was 775 mm long with an diameter of 52 mm. The annular gap was 2 mm wide.

Also EMP remained partly filled at the end of phase V. It was molten out in air. The average Li concentration in the molten out mixture was 13±1 at.%. Probably during melt-out the mixture was partly oxidized and only the remaining metal analyzed. The concentration of particles was between 0.001 and 0.005 wt.%. After melt-out EMP was cut open, tube and ferritic core analyzed separately.

Not much material was deposited in the TZM tube, **Fig.14,** merely Pb-15.8Li droplets are visible. Nevertheless because of the large surface, 6.25 grams of lithium-lead with 0.8 grams mainly magnetic particles were found.

Much more material was found at the ferritic core, **Fig.15**. 184 g with 14 wt.% particles contained more than 25 grams corrosion products. Again nearly all particles were magnetic. The high concentration of particles can be seen in **Fig.16.**

2.4 Cold Trap 1

Fig.17 shows a photo of the arrangement of Cold Traps. CT1 (cooler) was unchanged between phase I to V, **Fig.13**. After phase V the cooler remained partly filled with Pb-15.8Li.

CT1 was an 0.72 meter long 8 mm wide annular gap. The LM cross section was 23 cm^2, the volume 1750 cm^3, about 5000 cm^2 steel 1.4422 were in contact with molten Pb-15.8Li. Compared to main pipes the flow velocity in the cooler was 13 times lower. The temperature profile is shown in **Fig.18**. Supersaturation of dissolved metals will occure along CT1, deposits there were expected.

After removing thermal insulation, heater and cooling rips, CT1 was cut into 11 pieces, the smaller disks investigated chemically and by metallography, **Fig.19 .** Results of chemical analysis are shown in **Fig.20**. The Li concentration was within analytical errors in the range of the eutectic (average 15.6 at.%). About 0.1 wt.% particles of corrosion products were found, with one value as high as 0.44 wt.%. 28 grams corrosion products were deposited in the cooler.

Metallography of CT1 samples were done by Mrs.Echtle[1]. During solidification lead-rich dendrites are formed in the eutectic. The amount depended on temperature and cooling rate. While the average Li concentration was constant at all temperatures, dendrites were seen at the low-temperature side (outlet). There was the lowest cooling rate. An example is shown in **Fig.21.** Spherical metallic particles of corrosion products were found mainly near steel surfaces, **Fig.22,** other forms only in the low temperature range range of CT1, **Fig.21.** Microprobe analysis showed at least three different Cr to Fe ratios in particles, **Fig.23.**

Profiles of Li and corrosion products were seen in the tube between CT1 and CT2. The outlet of CT1 was comparable to CT1. At the inlet to CT2, 53.3 at.% Li and 9.5 wt.% particles were found.

[1] Mrs.Echtle, Universität Karlsruhe, Institut für Werkstoffkunde 1

2.5 Cold Trap 2

CT2 was opened after phase IV (1.2), most deposits removed mechanically and analyzed, deposition rings replaced. Then it was operated in phase V, **Fig.24.**

CT2 was considered to have no temperature profile. It consisted of a tank and a basket, filled with deposition rings of 1.4922, **Fig.25.** The eutectic mixture is coming from CT1, bottom right, flowing through a dome to above the basket, through the basket and out to the main loop, bottom left. The LM cross section in the basket was 67 cm^2, the volume 570 cm^3, about 1500 cm^2 steel were in contact with molten Pb-15.8Li. Compared to main pipes the flow velocity was 40 times lower. The analysis of cold trap samples was difficult. Because of high Li concentrations a fraction of particles were dissolved even in 2% acetic acid+0.5% H_2O_2. Often it was not possible to distinct between different kinds of particles.

2.5.1 Tank

Fig.26 shows a photo of the **tank** after removing the basket. Sampling positions and results are shown in **Fig.25**. Besides crusts at the wall, the dome was partly filled, **Fig.27**. Furthermore the bottom was covered with Pb-15.8Li from drain. (Average Li concentration there 15.1 at.%, concentration on corrosion products 0.004 wt.%.) Only small amounts of crusts from the wall could be gained, with 38.5 at.% Li and 1.2 wt.% corrosion products. In the dome the Li concentration was going up from 20 at.% at the inlet to 56 at.% at the top, the concentration of metallic particles from 0.8 to 6.4 wt.%. Even if some oxides may be lost during preparation, at least the main fraction was metallic Pb-Li, as seen after preparation by Mrs. Echtle, **Fig.28.**

2.5.2 Basket

Deposition rings, **Fig.29** were metallic clean with 44±5 mg/cm^2 deposit, a value in the range of that for the whole loop. The drain temperature of CT2 after phase V was nearly 400°C [3]. Inspite of the high Li concentration up to 44 at.%, there was clearly a metallic layer at the surface of rings. 1.6 wt.% particles were found in this layer at all positions. (In the dome up to 1 gram/cm^2 were deposited, with up to 6.4 wt.% particles !)

2.6 Valves

Valves were operated in phase I to V, **Fig.13.**

Valves 3, 5 and 6 were investigated[2]. More than 95% of crusts were found at stems, less than 5% at tubes, **Fig.30**. Aerosol deposits were measured at V3 and V6 (Part I). The Li concentration in crusts was higher than 50 at.%, showing that a fraction was oxidized. The low fraction of magnetic particles on V6 may be an analytical error, the ratio NM1/NM2 was the same as in other crusts.

2.7 Sampling Station and Expansion Tank

ET and SS's were operated in phase III to V, **Fig.9.**

Not much crust material was in tanks of SS1 and ET, **Fig.31,** more was found in SS2 and at the permeation membrane of ET, **Fig.32**. The concentration of particles was between 3 and 7.6 wt.%. No detailed analysis was performed.

[2] Valve 5 was until phase V located behind CT2. No V5 was installed in phases VI and VII.

2.8 Test Sections

TS were operated in phase IV and V, **Fig.33.**

Two TS with permeation membranes were installed in phase IV. Between TS1 and TS2 was a chamber with vanadium wire. Only small amounts of crusts were found, with about 1 wt.% of particles. Not much investigations were done.

2.9 Drain Tank

DT was operated in phase I to V, **Fig.13.**

TRITEX was drained during phases I to V about 10 times. Always a fraction of corrosion products and other deposits were washed down from loop surfaces. Thick crusts were seen, **Fig.34,** and a larger amount of corrosion product particles found in DT. Four kinds of deposits were analyzed. In the upper part, a thin layer of light gray material was deposited (A). In the middle part, the layer was thicker and more dark (B). Then a narrow crust was seen (C). Finally above the Pb-15.8Li surface a thick crust was deposited (D). Crust D contained droplets of the eutectic mixture. In addition there was a thin layer of oxides at the eutectic surface. This thin layer contained only 0.001 wt.% particles. Deposits A to D were analyzed separately. Furthermore aerosol deposits in covergas spaces were investigated (Part I).

3. Phase VI

Before phase VI; the whole loop was cleaned and new eutectic mixture with 17 at.% Li filled in the drain tank [3]. A new magnetic trap 1 and a second magnetic trap were constructed and installed. Completely new cold traps CT1 and CT2 and a diffusion type CT3 replaced the old system. After phase VI mainly these traps were investigated, all operated only in phase VI, **Fig.35.**

3.1 Magnetic Trap 1

More details of MT1 are given in chapter 4.1 It consisted of a 98 mm long and 18x35 mm wide vanadium capsule, welded on both sides to steel 1.4922. Inside was a core of ferritic steel. The total amount of deposited material was 2.7 grams, with about 1 wt.% particles. MT1 did not act as a magnetic trap, a large fraction of particles was non-magnetic !

3.2 Magnetic Trap 2

MT2 behind the cold traps did not contain any visible deposits. Only a thin film of Pb-15.8Li remained. No investigations were done.

3.3 Cold Trap 1

The new cold traps can be seen in **Fig.36,** a drawing of CT1 in **Fig.37.**

CT1 was an 0.75 meter long tube, outer diameter 140 mm, heated by a heat road in the center and cooled from the outside by air. Pb-15.8Li was flowing through an annular gap of 6 mm to a chamber, 50 mm in diameter and 45 mm high. From the bottom of the chamber it was flowing through another annular gap to the next chamber, and so on. There were 7 chambers along CT1, each with a thermo couple. **Fig.38** shows this arrangement, the temperature profile was as shown in **Fig.18.** Each chamber contained 48 grams of ferritic steel 1.4937 [3] wire, with a surface of 125 cm^2 . The liquid metal cross section in the gap was 24 cm^2, in the chamber 20 cm^2, flow velocities 1/13 resp. 1/11 of those in main pipes. All construction material was 1.4922.

Similar as described under 2.4, CT1 was cut into sections and analyzed. This was more difficult than before. In chambers, particles were adhering to wire surfaces. For analysis they were separated under a stereo-microscope. Other samples were taken from annular gaps.

Fig.39 shows the distribution of Li and corrosion products in CT1. The Li concentration was increasing from 15.1 to 16.4 at.% . This was different from CT1 after phase V (**Fig.20).** The average value is the concentration of the eutectic mixture, 15.8 at.%. The average particle concentration was 0,13 wt.%, **18.5 grams** corrosion products were deposited in the cooler.

3.4 Cold Trap 2

The new cold traps can be seen in **Fig.36,** a drawing of CT2 in **Fig.40.**

To check a model for corrosion product deposition, an isothermal CT2 with **1.7 m^2** deposition surface of ferritic steel was build. A tube with 58 mm diameter was filled with wire mesh of steel 1.4104 [4], **Fig.41.** The flow velocity was 1/15 of those in main pipes. Heating was done from outside, in the center was a thimble with 10 thermo couples. CT2 was operated most of the time at 260 ±1°C, **Fig.35.** A Philips KS4290 controller was used to keep the temperature between inlet and outlet constant.

Phase VI ended because of the blocked cold trap system. CT2 remained filled with Pb-15.8Li after drain. The outlet pipe was molten out in a glove box. An one cm long plug of LiPb remained. While the Li-Pb mixture in the inlet pipe contained 16.3 at.% Li (compare **Fig.39),** 48.0±1.0 at.% Li were found in the plug.

Because of wire mesh, analysis was again difficult. CT2 was cut in 25 disks. Many samples were analyzed. The Li concentration was increasing from 15.2 to 19.6 at.%, even stronger than in CT1, **Fig.42.** Values for corrosion products were scattered over a factor of 10. The average particle concentration was 0.018 wt.%, **2.2 gram's** corrosion products were deposited.

---

[3] Steel X25CrMoV 12 1. Analysis Cr :12.0%, Mo:1.0%, Mn: 0.6%, Ni:<1%, V:0.3%, (W:0.5, Si :0.4%, S:0.015 %).

[4] Steel X12CrMoS17.Analysis Cr :13.6%, Mn: 1.8%, Mo:0.25%, Ni:044%, (Si :1.0%, S:0.15-0.25%). CT2 with this steel was operated only at low temperature.

3.5 Cold Trap 3

The lowest possible temperature in a system with molten Pb-15.8Li is the eutectic melting point 234 °C. Any excess of Li will deposit at the liquid/solid phase boundary in form of LiPb, a lead phase will be formed in case of an under-stoichiometric mixture [5][6]. Bismuth (and Po-210) were also found deposited at this position [9][24]. Freeze valves in TRITEX were such components with a solid phase.

A diffusion type cold trap, CT3 was installed between main heater and expansion tank : a loop pipe was going out of the thermo box. There was no liquid metal flow in this pipe, transport of impurities or lithium to the colder part was by diffusion. The solid phase, point 234 °C, was 390 mm from flowing Pb-15.8Li.

Fig.43 shows the distribution of Li and Bi in CT3. The maximum Li concentration was 50 at.%, those of Bi 1.3 wt.%. No enrichment of steel elements has been seen. Corrosion products are mainly in particles, which do not diffuse to colder positions.The oxidation rate of Pb-Li mixtures at room temperature in air depend on the Li concentration. **Fig.44** shows this for the low temperature part of CT3. Areas with higher Li concentration oxidizes faster, even the 'minima' of **Fig.43** are visible.

3.6 Valve 7

There was an air leak in V7, causing the formation of 1.46 grams oxide crusts. As expected for oxides the Li concentration was between 17.5 and 76 at.%, [13]. The total amount of particles was 22 mg, only some small fractions contained up to 4.2 wt.%. No detailed analysis was done.

4. Phase VII

Cold traps and magnetic traps were new in phase VII. CT2 was a new design. Phase VII ended because of blocked MT1 and FM1. Because of the end of the experimental program, nearly all components were investigated as before.

4.1 Magnetic Trap 1

MT1 was operated in phase VII, **Fig.45.** At the end of phase VII, MT1 was blocked.

MT1 was of the same design as in phase VI. **Fig.46** shows the installation in TRITEX. It consisted of a 98 mm long and 18x35 mm wide vanadium capsule, welded on both sides to steel 1.4922. Inside was a ferritic core. **Fig.47** shows a foto of an cross section. The flow velocity was about the same as in main pipes.

While the inlet side of MT1 was filled with | Li-Pb+particles| , the outlet side was only partly filled. MT1 was cut through at the position of the magnet, **Fig.48.** At the upper and lower rim vanadium was machined away. Samples for analysis were taken at 15 positions.

As in other parts of TRITEX LiPb was deposited in MT1. The main flow is passing through the bottom part, **Fig.47.** The Li concentration there was lower than in the upper range, **Fig.49.** The mixture there contained more Pb-15.8Li. The concentration on particles in deposits reflects the flow distribution : 2.1 wt.% in the upper and 4.0 wt.% in the lower part of CT1. Because of higher flow rate more particles were transported.

No detailed particle analysis was performed, but all contained 3±1wt.% chromium, showing that more than 90% were magnetic. The total amount of corrosion product particles in MT1 was 3.4 grams, more than in any magnetic trap or flow meter before.

4.2 Magnetic Trap 2

MT2 was was located behind cold traps, it was operated in phase VII, **Fig.45.** It constisted of a vanadium capsule without core, the magnet was fixed on the top, **Fig.50.** Only below the magnet were deposits, **Fig.51.** 0.18 grams corrosion products were deposited, all of them magnetic.

4.3 Flow Meters

As described before electromagentic flow meters were vanadium tubes with 12 mm diameter. They were operated in phase VI+VII, **Fig.52.**

FM1 was blocked after phase VII like MT1. It was axially cut, **Fig.53.** One half was for chemical, the other for metallographic investigations. 0.94 grams of corrosion products were deposited, nearly all magnetic. **Fig 54** shows, that the particles are distibuted in deposited LiPb/Pb-15.8Li.

Deposits in **FM2** were at magnet position, similar as seen in **Fig 10.** 0.12 grams particles with the same composition as in FM1 were found.

4.4 Electro Magnetic Pump

EMP was operated in phase VI+VII, **Fig.52.**
EMP was of the same construction described before : a TZM liner in an austenitic steel tube, welded to steel 1.4922. The core of steel 1.6770 was 775 mm long. with an diameter of 46 mm. The annular gap was increased to 5 mm. EMP was analyzed by the same way as after phase V. The only seen difference was that after phase VII, TZM and austenitic steel were not soldered together (poor wetting), but a ferritic zone because of Ni-leaching was also formed.

Again, the main fraction of particles was found at the core, alltogether 6.4 grams. In the tube only 0.71 grams were found. The composition was comparable to particles in MT's and FM's.

4.5 Cold Trap 1

CT1 was operated in phase VII, **Fig.45.** It was described in chaper 3.3. A reduced investigation program was performed. About 2 grams corrosion products were deposited.

4.6 Cold Trap 2

Also CT2 was operated only in phase VII. Always a large fraction of corrosion product particles were at boundaries liquid metal-steel-covergas. A new CT2 with a large boundary was installed, operated as before isothermally. The liquid metal-steel-covergas line was increased to 750 cm, compared to CT2 in phase I to V of only 50 cm, and that the main loop of 170 cm. **Fig.55** shows CT2, the liquid metal-covergas line was in the center of the small tubes. Unfortunately phase VII was short because of blocking. After phase VII the whole program ended.

CT2 was operated mainly at loop temperature. As can be seen no deposits were in CT2. The Pb-15.8Li at the bottom contained 15.2 at.% Li and only 0.004 wt.% corrosion products. Both values are well in the range of all Pb-15.8Li samples.

At the beginning of operation CT2 was accidentally filled up to the gas pipes. These go out of the thermo box, and had a liquid/solid metal interface. The pipes remained partly filled. As in CT3 up to 42.9 at.% Li and up to 3 wt.% Bi were found in these plugs. The pipes were filled for less than 300 hours, this shows the efficiency of the system cold trap 3.

4.7 Cold Trap 3

CT3 was cut open as before and analyzed. All results of chapter 3.5 were confirmed.

4.8 Valves

Valves 3, 4 and 7 were investigated as before, crust deposits analyzed. V7 was operated in phase VII, **Fig.45**, V3 and V4 were operated in phase VI+VII, **Fig.52**. Crusts from all valves contained a large fraction of non-magnetic particles with high chromium content. Valve 6 was only visually inspected, it was similar to V3.

4.9 Sampling Station, Expansion Tank and Test Section

The appearance of SS, ET and TS was as described before. All were operated in phase VI+VII, **Fig.52.** Deposited crusts were analyzed. As in valves the fraction of non-magnetic particles was high.

4.10 Drain Tank

Also DT was operated in phase VI+VII, **Fig.52.** The appearance was as shown in **Fig.34**, with thinner crusts. No distiction between different positions as in chapter 2.9 was made. The total amount of corrosion products in DT is only 70 mg, compared to more than 5 grams after phase V. Remarkable in all DT deposits is the high concentration on Ni and Mn. Probably the compound NiMn [18][19] was washed down from the loop.

Tables

Table 1

Operation phases of TRITEX.

Phase I	960 hours	June 26, 1989	-	August 5, 1989
Phase II	1866 hours	September 14, 1989	-	December 1, 1989
Phase III	483 hours	August 1, 1990	-	August 21, 1990
Phase IV	3143 hours	November 12, 1990	-	March 22, 1991
Phase V	3431 hours	October 28, 1991	-	March 19, 1992
Phase VI	2398 hours	August 2, 1994	-	November 10, 1994
Phase VII	722 hours	October 31, 1996	-	December 12, 1996

Table 2

Materials in contact with Pb-15.8Li.

1.4922 : (different companies) About 1.2 m^2 wetted surface were from this steel. Own analysis in wt.% : Cr-12.1, Ni-0.31, Mn-0.53 , Mo-0.54, V-0.30, Cu-0.07 and Si-0.37.

1.6770 : 0.13 m^2, core of the EMP, similar to 1.4922, but only 2 wt.% Cr
1.4104 : 1.7 m^2, wire mesh of CT2 in Phase VI, similar to 1.4922*

Vanadium 99.5 : Less than 160 cm^2 wetted surface. Mainly used in MT's and FM's, in phase IV and VII also in TS2. Analysis as specified, Kelpin or GoodFellow company

TZM : 0.13 m^2 wetted surface (EMP). It was used as tubes for EMP, MT, and FM's. TZM is an alloy with Mo-99.5%, Ti-0.5%, Zr-0.08%, Cr-0.02%. Chemically similar to pure Mo, but with a better workability. It was always used instead of pure Mo.
Analysis as specified , PLANSEE, Reuthe, Austria

Fe-99.6 (armco-iron) : 0.19 m^2 wetted surface (TS). It was used for the test sections, which were heated under Argon, and for permeation membranes. Analysis as specified, GoodFellow and others.

Covergas : Ar-6.0, at inlet to TRITEX purified by OXISORB^R, Messer Griesheim company. The specified purity of <0.1vpm O_2 and <0.5vpm H_2O was confirmed in our laboratory.

* Used only at low temperature.

Table 3

Analysis of as received bars. Average concentrations.

Pb-17Li as received			
		MG	MetSpec
		1990/93	1992/95
Pb			
Li	at.%	av. 16.6	av. 17.0
Fe	wppm	7,00	4,30
Cr	wppm	0,85	0,21
Ni	wppm	1,40	0,35
Mn	wppm	0,50	0,04
Mo	wppm	0,40	0,02
V	wppm	0,05	0,05
Na	wppm	38,50	4,60
K	wppm	5,90	0,82
Be	wppm	0,00	0,05
Mg	wppm	0,47	0,33
Ca	wppm	3,10	2,40
Sr	wppm	0,00	0,01
Ba	wppm		0,02
B	wppm	2,10	0,36
Al	wppm	1,20	0,36
In	wppm		0,17
Tl	wppm	2,20	0,34
Si	wppm	3,30	
Sn	wppm	0,07	0,09
As	wppm	1,50	0,50
Sb	wppm	0,35	
Bi	wppm	53,00	29,40
Cu	wppm	0,51	1,35
Ag	wppm	11,50	3,47
Zn	wppm	0,42	0,49
Cd	wppm	1,86	1,12
Sc	wppm		0,01
Sb	wppm	0,35	
Se	wppm	0,40	0,50
Te	wppm	0,30	

Table 4

Analysis of Pb-15.8Li, taken during operation.

Analysis of Li-15.8 samples

		DT	DT	DT	DT	DT	TS	TS	CT1	5 posit.	MH	FM1	SS2	TS	CT1
		Aug.	Dec.		Febr.	Nov.	Febr.	March	Nov.	Nov.	Febr.	Febr.	Oct.	Nov.	march
		.1989.	.1989.	.1990.	.1991.	.1994.	.1991.	.1992.	.1992.	.1992.	.1993.	.1993.	.1994.	.1994.	.1996.
Pb															
Li	at.%	16,7	15,3	15,3	15,6	16,6	15,5		15,4	15,6	15,1	15,5	16,6	16,4	15,8
Fe	wppm	4,00	6,00	4,60	6,70	12,00	6,60	6,20	2	6	1,1		13,00	8,00	
Cr	wppm			0,80	0,54		1,70	0,86	0,9	8,4				4,00	
Ni	wppm	5,00	4,00	7,00	12,00	6,00	14,40	10,50	9,4	15,3	11,4	13,7	9,00	16,00	
Mn	wppm			1,30	1,45	1,00	1,32	0,26	0,85	0,28	0,55	0,4	2,00	2,00	
Mo	wppm				0,09		0,17								
V	wppm				0,07		0,37								
Bi	wppm	26,00		23,50	32,00	26,40	45,20	8,50	10,1		5,4	7	12,50	17,00	5,60
Cu	wppm	1,40		1,00	1,25		1,35	1,50	1						6,30
Ag	wppm			8,50	9,90		8,60	7,70	5,7						3,50
Zn	wppm			2,60	1,20		0,80		4,7						0,80
Cd	wppm				1,00		0,14	0,14	0,05	0,05				1,01	1,12

Table 5

Composition of particles from crusts and deposits.

Composition of crusts and deposits

		total	Li	particles		fraction of particles			
after			(Pb+Li)			M	NM1	NM2	NM3
Phase	Sample	g	at.%	g	w.%	%	%	%	%
II	ET - crust	12,0	34,1	0,204	1,7				
II	SS1 - crust	3,0	33,8	0,054	1,8				
IV	MT1 - deposit	3,3	16,3	0,066	2,0	27,8	45,1	23,7	3,5
IV	FM1 - deposit	0,15	15,3	0,00014	0,9	87,5	12,5		
IV	FM2 - deposit, magnet	3,23	14,1	0,081	2,51	95,0	4,9	0,074	
IV	FM2- deposit, out of magn.	0,28	16,3	0,0035	1,25	98,0	1,95		
IV	CT-2, crust	20,5	50,2	2,09	10	67,3	32,0	0,75	<0.02
IV	CT-2, deposition rings	25,7	55	2,09	11,6				
IV	CT-2, lead phase	3,0	0.1-4.8						
IV	TS-crust, membrane	0,57	38,3	0,0014	0,25				
IV	TS-crust, tank	3,3	45,8	0,01	0,3	61,7	all 38,3		
V	MT1	2,3	31	0,01	0,44	92,2	3,4	4,3	
V	FM1	1,44	12,6	0,072	4,98	98,9	0,76		
V	FM2 - estimated	1,5		0,072	5,0				
V	EMP tube	6,25	11,7	0,83	13,2	99,9	0,06		
V	EMP core	184	14,8	25,8	14,0	99,9	0,5		
V	CT1 cooler	16600	15,6	28,2	0,17	74,7	3,0	22,4	
V	CT1/2, tube (outlet CT1)	75,0	15,7	0,38	0,5				
V	CT1/2, tube (inlet CT2)	75,0	53,3	7,16	9,54	74,2	25,7		

Composition of crusts and deposits , continue

		total	Li	particles		fraction of particles			
after			(Pb+Li)			M	NM1	NM2	NM3
Phase	Sample	g	at.%	g	w.%	%	%	%	%
V	**CT2,** tank, No.2, bottom	58,0	15,1	0,0023	0,004				
V	**CT2,** tank, No.3, lower crust	0,06	35,9	0,00076	1,26				
V	**CT2,** tank, No.4,upper crust	0,55	40,8	0,0062	1,13	93,8	6,2		
V	**CT2,** inlet dome, No.1	85,0	25,3	1,07	1,26	75,0	25,0		
V	**CT2,** dome, No.5, lower part	15,0	20	0,11	0,75	(100.)			
V	**CT2,** dome, No.6, center	4,4	49,3	0,24	5,4	99,1	0,88		
V	**CT2,** dome, No.7, top	7,0	55,7	0,45	6,41	96,6	3,35		
V	**CT-2,** basket,dep.ring, top	4,9	39,5	0,084	1,72	(100.)			
V	**CT-2,** basket,dep.ring, bottom	3,9	43,7	0,062	1,59	(100.)			
V	**CT-2,** basket,wall-crust,No.10	0,3	41,2	0,011	3,6				
V	**CT-2,** basket,wall-crust,No.11	1,53	30,7	0,063	4,14	84,3	14,4	1,38	
V	**V3**-crust	2,9	52,4	0,046	1,58	38,4	43,3	18,4	
V	**V5**-crust	3,27		0,051	1,55				
V	**V6**-crust	3,0	62,9	0,048	1,61	1,1	66,7	32,3	
V	**ET**	11,5		0,35	3,0				
V	**SS1**	1,0	20,8	0,076	7,6				
V	**TS1** estimated	0,56		0,0056	1,0				
V	**TS2**	0,45		0,0037	0,82	78,3	21,6		
V	**SS2**	12,1		0,36	3,0				
V	**DT** upper part, A	1,3	19,2	0,0009	0,07	69,4	30,4		
V	**DT** upper part, B	67,0	48,9	0,88	1,31	81,8	13,2	5,0	
V	**DT** middle crust, C	69,4	39,4	0,38	0,54	62,5	37,5		
V	**DT** lower crust, D	486	39,0	4,08	0,84	41,9	49,7	8,41	

Composition of crusts and deposits , continue

		total	Li	particles		fraction of particles			
after			(Pb+Li)			M	NM1	NM2	NM3
Phase	Sample	g	at.%	g	w.%	%	%	%	%
VI	MT1 V-sheet	0,33	23,4	0,0017	0,49	13,1	86,0		
VI	MT1 core, deposit	1,21	25,8	0,0092	0,76	9,7	87,5		
VI	MT1 core, crust	1,15	25,3	0,014	1,19	18,0	59,0	23,0	< 1.0
VI	CT1 all particles	14250		18,5	0,13	(no separate analysis)			
VI	CT2 all particles	11400		2,05	0,018				
VI	V7 total	1,46		0,022	1,5				
VII	MT1 inlet	20,4	40,9	1,55	7,61	>90			
VII	MT1 gap at top part	32,4	39,4	0,67	2,08	>90			
VII	MT1 gap at bottom part	15,6	28,6	0,62	3,99	>90			
VII	MT1 outlet	15,3	21,2	0,57	3,73	>90			
VII	MT2 all	6,77	16,2	0,185	2,73	>99			
VII	FM1 all	19,7	30,1	0,94	4,76	97,7	1,76	0,34	
VII	FM2 all	5,2	29,5	0,12	2,22	94,0			
VII	EMP core	119,3	25,7	6,36	5,33	93,8	1,68	4,31	
VII	EMP tube	12,5	44,1	0,71	5,69	94,9	1,25	3,75	
VII	CT1 **(estimated)**			2,0					
VII	V3 all	1,85	50,1	0,031	1,7	63,9	20,6	15,3	
VII	V4 all	18,3	60,7	0,24	1,33	56,4	32,0	10,9	
VII	V6 all	1,85	(50.1)	0,031	1,7				
VII	V7 all	4,9	51,4	0,049	1,0	28,4	49,4	21,6	
VII	ET crust membrane	14,4	52,0	0,17	1,21	45,5	31,7	22,8	
VII	ET crusts	4,17	47,4	0,083	1,98	53,6	4,86	41,4	
VII	SS1,2 crusts	13,2	38,3	0,37	2,84	59,1	12,9	28,0	
VII	TS1 all crusts	2,61	40,4	0,052	1,96	19,4	48,4	32,2	
VII	TS2 all crusts	4,63	39,3	0,0145	0,33	11,3	53,9	34,6	
VII	DT all wall deposits	61,3	39,1	0,058	0,094	42,9	52,2	4,9	
VII	DT oxides from surfcae	41,5	31,8	0,011	0,027	39,2	52,0	8,8	

Table 6

Composition of magnetic particles.

Composition of magnetic particles							
after Phase	Sample	wt.% Fe	wt.% Cr	wt.% Ni	wt.% Mn	wt.% Mo	wt.% V
II	ET - crust	(total 90.1% Fe, 9.7% Cr, 0.17% Ni)					
IV	MT1 - deposit	80,5	19,1	0,32	0,36	0,25	0,036
IV	FM1 - deposit	85,3	13,3	1,25	0,36		
IV	FM2 - deposit, magnet	87,6	12,0	0,20	0,09	0,10	
IV	FM2- deposit, out of magnet	89,2	10,6	0,12	0,09		
IV	CT-2, crust	80,9	16,6	1,12	1,12	0,088	0,035
IV	CT-2, dep.rings/ *total*	94,4	4,5	0,50	0,21	0,12	0,078
IV	TS-crust, membrane	91,9	7,1	0,70	0,42	0,42	0,11
IV	TS-crust, tank	79,0	16,0	0,60	1,10	2,60	0,40
V	MT1	88,7	7,4	0,32	0,19	2,95	0,43
V	FM1	96,4	3,3	0,27	0,03	<0.05	<0.01
V	EMP tube	97,3	2,5	0,20	0,01	< 0.05	< 0.005
V	EMP core	94,1	4,9	0,20	0,05	0,75	< 0.01
V	CT1 cooler	90,3	9,0	0,25	0,17		
V	CT1/2, tube (inlet CT2)	90,3	9,3	0,27	0,13		
V	CT2, tube bottom of CT2	88,2	10,8	0,50	0,21		
V	CT2, tank, No.2, bottom	86,9	12,3	0,52	0,33		
V	CT2, tank, No.3,upper crust	74,9	22,9	1,26	0,97		
V	CT2, dome, No.5, lower part	87,1	12,1	0,59	0,28		
V	CT2, dome, No.6, center	88,9	10,1	0,52	0,26		
V	CT2, dome, No.7, top	56,3	41,3	1,31	0,97		
V	CT-2, basket,dep.ring, top	55,8	40,0	2,79	1,52		
V	CT-2, basket,dep.ring, bottom	56,5	40,0	2,31	1,25		
V	CT-2, basket,wall-crust,No.11	56,3	39,8	2,51	1,41		

Composition of magnetic particles , continue							
after Phase	Sample	wt.% Fe	wt.% Cr	wt.% Ni	wt.% Mn	wt.% Mo	wt.% V
V	V3- crust	94,4	2,8	0,28	0,09	2,32	0,026
V	V6 -crust	99,0	0,4	0,09	0,08		0,010
V	TS2	81,1	10,9	5,83	2,20		
V	DT upper part, A	92,4	7,6				
V	DT upper part, B	84,6	13,5	0,69	0,52	0,52	0,15
V	DT middle crust, C	85,4	14,0	0,13	0,40		
V	DT lower crust, D	79,4	16,9	2,36	0,54	0,71	0,094
VI	MT1 V-sheet	88,4	8,2	2,30	1,10		
VI	MT1 core, deposit	94,8	5,3	<0.9	<0.6		
VI	MT1 core, crust	93,8	4,4	0,39	0,38		0,98
VII	MT1 all particles	96,2	3,0	0,24	0,07	0,11	0,27
VII	MT2 all particles	97,8	2,1	0,09	0,01	0,014	0,007
VII	FM1 all	97,0	2,7	0,08	0,05	0,045	0,15
VII	FM2 all	95,4	3,7	0,14	0,11	0,26	0,37
VII	EMP core	97,7	2,1	0,07	0,03	<0.05	<0,01
VII	EMP tube	95,6	4,0	0,23	0,11		0,021
VII	V3 all	93,2	6,0	0,17	0,51	<0,1	0,18
VII	V4 all	93,9	4,4	0,15	0,34	1,0	0,24
VII	V7 all	93,6	5,5	0,37	0,34	<0,1	0,16
VII	ET crust membrane	91,9	6,3	<0.02	1,00	0,81	0,13
VII	ET crusts	77,3	14,7	0,42	0,98	6,17	0,38
VII	SS1,2 crusts	96,8	2,7	0,17	0,12	0,19	0,044
VII	TS1 all crusts	93,1	5,6	0,19	0,23	0,66	0,17
VII	TS2 all crusts	92,5	4,9	1,17	0,72	0,52	0,19
VII	DT all wall deposits	82,2	7,4	7,28	2,55	0,89	0,17
VII	DT oxides from surfcae	40,3	4,5	36,80	18,40	<2	<1

Table 7

Composition of non-magnetic particles I.

Composition of non-magnetic particles - 1							
after		wt.%	wt.%	wt.%	wt.%	wt.%	wt.%
Phase	Sample	Fe	Cr	Ni	Mn	Mo	V
IV	MT1 - deposit	29,3	68,6	0,09	1,55	0,83	0,18
IV	FM1 - deposit	68,8	28,1	2,32	0,69		
IV	FM2 - deposit, magnet	42,7	50,3	0,42	0,76	5,2	1,0
IV	FM2 - deposit, out of magn.	48,4	48,7	2,10	0,83		
IV	CT-2, crusts	71,9	25,8	0,32	1,51	0,16	0,055
IV	TS - crust, tank	65,0	29,0	1,60	2,00	1,7	0,3
V	MT1	68,0	29,6	1,68	0,70		
V	FM1 all	41,1	58,0	1,30	0,70	<0.01	<0.01
V	EMP tube all	92,5	7,2				
V	EMP core all	44,8	52,6	0,67	0,89	0,77	0,34
V	CT1 cooler	66,6	32,5	0,33	0,55		
V	CT1/2, tube (inlet CT2) all	82,6	15,5	0,13	0,67	< 0,4	0,1
V	CT2, tank, No.3,upper crust	27,9	69,3	1,03	1,83		
V	CT2, dome, No.6, center	29,6	66,8	2,10	1,79		
V	CT2, dome, No.7, top	35,2	52,3	9,20	3,40		
V	CT-2, basket,wall-crust,No.11	55,6	38,6	3,94	1,84		
V	V3 crust	89,3	7,6	0,23	1,12	1,7	0,089
V	V6 crust	81,6	12,2	0,19	1,06	4,53	0,41
V	TS2 all	82,9	11,3	4,81	1,00		
V	DT upper part, A -all	92,1	7,9				
V	DT upper part, B	74,2	22,6	1,61	1,18		0,47
V	DT middle crust, C - all	66,1	30,0	0,49	1,07	1,93	0,36
V	DT lower crust, D	85,2	11,6	0,25	1,02	1,63	0,31

Composition of non-magnetic particles - 1 , continue							
after		wt.%	wt.%	wt.%	wt.%	wt.%	wt.%
Phase	Sample	Fe	Cr	Ni	Mn	Mo	V
VI	MT1 V-sheet -all	59,2	38,5	<0.5	2,33		
VI	MT1 core, deposit- all	63,5	34,9	<0.3	2,10		0,1
VI	MT1 core, crust	59,0	38,9	<0.3	2,10		0,21
VII	FM1 all	43,3	51,4	0,85	1,27	3,17	
VII	EMP core	85,7	13,0	<0.7	0,26	1,5	<0,5
VII	EMP tube	87,7	11,5	0,41	0,27		0,14
VII	V3 all	85,5	7,9	0,12	1,42	4,94	0,15
VII	V4 all	82,9	12,4	0,16	2,20	2,1	0,2
VII	V7 all	95,4	1,9	0,10	0,68	1,84	0,076
VII	ET crust membrane	75,8	21,2	0,35	1,73	0,8	0,18
VII	ET crusts	63,9	34,7	0,19	0,58	0,41	0,37
VII	SS1,2 crusts	66,5	29,8	0,22	0,84	2,47	0,11
VII	TS1 all crusts	86,6	11,3	0,12	0,50	1,18	0,30
VII	TS2 all crusts	89,9	8,6	0,18	0,63	0,47	0,18
VII	DT all wall deposits	62,9	23,9	8,43	4,72	<6	<1
VII	DT oxides from surfcae	65,3	15,8	12,00	7,08	<2,6	<1

Table 8

Composition of non-magnetic particles II.

Composition of non-magnetic particles - 2							
after Phase	Sample	wt.% Fe	wt.% Cr	wt.% Ni	wt.% Mn	wt.% Mo	wt.% V
IV	MT1 deposit	33,8	64,8	0,025	1,39	0,19	0,03
IV	FM2 deposit, magnet	42,4	54,7	1,23	1,60		
IV	CT-2 crusts	40,1	57,8	0,71	1,31		0,11
IV	TS crust, tank	39,0	59,0	0,20	2,50	0,50	0,02
V	MT1	44,9	54,5	0,26	0,21		
V	CT1 cooler	45,9	50,8	0,38	2,90		
V	CT-2, basket,wall-crust,No.11	53,9	43,9		2,20		
V	V3 crust	11,8	86,1	0,08	1,07	0,20	0,59
V	V6 crust	6,0	89,8	0,10	0,86	1,67	1,59
V	DT upper part, B	45,7	54,3				
V	DT lower crust, D	9,1	90,9				
VI	MT1 core, crust	33,9	65,1	<0.7	1,10		<0.4
VII	FM1 all	10,2	77,8	2,80	1,85	7,41	
VII	EMP core	10,5	88,2	<0.3	1,25	<0.6	0,10
VII	EMP tube	22,5	75,9	0,43	1,03		0,20
VII	V3 all	77,8	19,4	0,22	1,36	1,01	0,22
VII	V4 all	12,3	84,7	0,29	1,65	0,47	0,59
VII	V7 all	13,3	84,2	0,28	1,69	<0.5	0,55
VII	ET crust membrane	12,2	86,6	<0,2	1,26	<0,5	<0,2
VII	ET crusts	44,0	53,7	0,18	1,29	0,59	0,39
VII	SS1,2 crusts	40,2	57,6	0,42	1,21	0,37	0,21
VII	TS1 all crusts	15,7	80,4	0,40	2,29	0,92	0,28
VII	TS2 all crusts	26,8	69,4	0,38	2,03	1,13	0,28
VII	DT all wall deposits	65,7	33,1		1,80		
VII	DT oxides from surfcae	64,2	26,7	7,40	1,71		

Table 9

Composition of non-magnetic particles III.

Composition of non-magnetic particles - 3							
after		wt.%	wt.%	wt.%	wt.%	wt.%	wt.%
Phase	Sample	Fe	Cr	Ni	Mn	Mo	V
IV	MF1 - deposit	18,5	81,5				
IV	CT-2, crusts	14	86				
VI	MT1 core, crust	2	98				
	average	**11,5**	**88,5**				
	sigma	6,9	6,9				

Figures

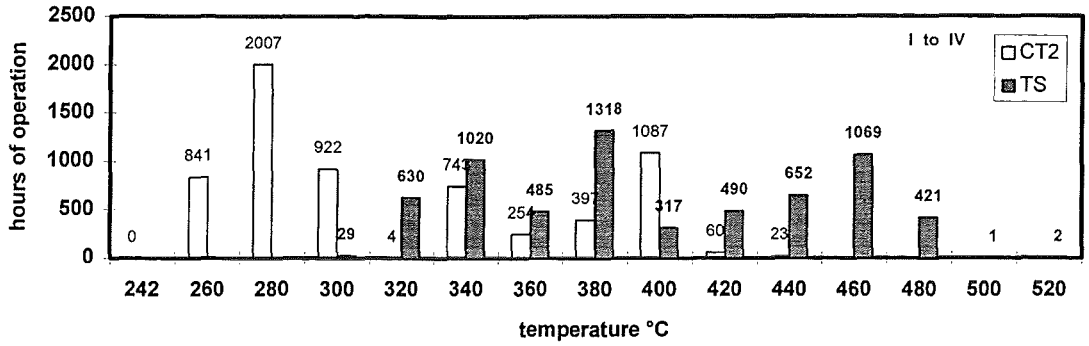

Fig.1 : Operation Phase I to IV.

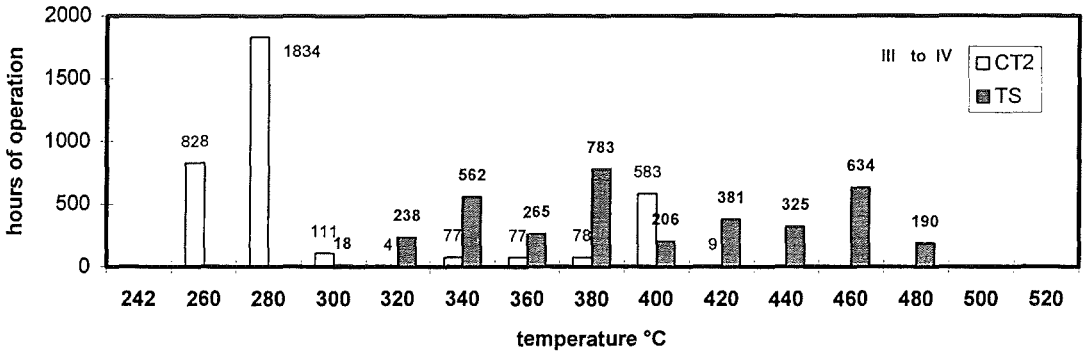

Fig.2 : Operation Phase III and IV.

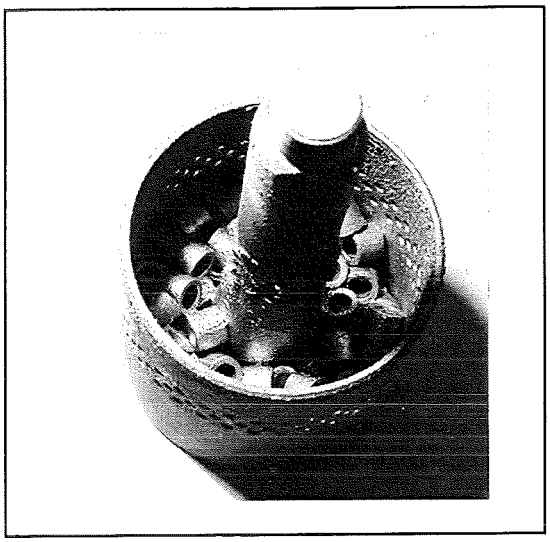

Fig.3 : Phase IV. Basket of cold trap 2, filled with rings of steel 1.4922.

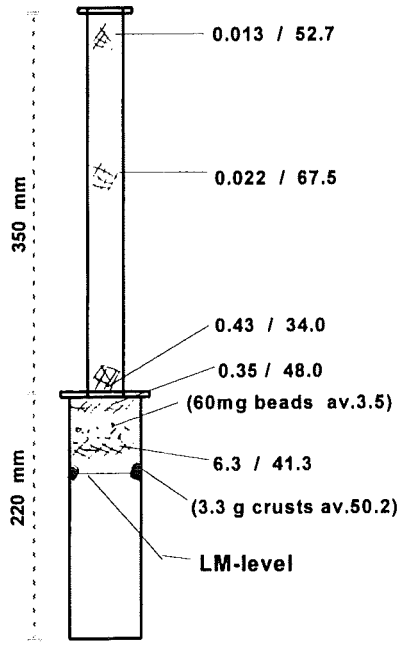

Fig.4 : Phase IV. Aerosol deposits in test section.
First number mg/cm^2 deposited material, second number at.% Li.

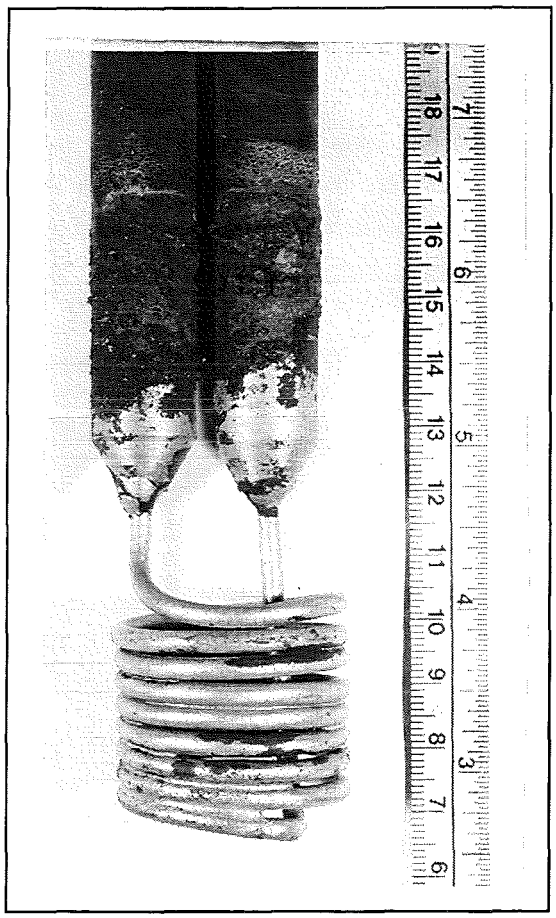

Fig.5 : Phase IV. Permeation membrane of test section with crusts.

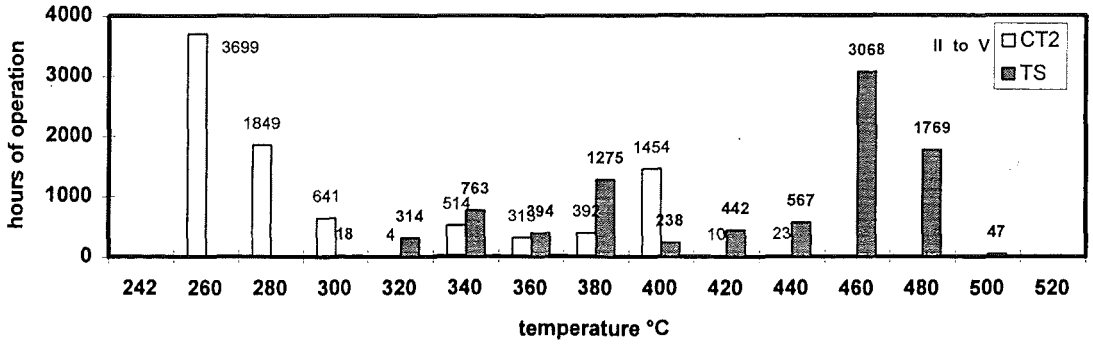

Fig.6 : Operation Phase II to V.

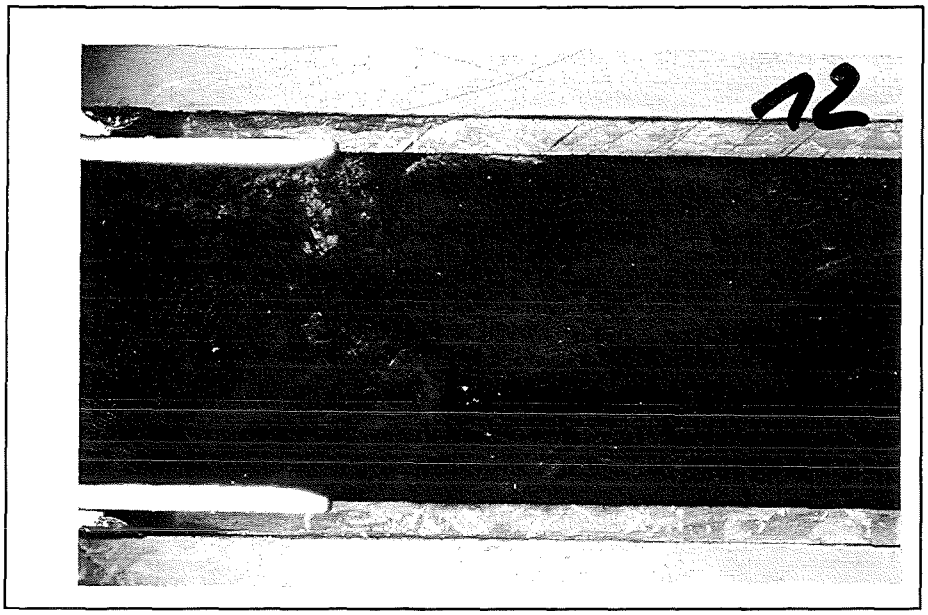

Fig.7 : Phase V , magnetic trap 1, about 3x. Main tube steel 1.4922, welded to austenitic steel (far left). Bright liner TZM. Inside the tube Pb-15.8Li with metallic particles as bright spots.

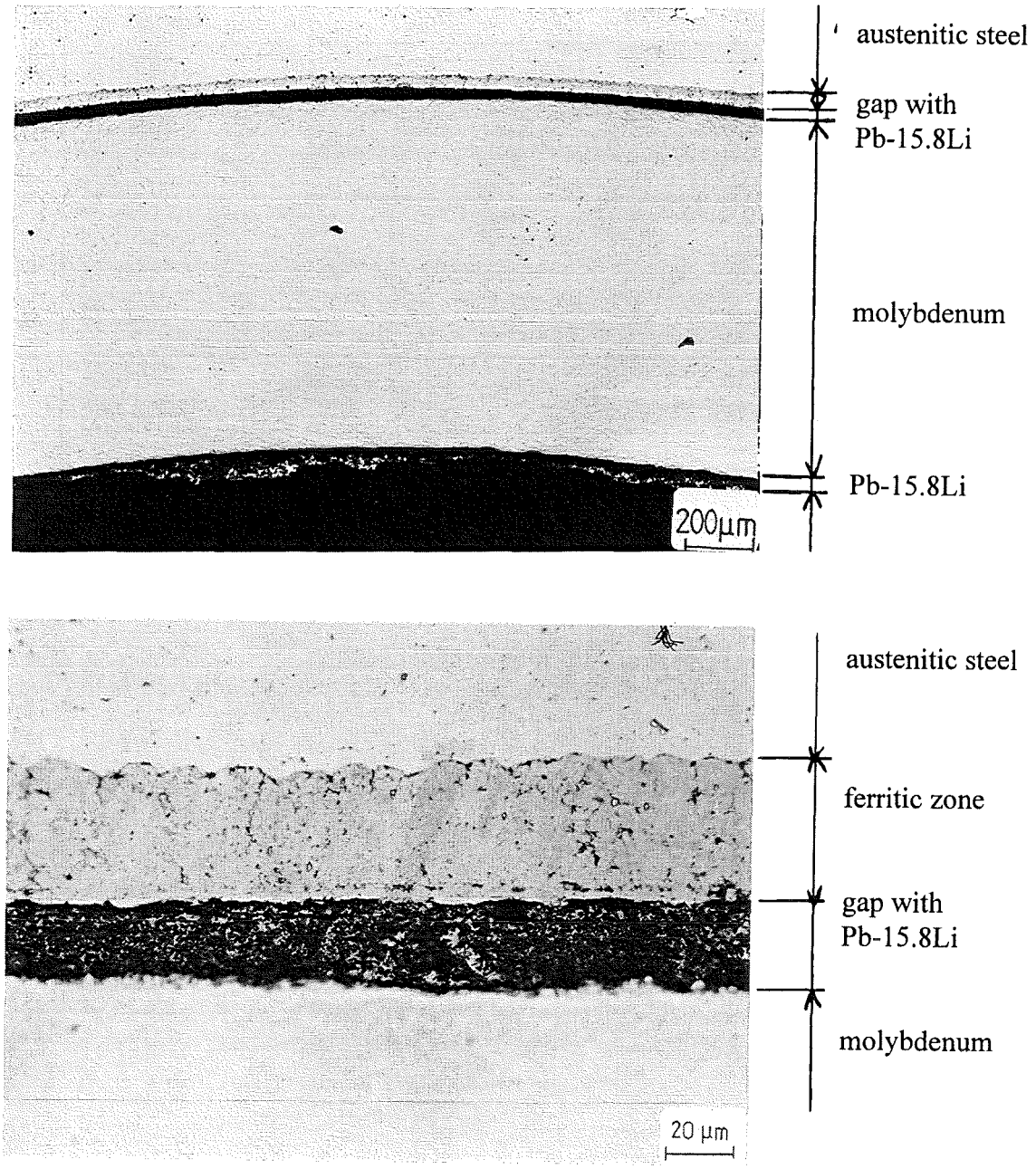

Fig.8 : Phase V , magnetic trap 1. Gap between austenitic steel 1.4301 and TZM filled with Pb-15.8Li. Ferritic layer on austenitic steel because of Ni-leaching.

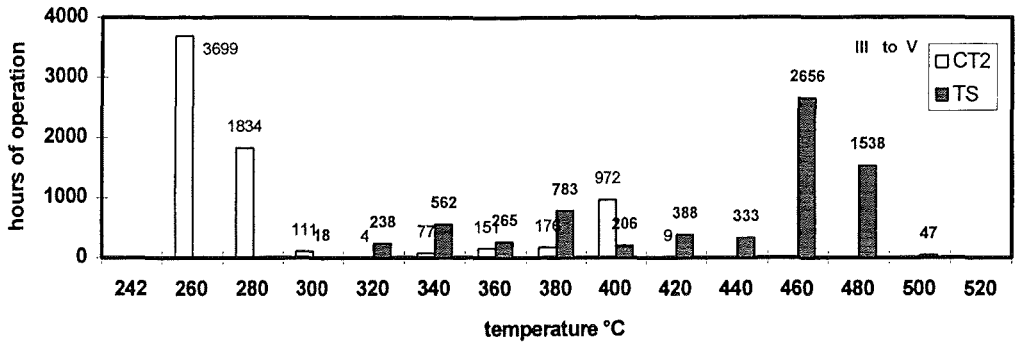

Fig.9 : Operation Phase III to V.

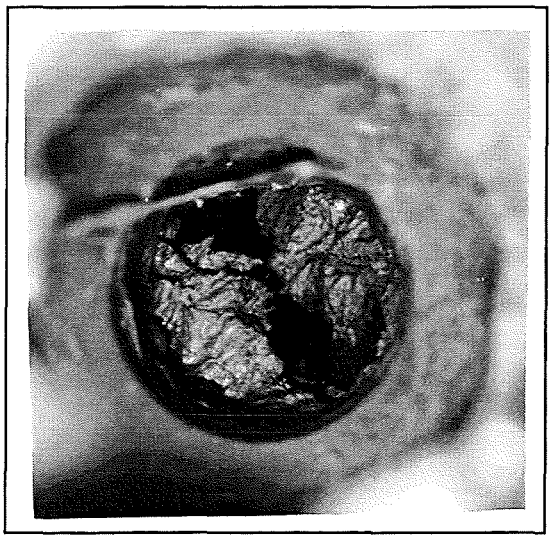

Fig.10 : Phase V. Looking into the tube of flow meter 1 after melt-out. ≈3x.

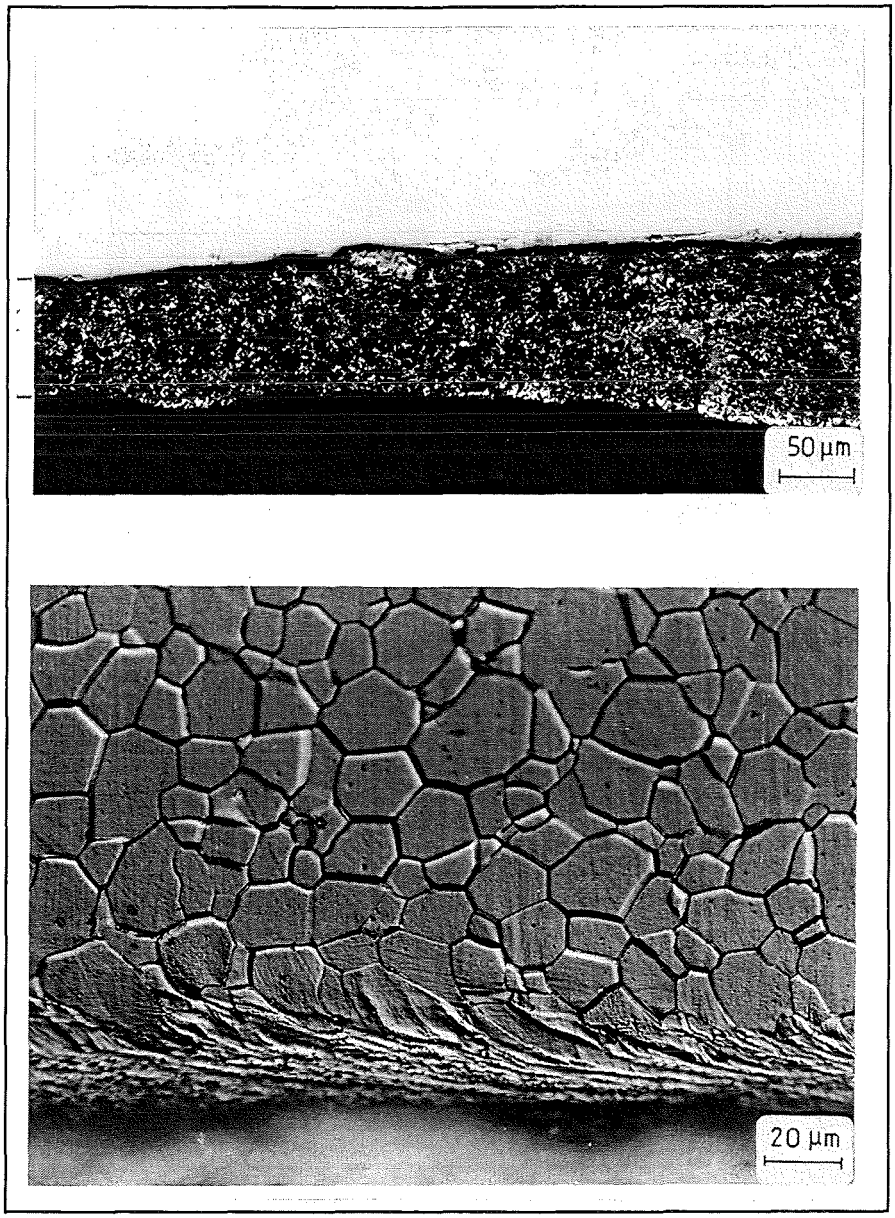

Fig.11 : Phase V, vanadium tube of flow meter 2. Metallographic examination. Upper picture mechanically polished, with Pb-15.8 adhering to vanadium. Lower picture after etching, Pb-15.8 removed, plastic deformed surface structure from manufacturing.

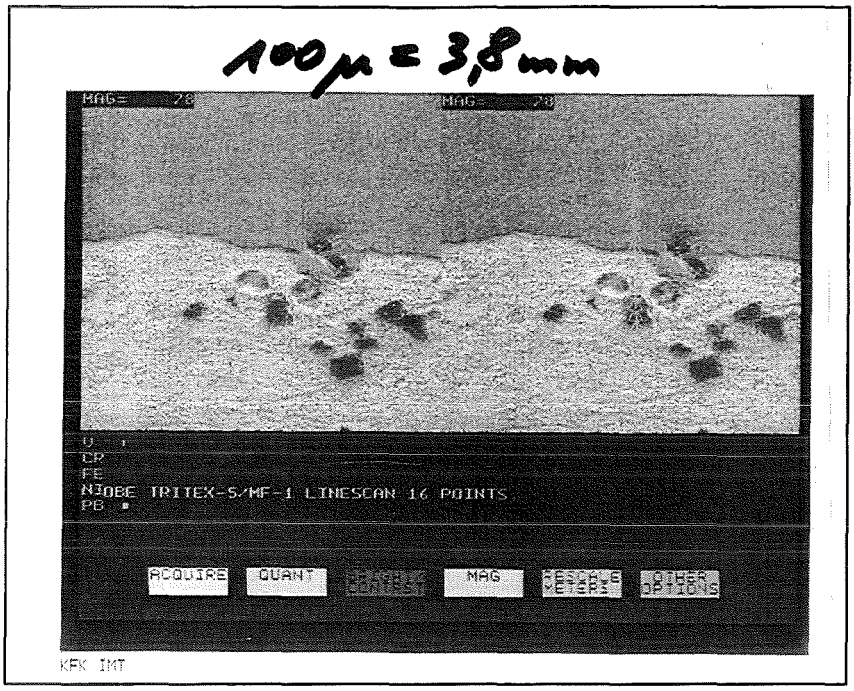

Fig.12 : Phase V, flow meter 1. Microprobe picture of Pb-15.8Li near the vanadium surface. Particles of $Ni_{1.2\text{-}1.9}V$.

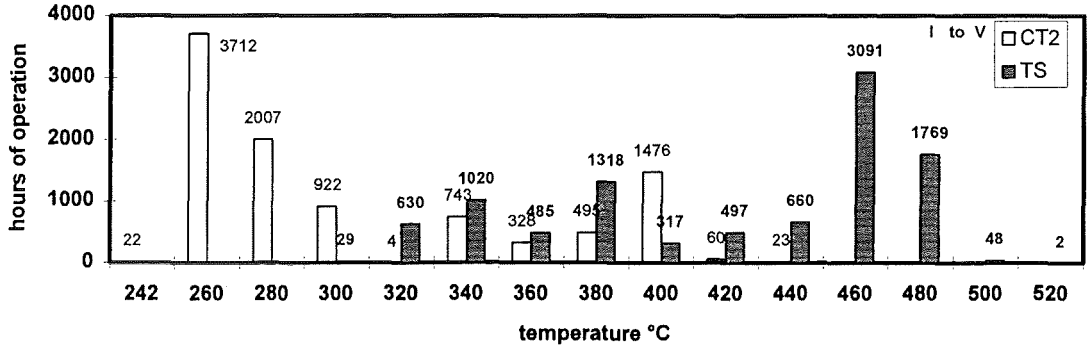

Fig.13 : Operation Phase I to V.

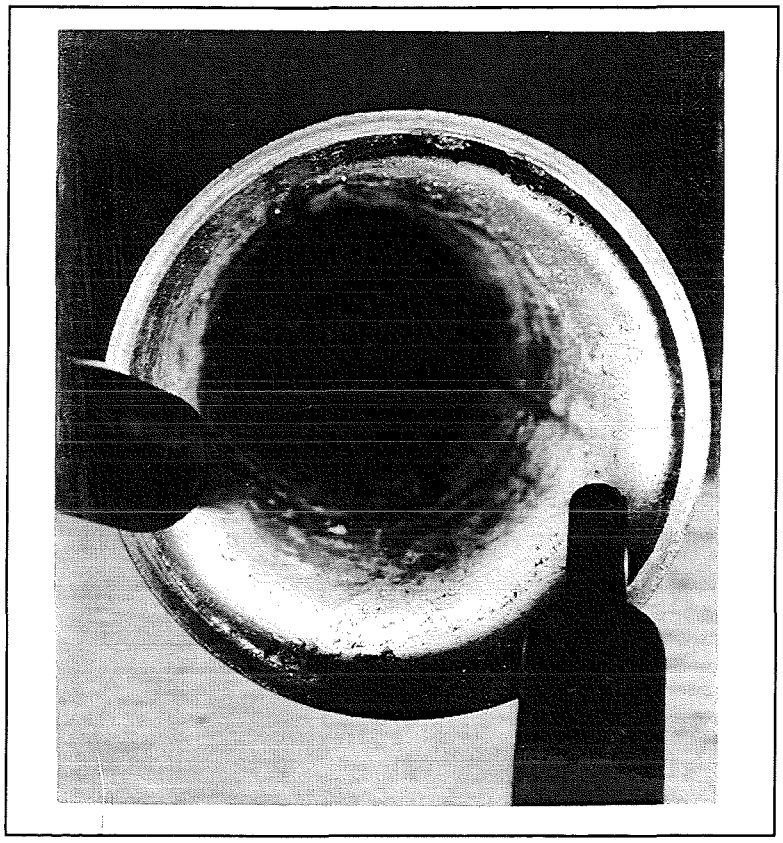

Fig.14 : Phase V, TZM tube of electro magnetic pump inlet.

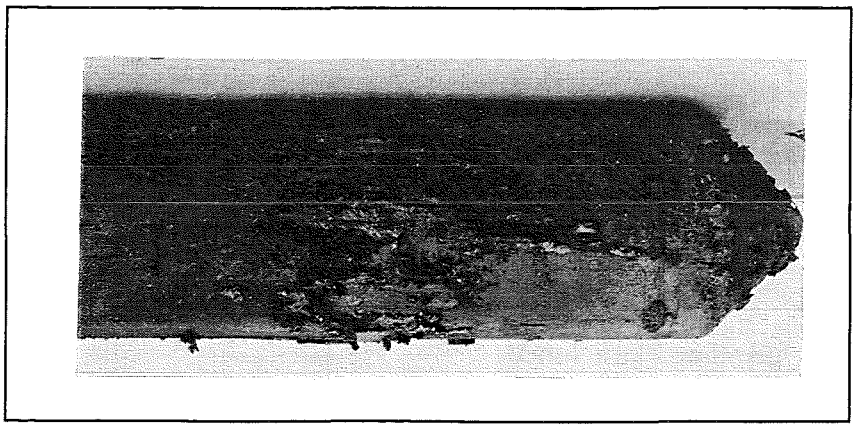

Fig.15 : Phase V, ferritic core of electro magnetic pump inlet.

Fig.16 : Phase V, core of electro magnetic pump. Corrosion product particles deposited at steel. Black parts are remaining Pb-Li mixture.

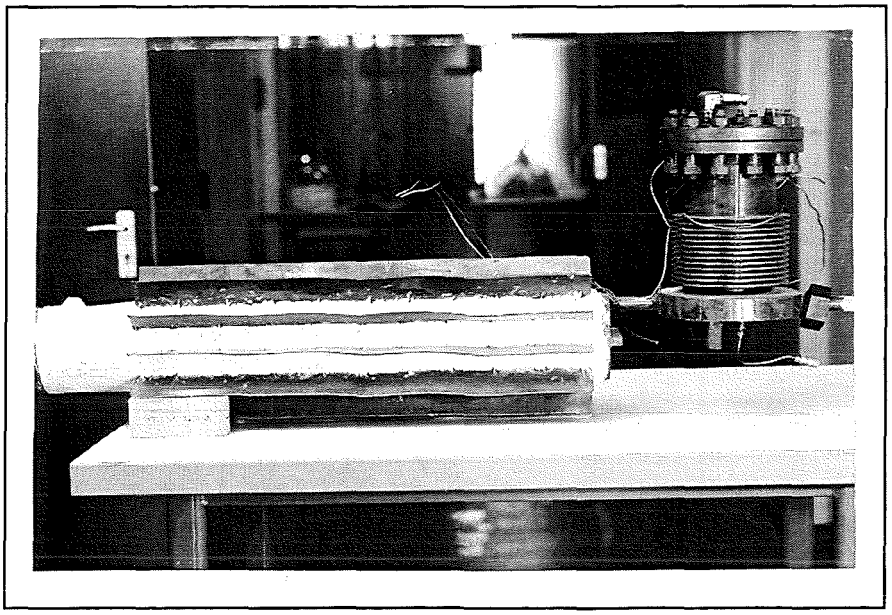

Fig.17 : Phase V. Cold trap 1 and cold trap 2 after phase V.

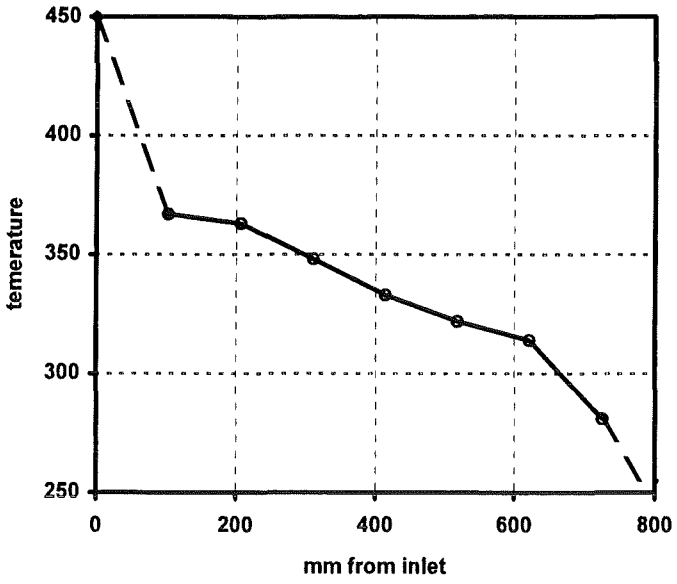

Fig.18 : Temperature profile in cold trap 1, 1990.

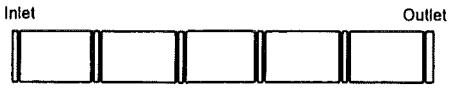

Fig.19 : Phase V. Sections of cold trap 1.

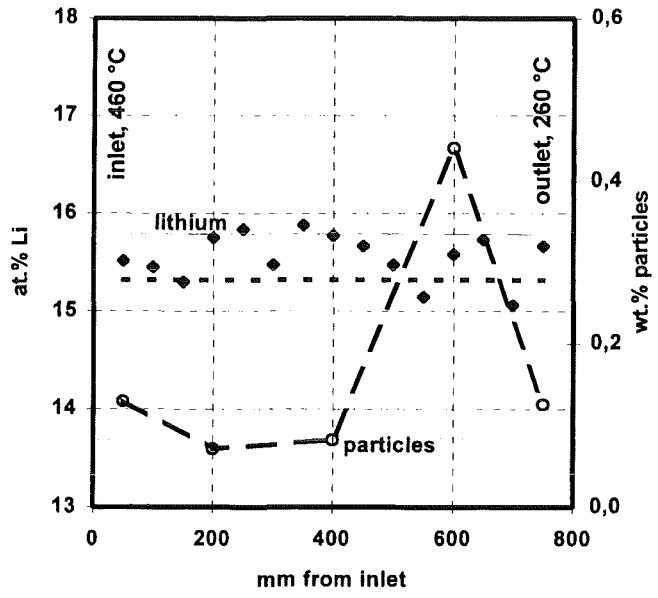

Fig.20 : Phase V. Cold trap 1, distribution of Li and corrosion products.

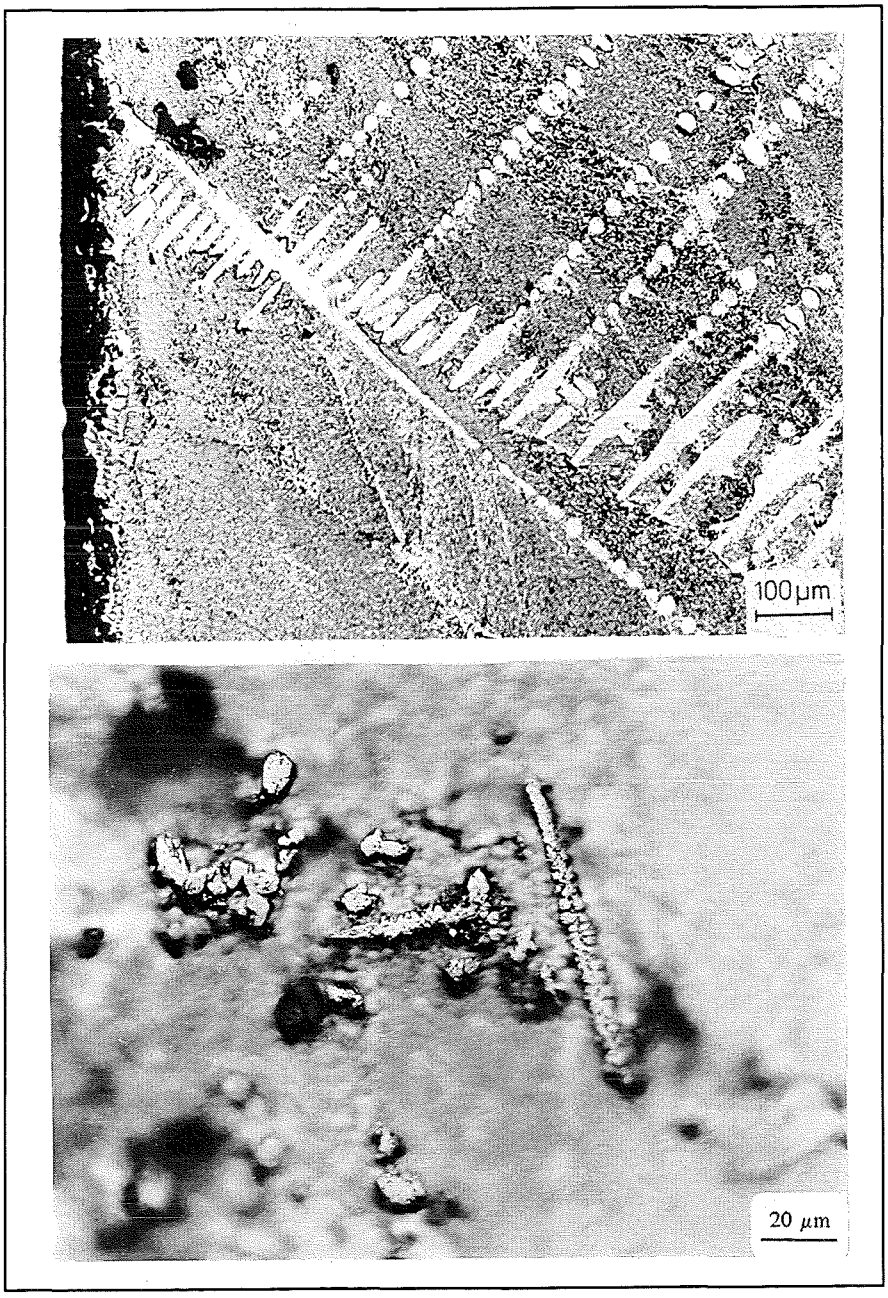

Fig.21 : Phase V. Outlet side of cold trap 1 (low temperature). Upper picture lead-rich dendrites, lower picture corrosion products particles after etching.

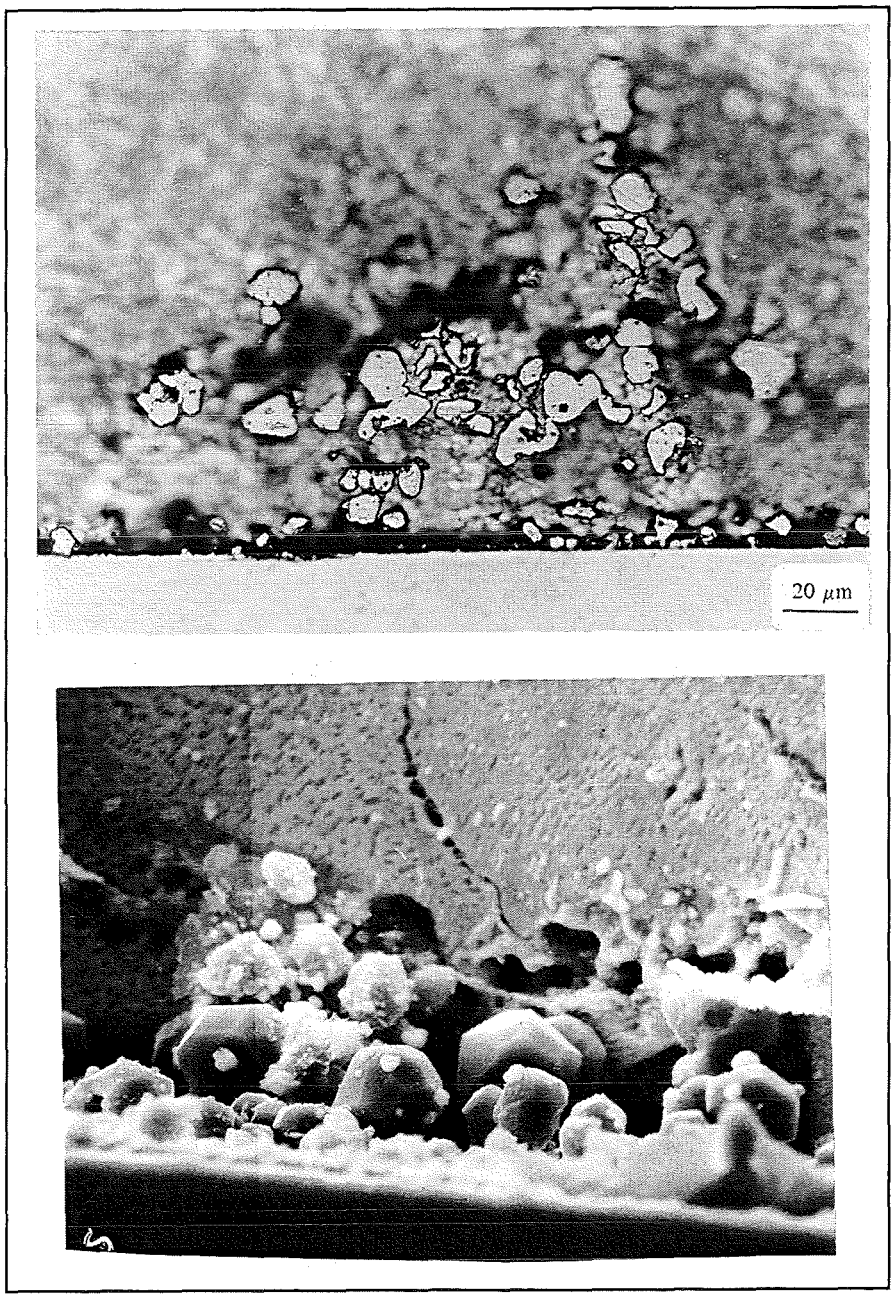

Fig.22 : Phase V. Cold trap 1 inlet (high temperature). Metallographic and SEM picture.

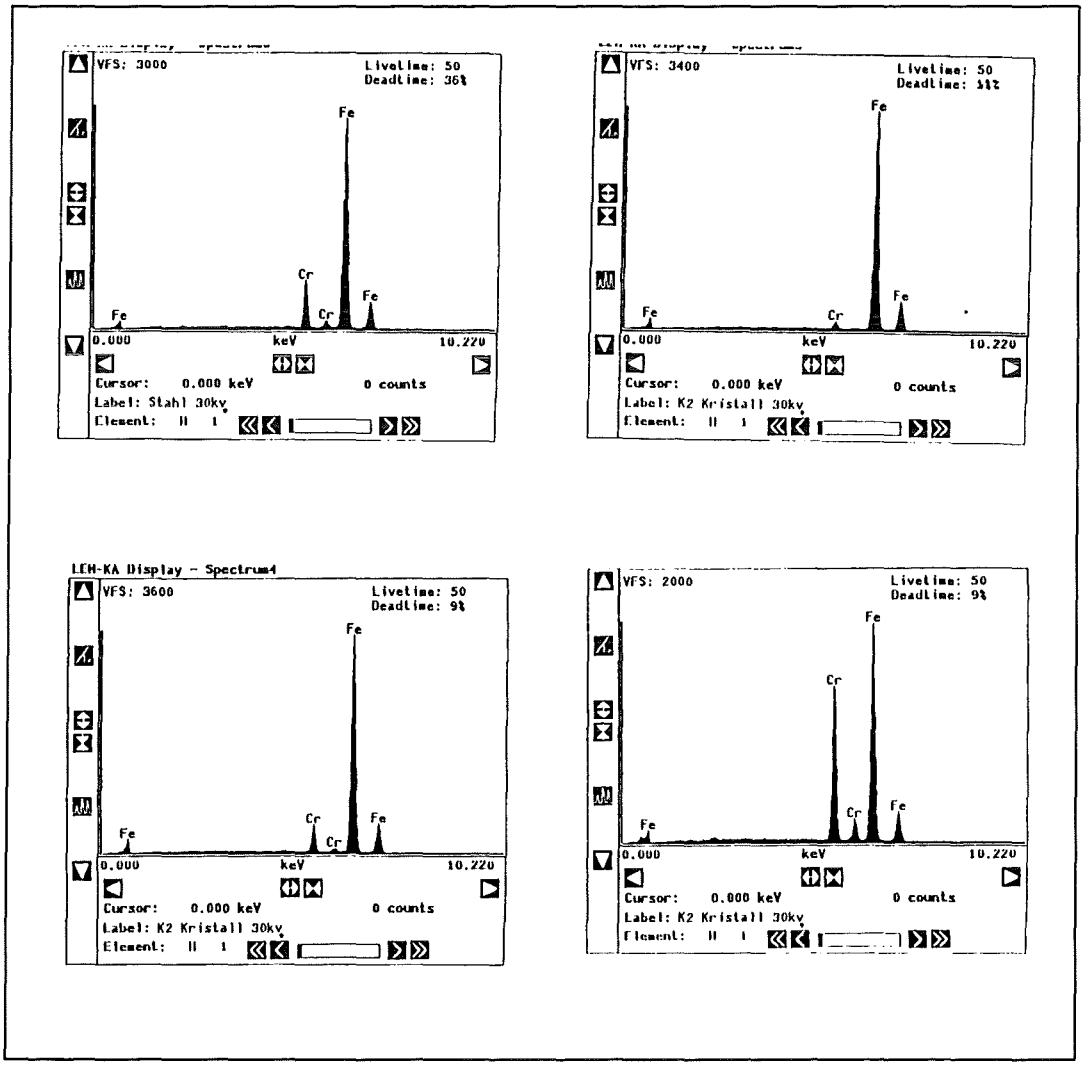

Fig.23 : Phase V. Cold trap 1 outlet (low temperature). Microprobe analysis of different particles. Upper left steel 1.4922.

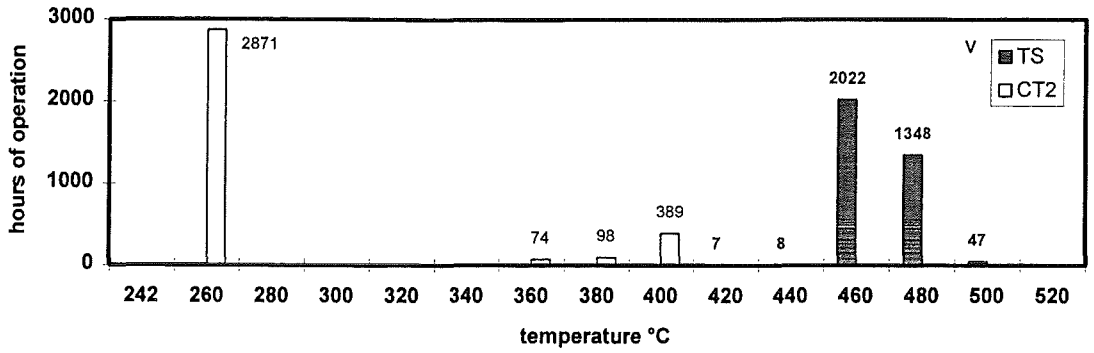

Fig.24 : Operation phase V.

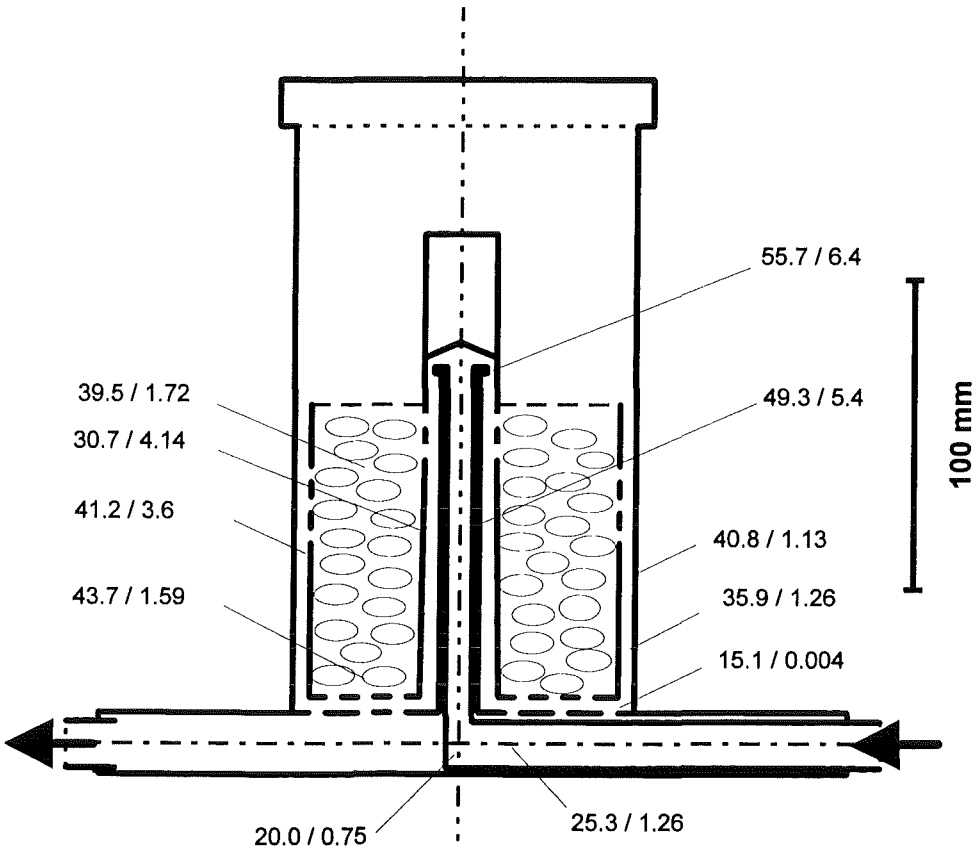

Fig.25 : Phase V. Cold trap 2. First value at.% Li, second value wt.% of corrosion product particles in deposit.

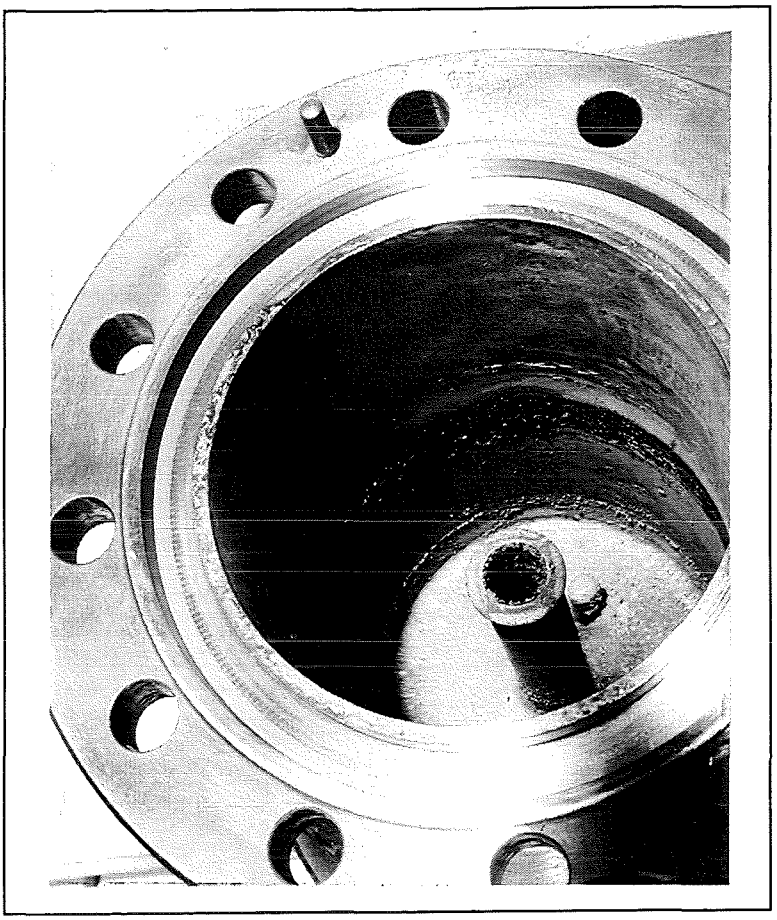

Fig.26 : Phase V. Cold trap 2. Tank without basket.

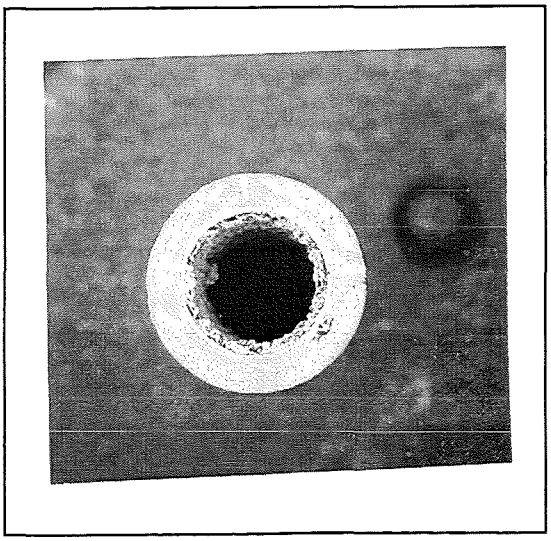

Fig.27 : Phase V. Cold trap 2. Dome.

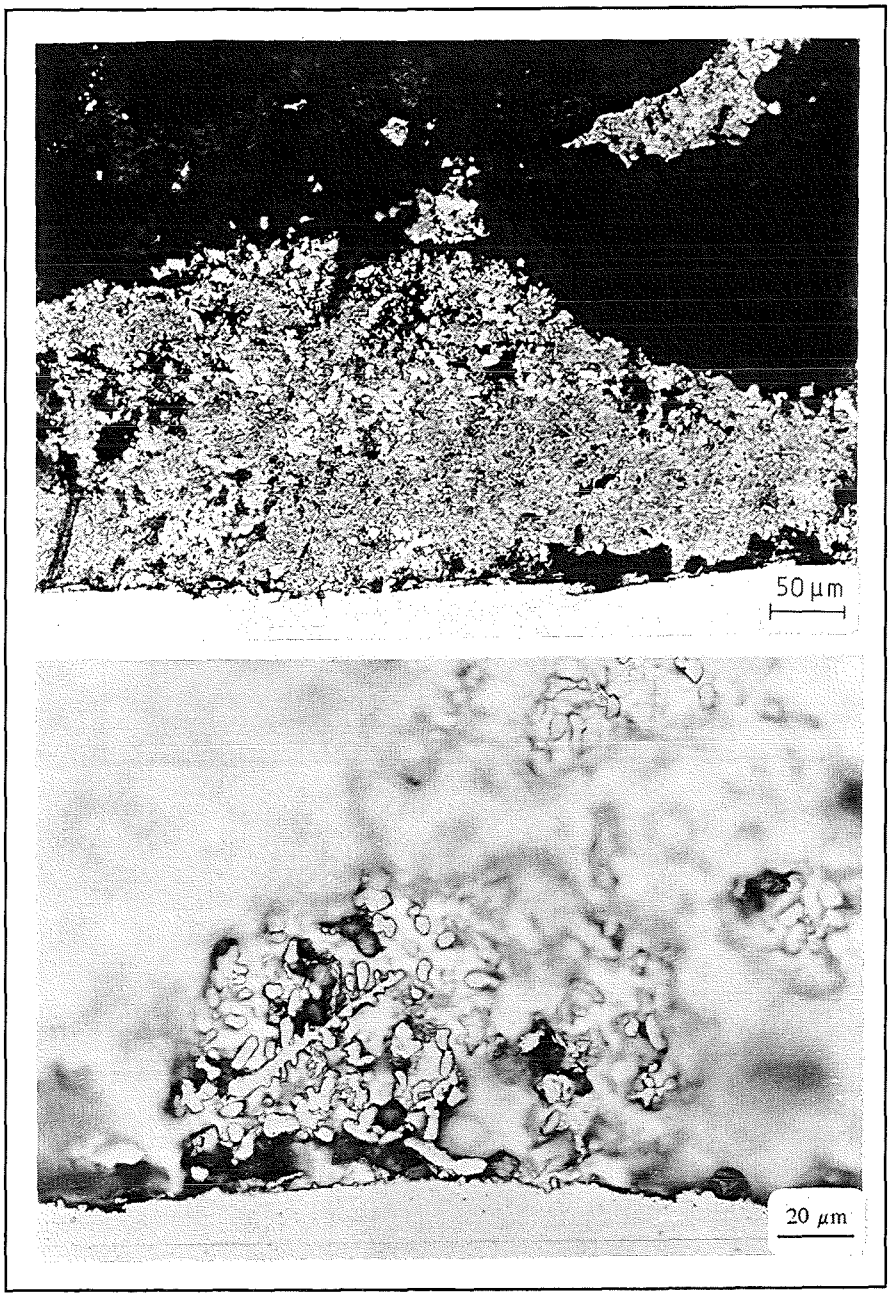

Fig.28 : Phase V. Cold trap 2. Dome. Upper picture Li-Pb phases with metallic particles, lower picture corrosion product particles after etching.

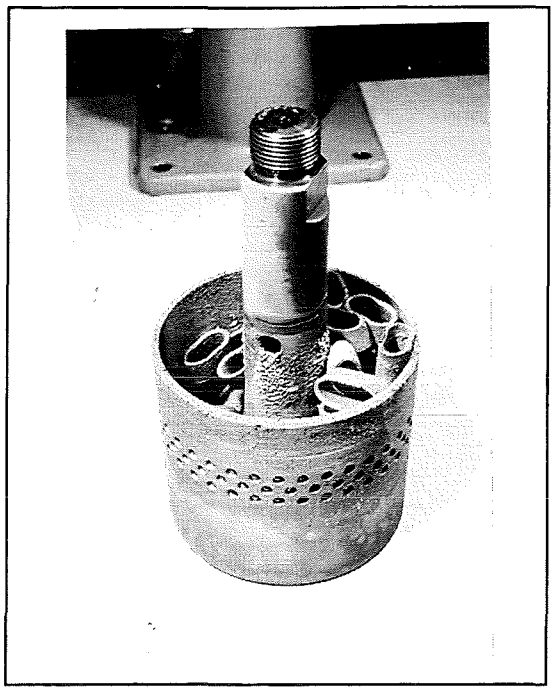

Fig.29 : Phase V. Cold trap 2. Basket with deposition rings.

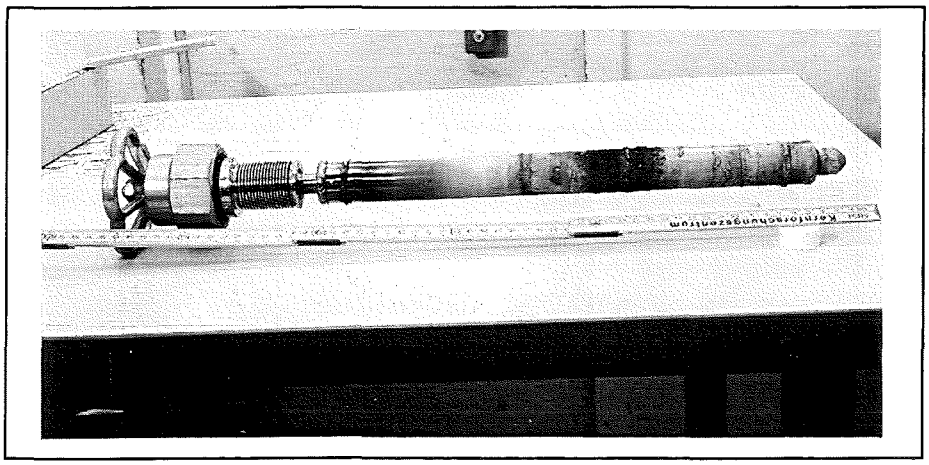

Fig.30 : Phase V. Stem of valve 5 with crusts.

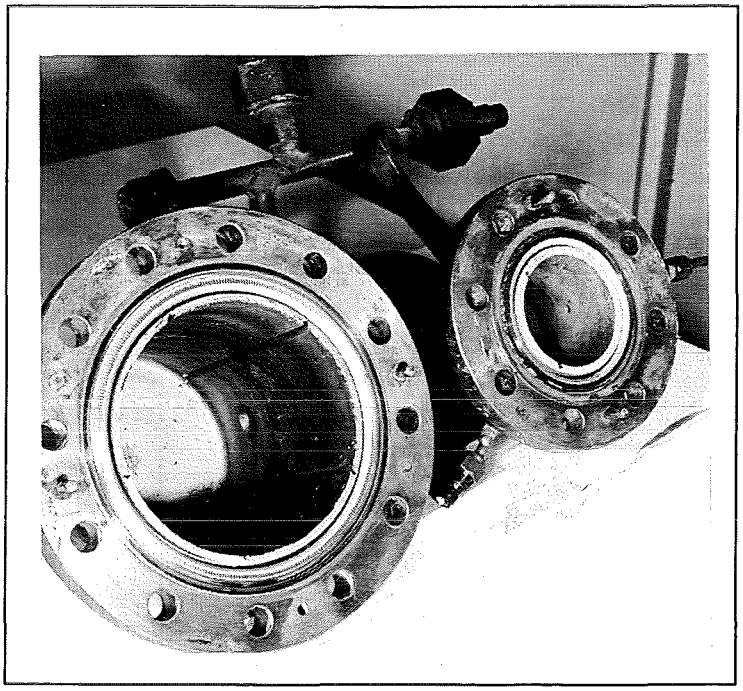

Fig.31 : Phase V. Photo of expansion tank (left) and sampling station 1.

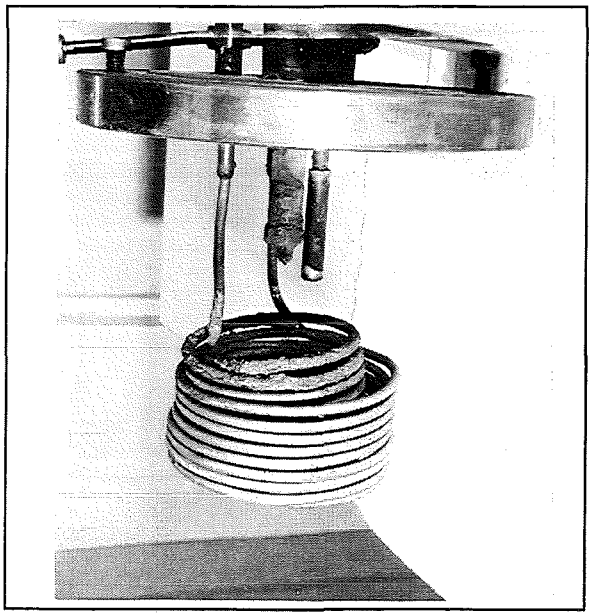

Fig.32 : Phase V. Permeation membrane of expansion tank.

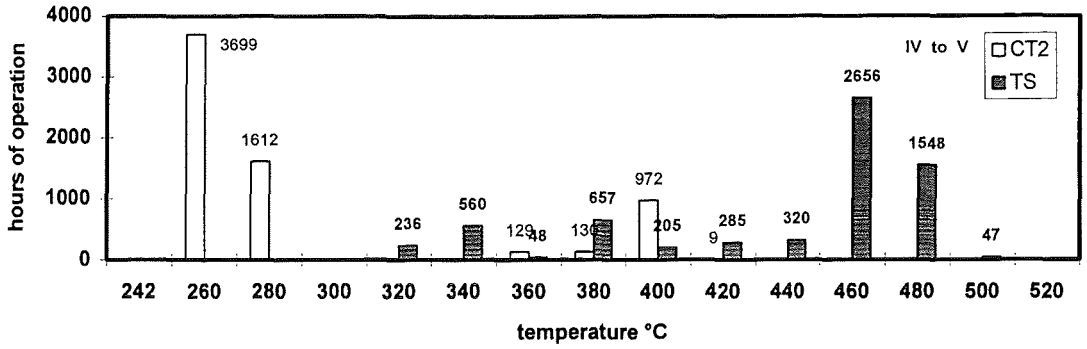

Fig.33 : Operation phase IV and V.

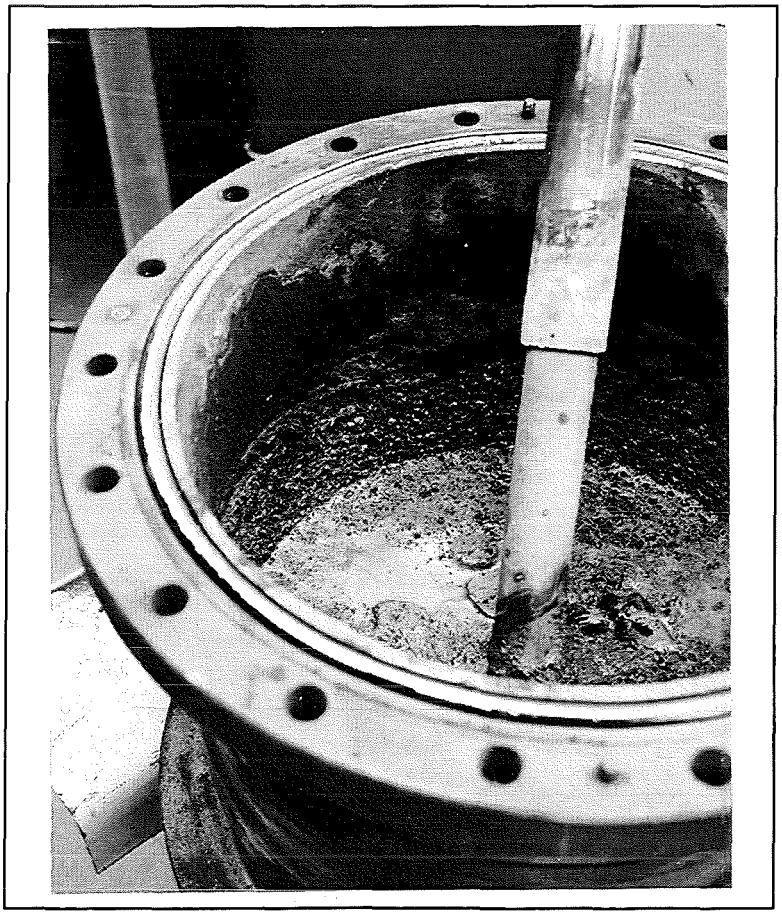

Fig.34 : Phase V. Drain Tank

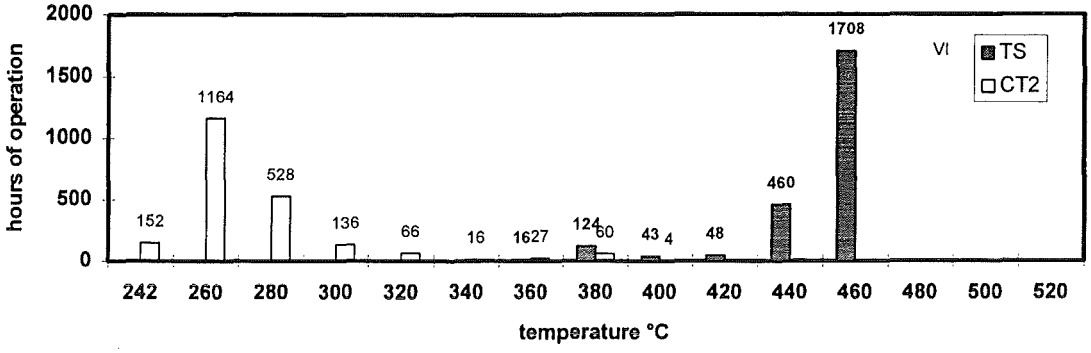

Fig.35 : Operation phase VI.

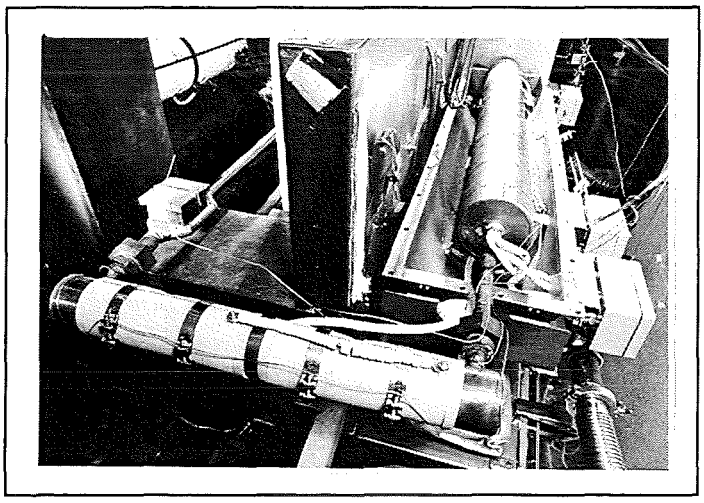

Fig.36 : Phase VI. Cold trap 1 (right), cold trap 2 (front) and magnetic trap 2 .

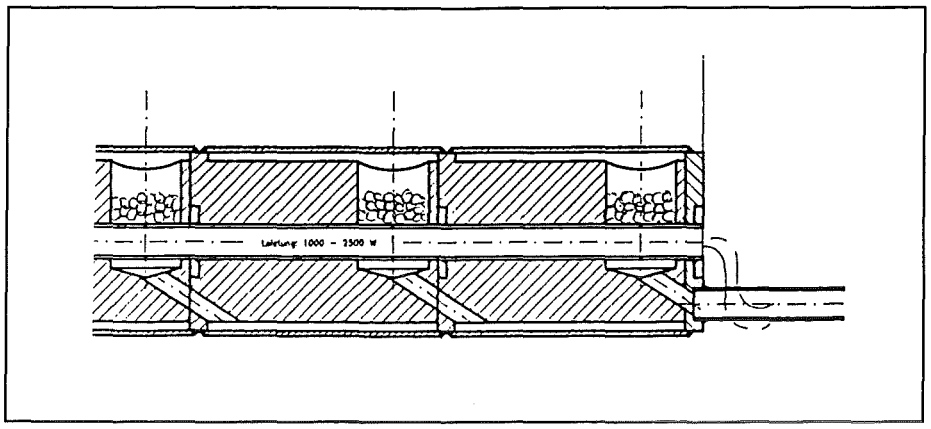

Fig.37 : Phase VI. Part of cold trap 1, outlet.

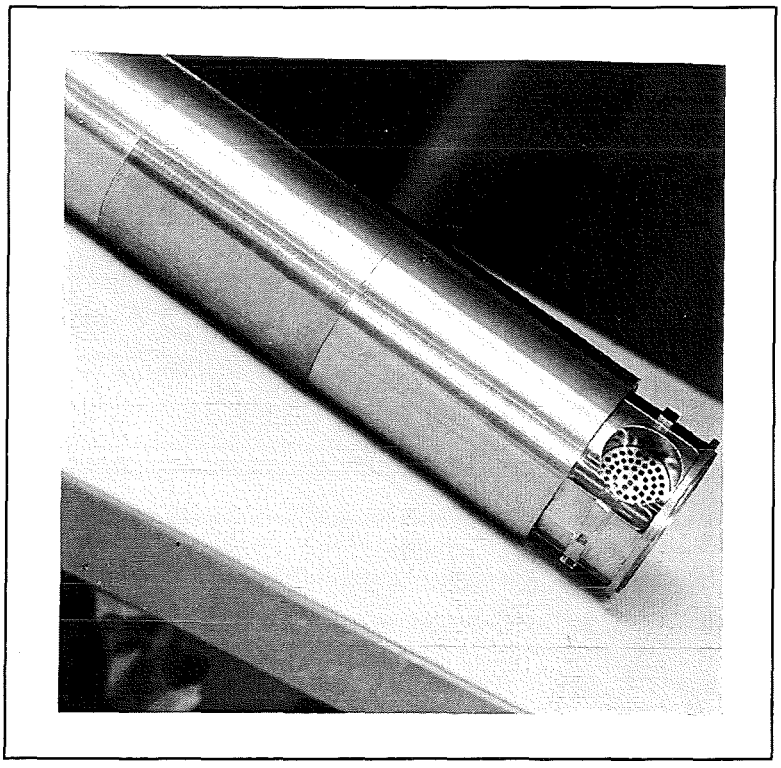

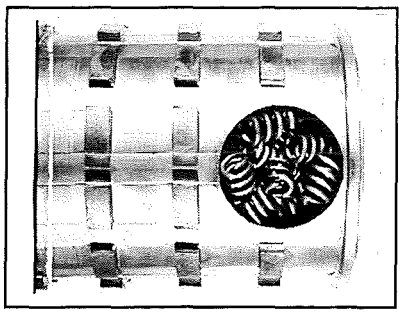

Fig.38 : Phase VI. Cold trap 1 and wire mesh filled chamber.

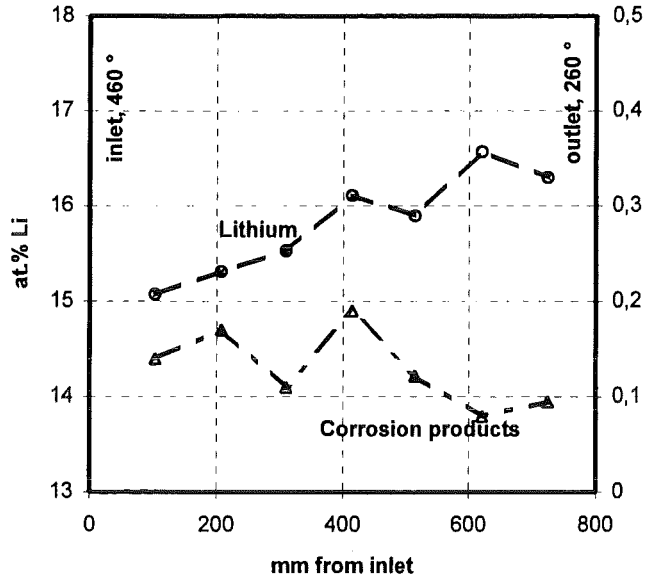

Fig.39 : Phase VI. Cooler, CT1. Distribution of Li and corrosion products.

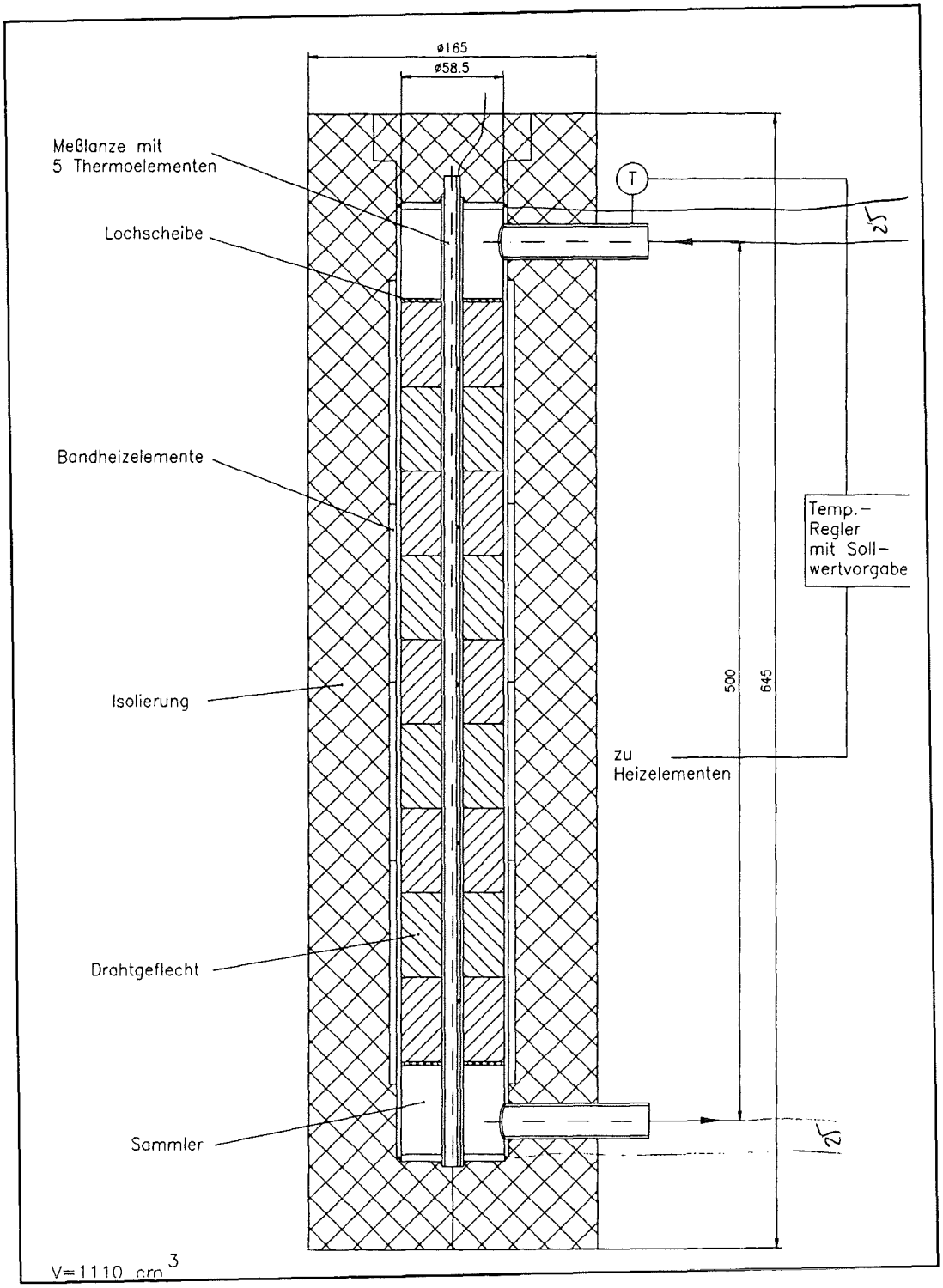

Fig.40 : Phase VI. Cold trap 2.

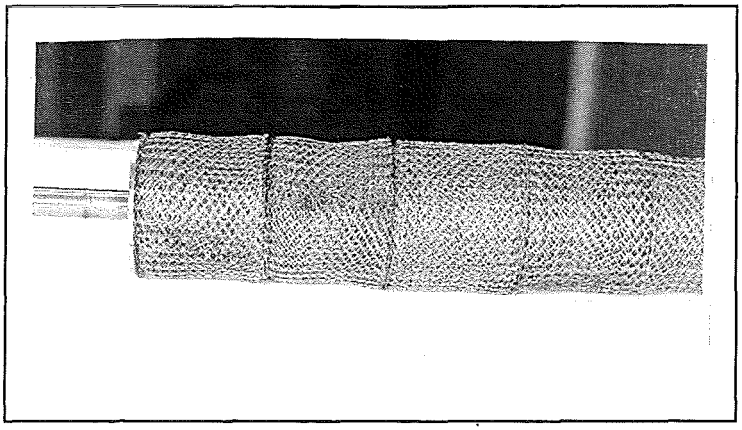

Fig.41 : Phase VI. Wire mesh packing of cold trap 2.

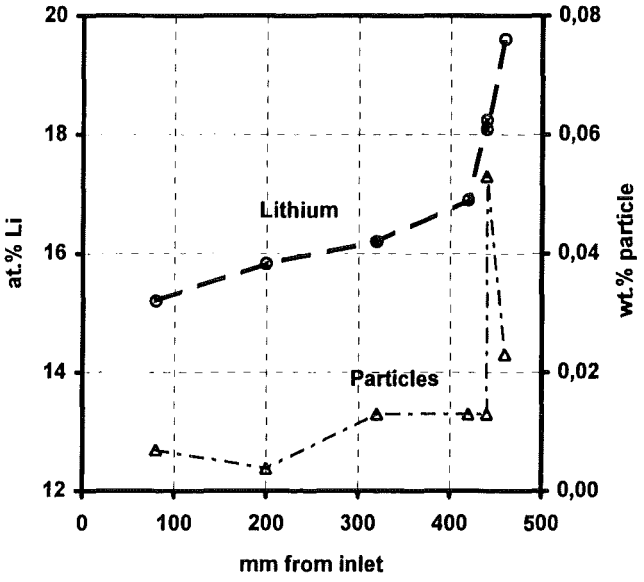

Fig.42 : Phase VI. Cold trap 2. Distribution of Li and corrosion products.

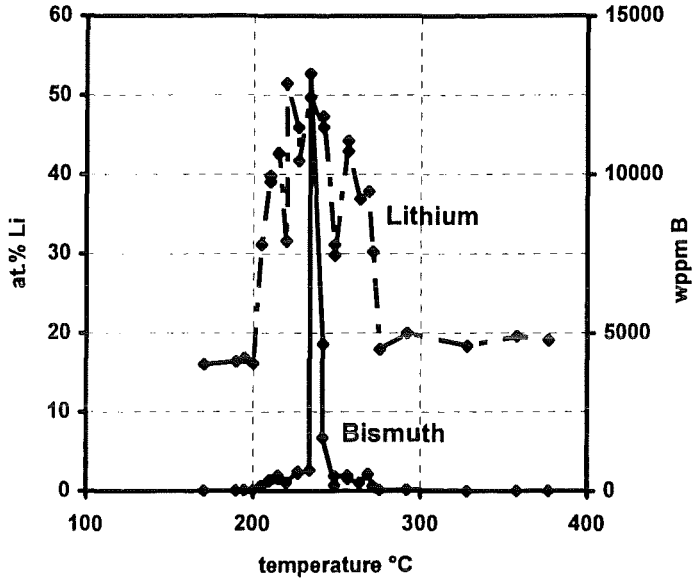

Fig.43 : Phase VI. Cold trap 3. Distribution of Li and Bi.

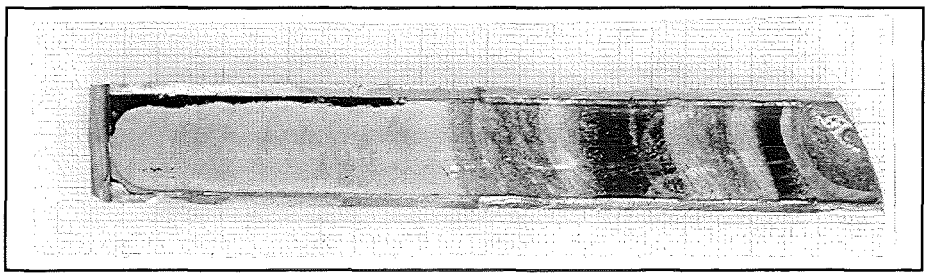

Fig.44 : Phase VI. Cold trap 3. Axial cut , after 5 hours oxidation in air at room temperature.

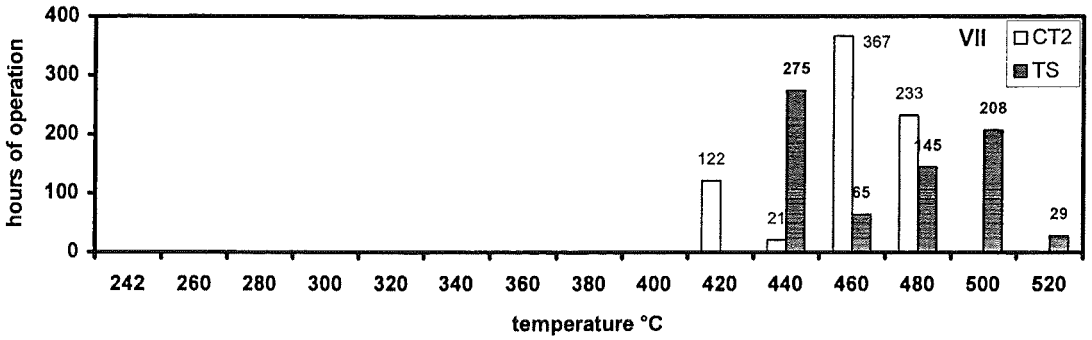

Fig.45 : Operation Phase VII.

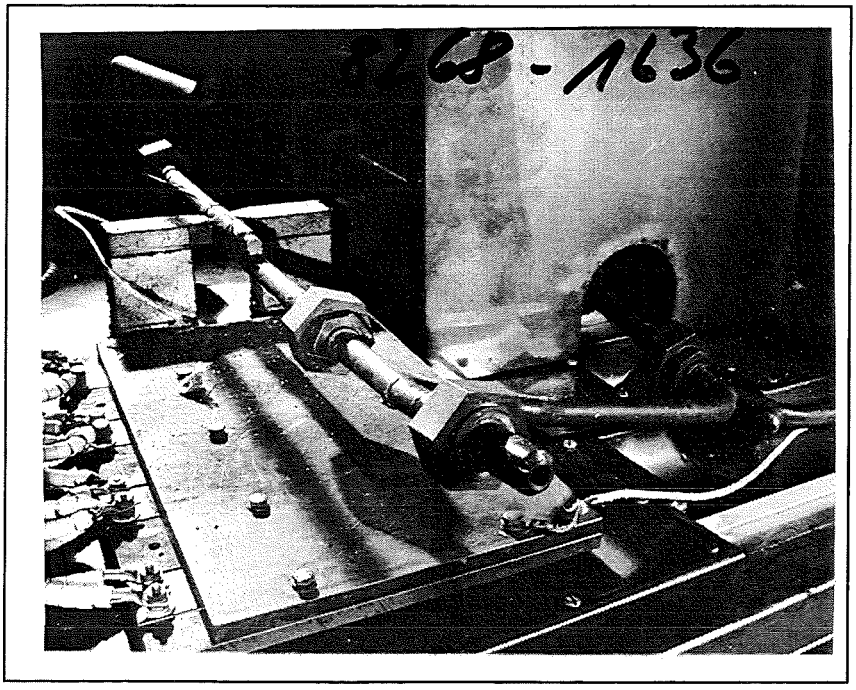

Fig.46 : Phase VII. Magnetic trap 1 in TRITEX. Front pipe going to inlet EMP.

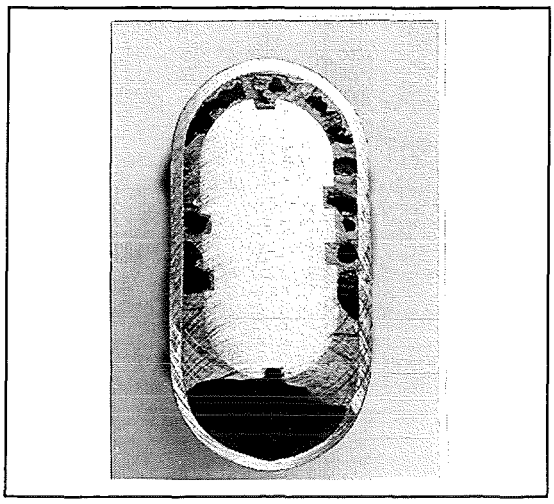

Fig.47 : Phase VII. Cross section of magnetic trap 1 near inlet. Scale 1:1.

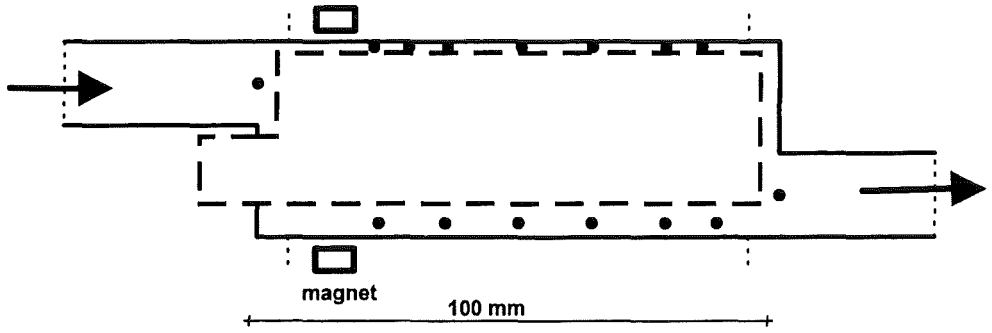

Fig.48 : Phase VII. Magnetic trap 1. Between dotted lines : vanadium part; black dots : sampling positions.

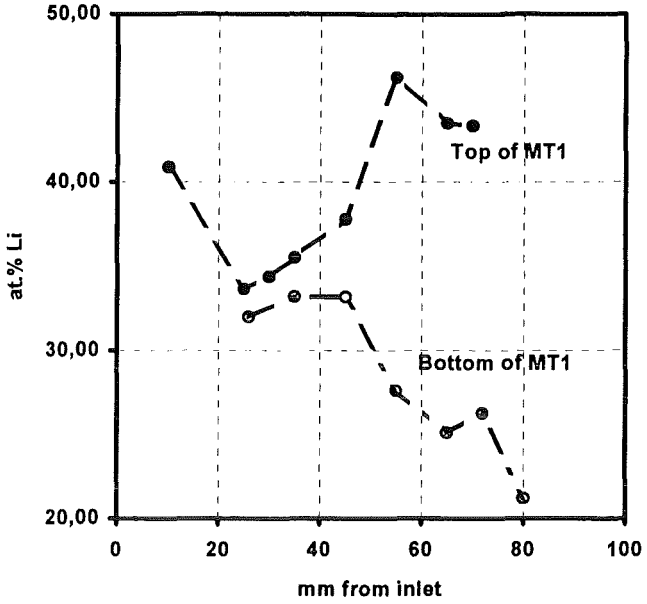

Fig.49 : Phase VII. Concentration of Li in magnetic trap 1.

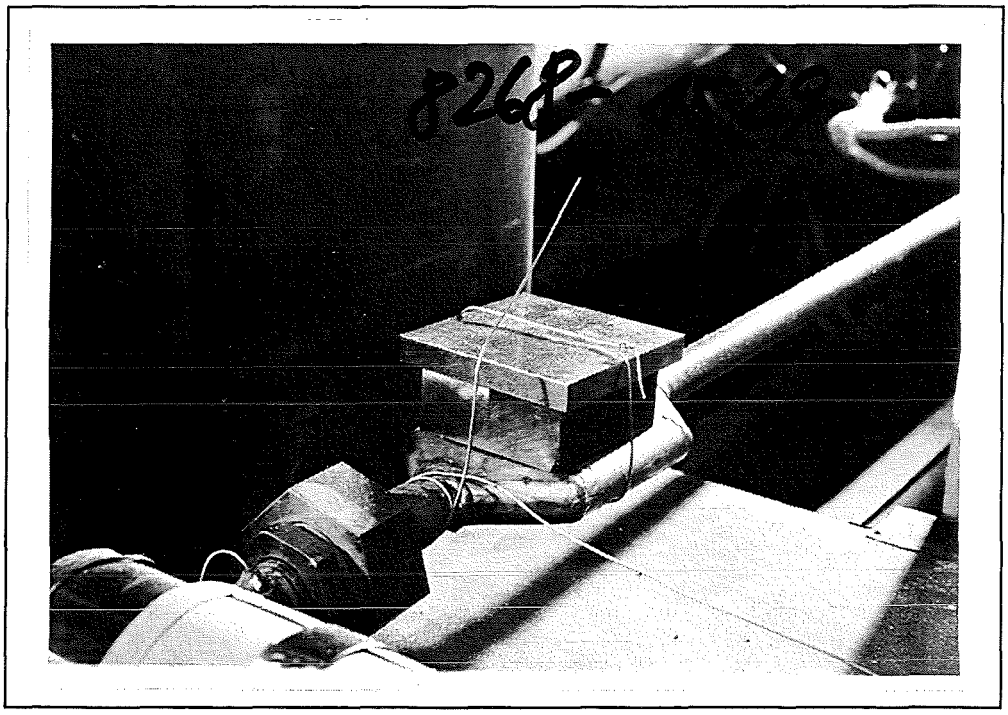

Fig.50 : Phase VII. Arrangement of magnetic trap 2.

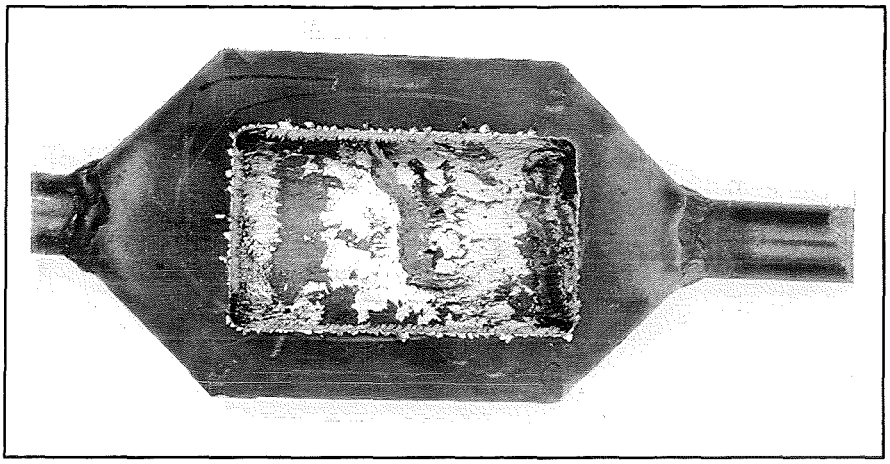

Fig.51 : Phase VII. Deposits in magnetic trap 2.

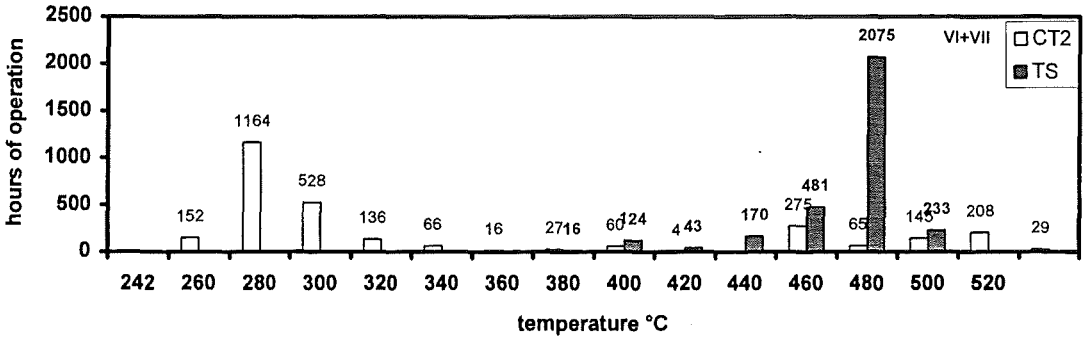

Fig.52 : Operation Phase VI+VII.

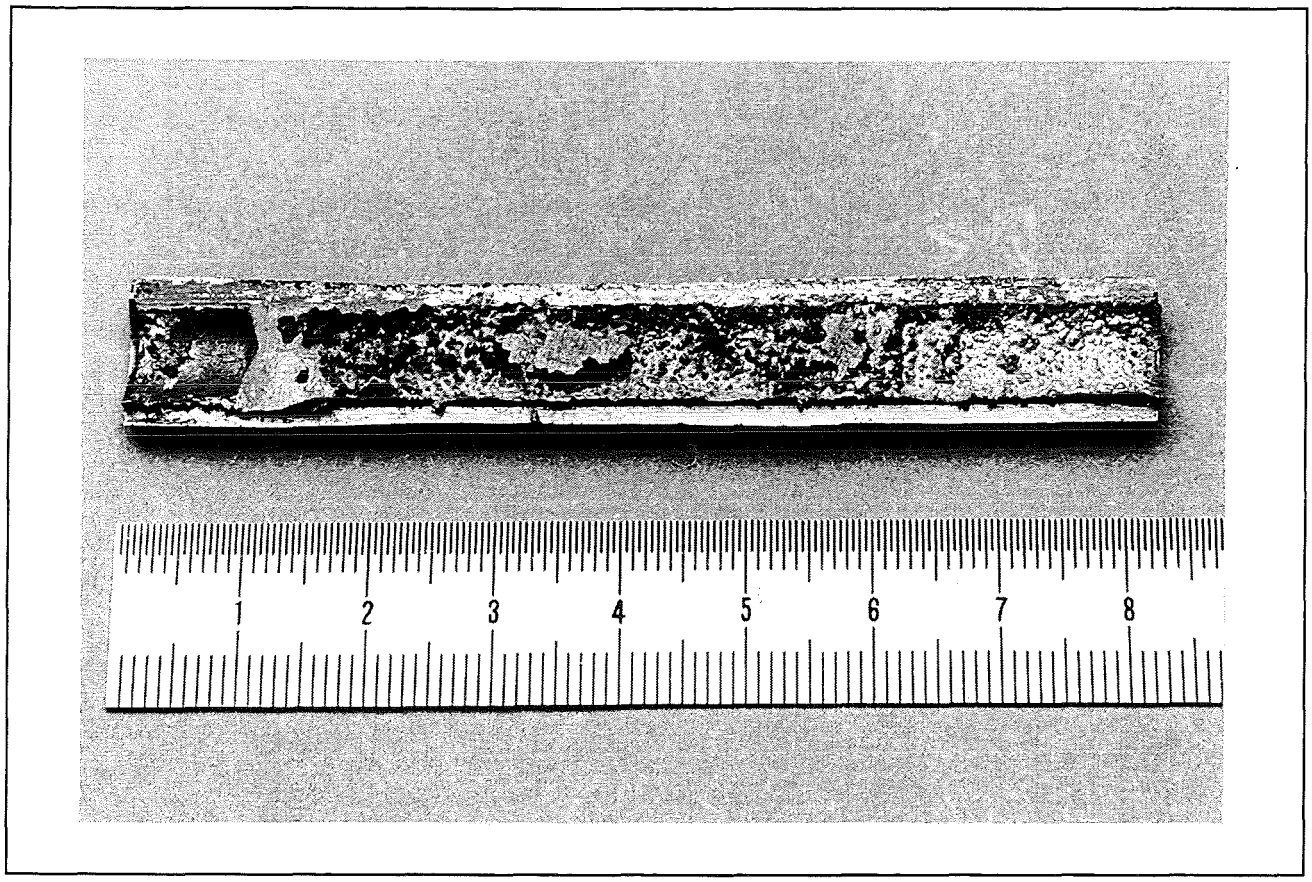

Fig.53 : Phase VII. Axially cut of flow meter 1. Main deposits at inlet side (left) at position of magnet. Scale 1:1.

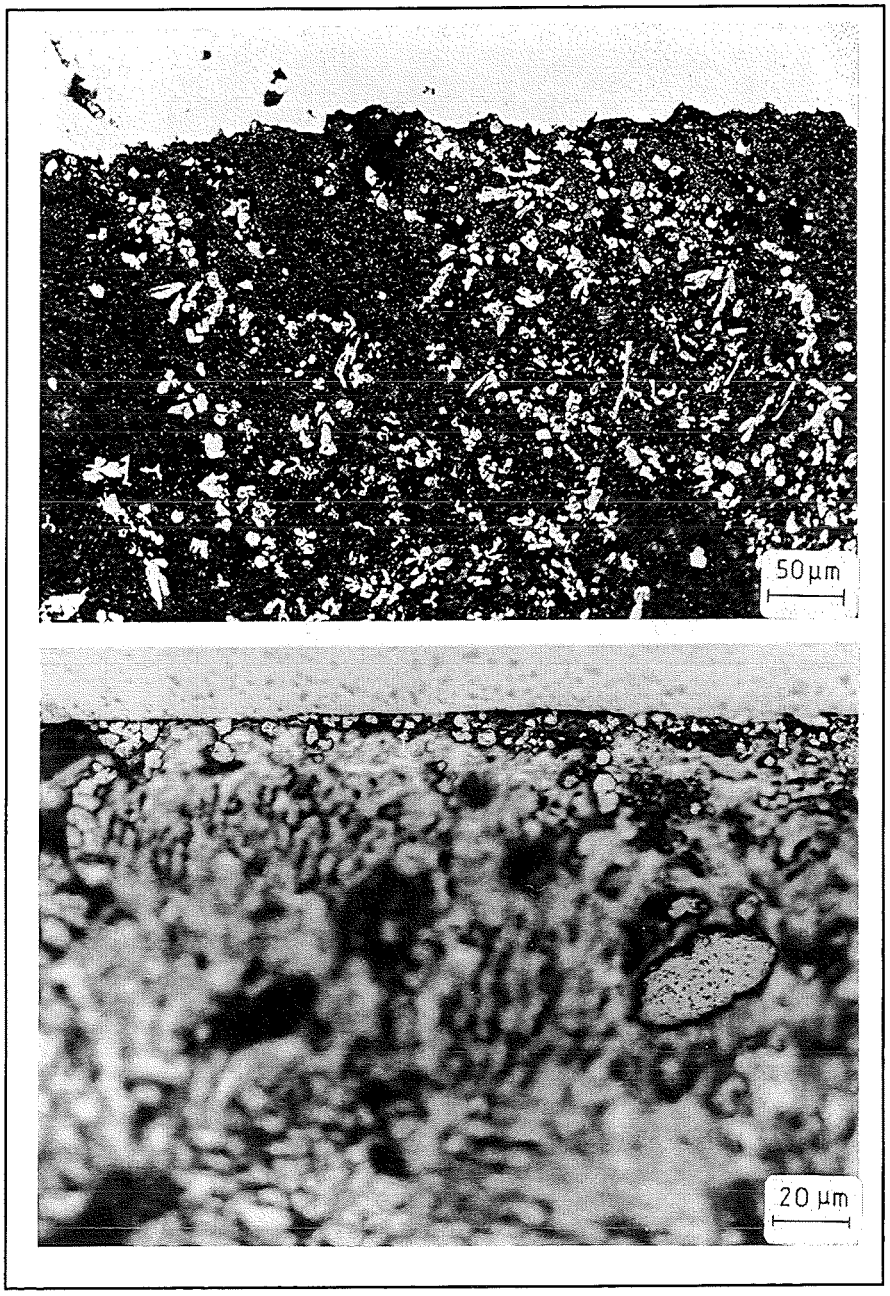

Fig.54 : Phase VII. Particle deposition in flow meter 1. Upper picture near magnet, lower picture 5 cm away from magnet.

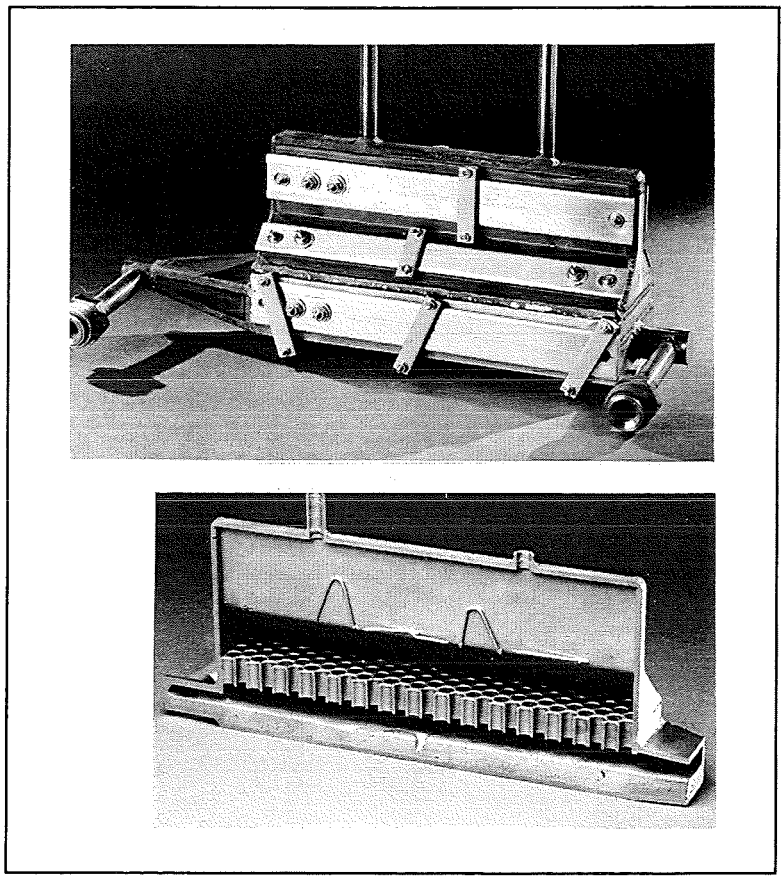

Fig.55 : Phase VII. Cold trap 2 after phase VII. Closed with heaters and cut open.

References

[1] M.Abdou (Editor), BCSS, Blanket Comparison and Selection Study, ANL/FPP 83-1 (1983)

[2] H.Feuerstein, H.Gräbner, G.Kieser, TRITEX, a forced convection loop with Pb-17Li, J.Nucl.Materials 155-157 (1988) 520

[3] H.Feuerstein, S.Horn, G.Kieser, TRITEX, A Ferritic Steel Loop with Pb-15.8Li. Facility and Operation, FZKA-6286 (1999)

[4] P.Hubberstey, T.Sample, M.G.Barker, Is Pb-17Li Really the Eutectzic Alloy ? J.Nucl.Materials 191-194 (1992) 283-287

[5] H.Feuerstein, L.Hörner, J.Oschinski, S.Horn, Behaviour of Lithium in Pb-17Li Systems, Liquid Metal Systems, p.357, Plenum Press, New York 1995, Edited by H.U.Borstedt

[6] H.Feuerstein, L.Hörner, S.Horn, Self adjustment of Li in Pb-17Li systems, J.Nucl.Materials 258-263 (1998) 505-507

[7] H.Feuerstein, H.Gräbner, J.Oschinski, J.Beyer, S.Horn,, L.Hörner, K.Santo, Compatibility of 31 metals, alloys and coatings with static Pb-17Li eutectic mixture, FZKA 5596 (1995)

[8] P.Judex, S.Heißler, C.Adelhelm, Determination of bismuth in lead and in a lead-lithium alloy by stripping voltametric assay, Fresenius Journal of Analytical Chemitsry 347 (1993) 413-416

[9] S.Bucké, H.Feuerstein, L.Hörner, J.Beyer, S.Horn, Behavior of Bismuth in Lithium-Lead Mixtures, 19th Symposium on Fusion Technology, Lisbon, Portugal, Sept.16-20, 1996

[10] H.Feuerstein, H.Gräbner, S.Horn, J.Oschinski, Transport of deuterium and rare gases in thermal convection loops with molten Pb-17Li, Fus.Engin.Design 14 (1991) 261-272

[11] M.C.Bloom, M.Krulfeld, W.A.Fraser, P.N.Vlannes, Corrosion Studies in High Temperature Water By a Hydrogen Effusion Method, Corrosion 13 (1957) 27-32

[12] H.Feuerstein, H.Gräbner, S.Horn, J.Oschinski, Extraction of tritium from molten Pb-17Li by use of solid getters, 16th Symposium on Fusion Technology, London, UK, Sept.3-7, 1990

[13] H.Feuerstein, L.Hörner, S.Horn, J.Beyer, J.Oschinski, H.Gräbner, P.Welter, S.Bender, Oxidation of Pb-17Li in Ar between 25 and 650 °C, KfK 4927 (Sept.1992)

[14] H.Feuerstein, D.A.Wirjantoro, L.Hörner, S.Horn, Eutectic mixture Pb-17Li - In-situ production an Li-adjustment, 18th Symposium on Fusion Technology, Karlsruhe, Germany, Aug.22-26, 1994

[15] H.Tas, P.Lemaitre, Ja.Dekeyser, W.Vandermeulen, F.DeSchutter, Austenitc stainless steel degradation in dynamic Pb-17Li systems, Fus.Engin.Design 14 (1991) 321-328

[16] O.J.Foust, Sodium-NaK Engineering Handbook, Gordon and Breach, NY, 1979

[17] M.G.Barker and T.Sample, The solubility of nickel, manganese and chromium in Pb-17Li, Fus.Engin.Design 14 (1991) 219-226

[18] H.Feuerstein, Contribution to European Liquid Metal Workshop, Nottingham 1990 (unpublished)

[19] F.Barbier, Influence of manganese on the nickel concentration in solution in Pb-17Li alloy, 18th Symposium on Fusion Technology, Karlsruhe, Germany, Aug.22-26,

[20] P.Nash, Ed., Phase Diagrams of Binary Nickel Alloys, ASM International , Materials Park, Ohio, 1991

[21] V.Coen and T.Sample, Pb-17Li : A Fully Characterized Liquid Breeder, Fusion Technology 1990, 248-252

[22] Ch.Adelhelm, H.U.Borgstedt, D.Lindner and G.Streib, Methods for the determination of lithium and impurities Pb-17Li, Fus.Engin.Design 14 (1991) 235-240

[23] R.Ainsly, L.P.Hartlib, G.Long, A.Pilbeam, R.Thompson, Behavior of carbon in sodium/steel systems, Proceedings of the International Conference on Liquid alkali metals, Nottingham april 1973, British Nuclear Energy Society , London 1976

[24] H.Feuerstein, L.Hörner, S.Horn, Chemistry of heavy metals in eutectic Li-Pb mixture, 20th Symposium on Fusion Technology, Marseille, France, Sept.7-11, 1998

[25] S.Malang and M.S.Tillack (Editors), Development of Self-Cooled Liquid Metal Breeder Blankets, KFK-5581 (1995)

[26]. H.Feuerstein, H.Gräbner, .Oschinski, S.Horn, S.Bender, Evaporation of Lead and Lithium from Molten Pb-17Li - Transport of Aerosols, Fus.Engin.Design 17 (1991) 203-207

[27] D.R.Lide (Editor) CRC handbook of chemistry and physics, 71.ed. CRC Press 1990

[28] S.G.Bankoff, Minimum Thickness of a draining Liquid Film, Intern.Journal of Heat and Mass Transfer 14 (1971) 2143-2146

ACKNOWLEDGMENT

This work has been performed in the framework of the Nuclear Fusion Project of the Research Center Karlsruhe and was supported by European Communities within the European Fusion Technology Program.

The authors have to thank Dr.Gräbner, Mr.Oschinski and Mr.Beyer which participated over many years in the program. All three are now retired. Many other people were involved over the years with experiments and evaluations. We have to thank especially the mechanical and electrical workshops for their ideas and manually help. We have also to thank Mrs.Echtle, Universität Karlsruhe, Institut für Werkstoffkunde 1 for metallographic preparations, and Mr.G.Schüler, IMT, FZK for REM pictures and Microprobe analysis.